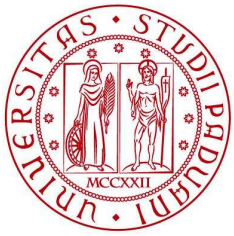

UNIVERSITÀ
DEGLI STUDI
DI PADOVA

Sede Amministrativa: Università degli Studi di Padova

Diperatmiento di Scienze Chimiche

SCUOLA DI DOTTORATO DI RICERCA IN SCIENZE MOLECULARI

INDIRIZZO: SCIENZE CHIMICHE

CICLO XXXI

CARBOHYDRATE RECOGNITION BY MONOLAYER PROTECTED GOLD NANOPARTICLES

Direttore della Scuola: Ch. mo. Prof. Leonard J. Prins

Coordinatore d'indirizzo: Ch. mo. Prof. Leonard J. Prins

Supervisore: Ch. mo. Prof. Leonard J. Prins

Dottorando: Carlos M. León Prieto

Table of contents

This research project have been carried out within the framework of the Marie Curie ITN "MULTI-APP" (Nº 642793).

Abbreviations

K_D = Dissociation constant

$CDCl_3$ = Deuterated Chloroform

CDCN = Deuterated Acetonitrile

CD_3OD = Deuterated Methanol

K_a = Association constant

D_2O = Deuterium oxide

DCC = Dynamic combinatorial chemistry

Neu5Ac = N-Acetylneuraminic acid

Cys = Cysteine

His = Histidine

AuNPs = Monolayer protected gold nanoparticles

d = Diameter

nm = Nanometer

TACN = 1,4,7-Triazacyclonone

FCS = Fluorescence correlation spectroscopy

ITC = Isothermal titration calorimetry

DOSY = Diffusion-ordered spectroscopy

Trp = Tryptophan

SPR = Surface Plasmon Resonance

XPS = X-ray photoelectron spectroscopy

IR = Infrared radiation

ATP = Adenosine triphosphate

ADP = Adenosine diphosphate

AMP = Adenosine monophosphate

Ac = Acetyl

Asp = Aspartic acid

Gly = Glycine

TGA = Thermogravimetric analysis

TEM = Transmission electron microscopy

DLS = Dynamic light scattering

F.I. = Fluorescence intensity

SSC = Surface saturation concentration

ex = Excitation

em = Emission

EP = Ether petroleum

t = Triplet

s = Singlet

m = multiplet

br = Broad

MeOH = Methanol

ESI-MS = Electrospray Ionization-Mass Spectrum

$CHCl_3$ = Chloroform

DCM = Dichloromethane

J = Joule

H = Enthalpy

N = Stoichiometry

G = Gibbs energy

S = Entropy

cal = Calorie

K = Kelvin

T = Temperature

D = Diffusion coefficient

Arg = Arginine

Ser = Serine

Asn = Asparagine

Glu = Glutamic acid

Tyr = Tyrosine

SPPS = Solid phase peptide synthesis

HPLC = High Performance Liquid Chromatography

UPLC-MS = Ultra Performance Liquid Chromatography – Mass Spectrometry

Fmoc = Fluorenylmethyloxycarbonyl

DMF = Dimethylformamideç

DIPEA = N,N-Diisopropylethylamine

TFA = Trifluoroacetic acid

TIS = Triisopropylsilane

ACN = Acetonitrile

AP = Alkaline Phosphatase

TMP = Thymidine monophosphate

dGMP = deoxy-guanidine monophosphate

PNPP = Para-nitro-phenyl phosphate

Chapter 1: Introduction

1.1 The relevance of carbohydrates in the biomolecular recognition

Carbohydrates represent one of the most versatile and interesting class of biomolecules since they play important roles in different biological processes.[1] For instance, in nature polysaccharides such as glycogen and starch serve as energy storage, while monosaccharides like glucose can be used as an immediate source of energy.[2] Other polysaccharides such as cellulose and chitin are rigid materials that are used to build up structural units in plants and crustaceans.[3]

Apart from the well-known roles mentioned above, nowadays we are also starting to understand and appreciate the profundity and complexity of information encoded within sugar structures. For instance, in the DNA chain and protein information systems, six monomers can be connected giving rise to 4096 nucleotide sequences or $6x10^7$ polypeptides.[4] Analogously, when factors such as ring size, anomeric configuration, linkages position, and branching are taken in consideration, six monosaccharides can form more than $1x10^{15}$ different oligosaccharides.[4a, 4b] So, it is not surprising that biology uses carbohydrates as more than just structural building blocks or sources of biochemical fuels.

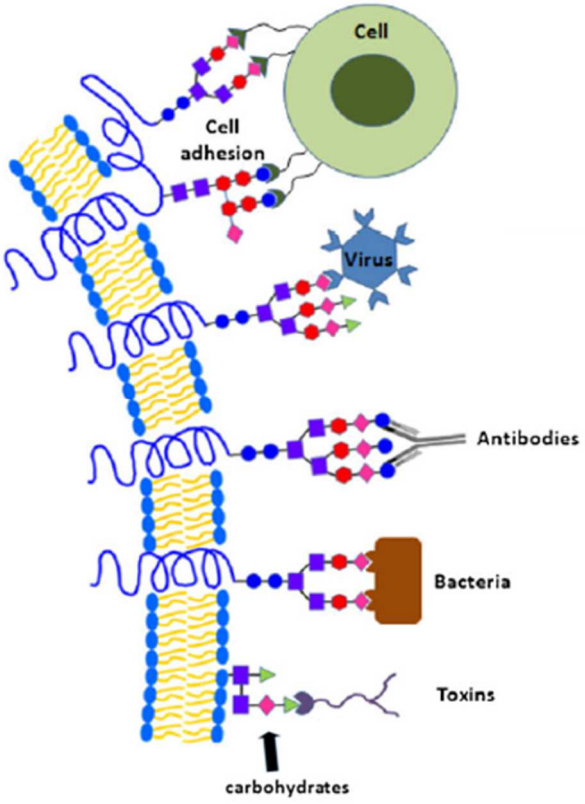

Figure 1: Multivalent protein-carbohydrate interactions at the cell surface.

In nature, carbohydrates are used to perform very delicate tasks. In fact, carbohydrates play a key role in the progression of human pathologies such as infection by pathogens,

diabetes, tumour development and metastasis, and immune system disorders (Figure 1).[5] Indeed, certain types of carbohydrates are biomarkers for pathologies such as cancer.[6] Carbohydrate recognition is obviously important in carbohydrate metabolism and for the transport of highly polar molecules across cell membranes.[1, 7]

Therefore, carbohydrate recognition in biological media is a very attractive target. The development of methodologies for carbohydrate recognition are useful for expanding the knowledge of biological processes from the theoretical point of view. For instance, Quiocho *et. al.* reported one of the first theoretical models of the recognition process between lectin and carbohydrates.[8] But apart from these methodologies, the capacity to recognize carbohydrates in a selective manner would enable the detection of specific sugars in biological media. It is a powerful tools in diagnostic[9] and medical fields[10] through the design of synthetic receptors that could also be used as drugs (for instance anti-infective agents),[11] to target cell types (acting as "synthetic antibodies"),[12] to transport saccharides or related pharmaceuticals across cell membrane (Figure 2).[7a]

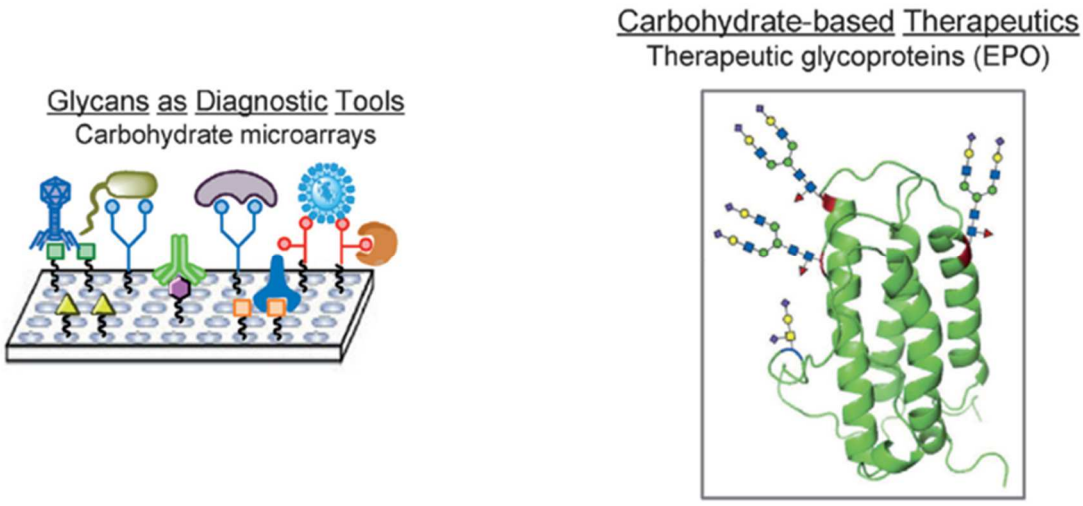

Figure 2: Applications of synthetic carbohydrates in medicine and biology.

1.2 Carbohydrate recognition

Owing to the important role that carbohydrates play in many biological processes and the vast number of applications that involve carbohydrate recognition, supramolecular chemists have been studying carbohydrate recognition since the late 1980's. Two main strategies can be identified, the first one based on reversible covalent bonds and the other one based on non-covalent interactions.[13] Many of the developed receptors are inspired by nature, since the natural carbohydrate receptors, a group of proteins called lectins, are able to recognize carbohydrate in a selective manner in water based on multiple non-covalent interactions.[14]

1.2.1 Natural carbohydrate receptors

In Nature, carbohydrate-recognition occurs by carbohydrate-binding proteins named lectins, which are of non-immune origin and which bind carbohydrates without enzymatically altering them (Figure 3).[15]

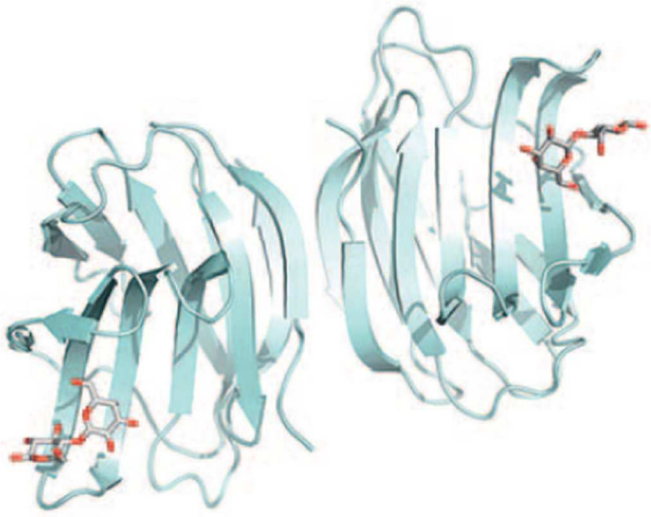

Figure 3: b-sandwich/jelly-roll fold of a galectin (human galectin-1; PDB 1GZW).

Lectins are present in all branches of the evolution tree, since they have been identified in all organisms, starting from microorganism moving all the way up to plants and animals.[14] Lectins are basically divided into three classical families, legume lectins, C-type lectins and galectins. There are also other plant lectins, viral proteins, toxins, anti-carbohydrate antibodies and pentraxins that have been found.

The binding between carbohydrates and lectins is usually weak since in general the lectins present shallow binding pockets that are exposed to solvent.[16] Lectins recognize carbohydrates via hydrogen bonding, metal coordination, Van der Waals and hydrophobic effects.[17] The impressive line-up of hydroxyl groups on carbohydrates allows the creation of networks of hydrogen bonds in which the hydroxyl group acts both as a donor and as an acceptor to promote the formation of cooperative hydrogen bonds between the saccharide and protein surface.[18] The hydrogen bonds between lectin and carbohydrates are both direct and water mediated. Furthermore, divalent cations, such as Ca^{2+} and Mn^{2+}, are involved in carbohydrate recognition by changing the shape of the binding site or by direct binding of the carbohydrates, such as what happens in C-type lectins, like serum lectin (Figure 4).

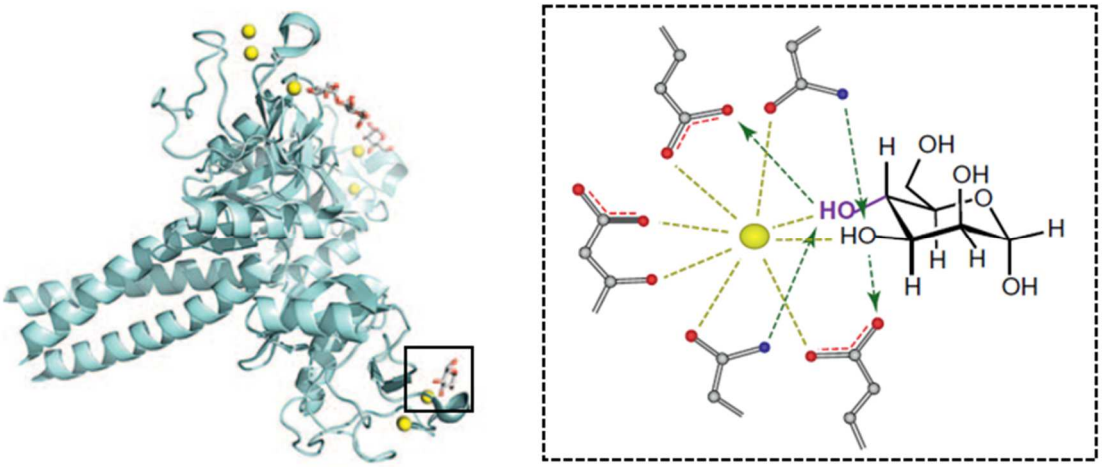

Figure 4: Mannose-binding C-type serum lectin involves a strategically presented Ca^{2+} ion (sphere) to probe or the presence of the equatorial 4-hydroxyl group, along with two H bonds.

In addition, carbohydrate-aromatic CH-π interactions participate in the lectin-carbohydrate recognition. These are dispersion interactions, which are modulated by electrostatic interactions and partially stabilized by hydrophobic effects that occur between the C-H bonds of carbohydrates and aromatic units present in the binding pockets of lectins stabilizing the complex formed between them (Figure 5).[19]

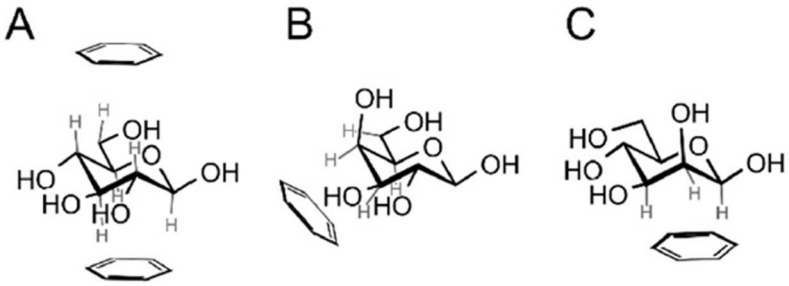

Figure 5: Prevalent geometries of carbohydrate–aromatic CH/π interactions: a) β-D-glucopyranosecan interact via both faces, b) α- or β-D-galacto- or D-fucopyranose interacts via hydrogens on atoms C3, C4, C5 and, c) β-D-mannopyranose interacts via hydrogen atoms on C1, C2 and C3.

The study of lectin-carbohydrates or protein-carbohydrates is challenging because of the complexity and heterogeneity of the cell surface, the intrinsic complexity of carbohydrates and also the typical weak binding affinities. The interactions between carbohydrates and proteins are weaker than protein-protein interactions, by about a factor of 10^6-10^{12} from characteristic antibody equilibrium constant (K_D). The K_D value of lectin binding with a simple monosaccharide is around 1 mM.[20] Nonetheless, in biological context, the limitations arising from a weak binding affinity have been overcome by multivalency. For instance, multiple contacts occur between clustered carbohydrates on cell surfaces and protein receptors that contain several carbohydrate recognition units.[21] Therefore, the interaction between carbohydrates and lectins is not a simple monomeric binding event, but involves multiple recognition events (Figure 6).[22]

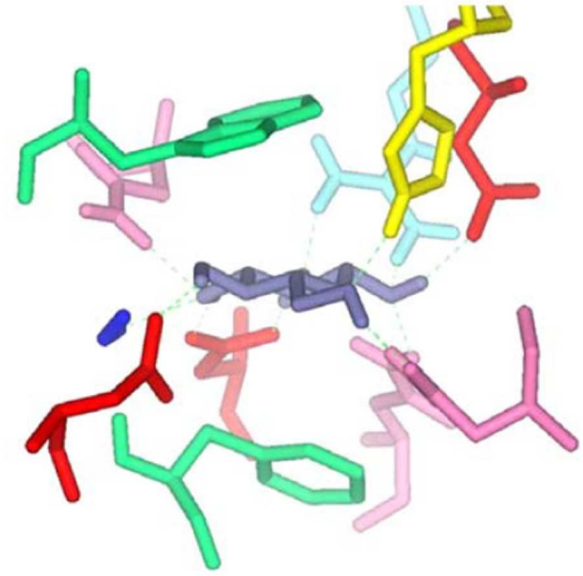

Figure 6: A glucose molecule in the active site of the E. coli. galactose chemoreceptor protein, as revealed by X-ray crystallography. The substrate makes contact with two apolar residues (phenylalanine and tryptophan, shown in light green), a water molecule dark blue), and eight polar amino acid residues (39 aspartate, red; 39 asparagine, pink; 19 histidine, yellow; and 19 arginine, light blue).

Usually, lectins present more than one carbohydrate binding site and it has been shown that when two binding events occur simultaneously it can improve the interaction by more than 100-fold and, on occasions, even up to 10.000 fold.[23] For instance, the interaction between cholera toxin and ganglioside G_{M1} was studied and a K_D from 1 nM to 1 pM were reported.[24] This affinity is similar to that of a typical antibody interaction. Another example is provided by the charged polysaccharides heparin and heparin sulfate that interact with high affinities with a variety of proteins. Lipoprotein lipase binds to heparin sulfate with a K_D of approximately 100 pM, human acidic fibroblast growth factor binds to heparin with a K_D~50 nM, and protease nexin-1 binds to heparin with a K_D~20 nM. As a result of multivalency, lectin-carbohydrate binding has been shown to significantly decrease the observed K_D values to the low nM region.[25] In general, the conclusion that can be drawn is that the high density of carbohydrates on the cell surface permits multivalent binding, which is referred to as the glycoside cluster effect (Figure 7).[26]
Since lectins are involved in several physiological events, an understanding of the interaction with carbohydrates is of utmost importance. For instance, the cellular protein glycosylation pattern is affected by several kinds of pathologies. Thus, changes in the glycoform population of a given glycoprotein can be diagnostic of the disease responsible for the alteration. The analysis of glycosylation as a result of cancer,[27] showed both quantitative and qualitative lectin-binding differences for cytosolic glycoproteins in malignant and benign thyroids neoplasms. It was observed that, in the majority of carcinomas, lectin-binding was weaker with regard to the adenomas and non-neoplastic specimens.[28]

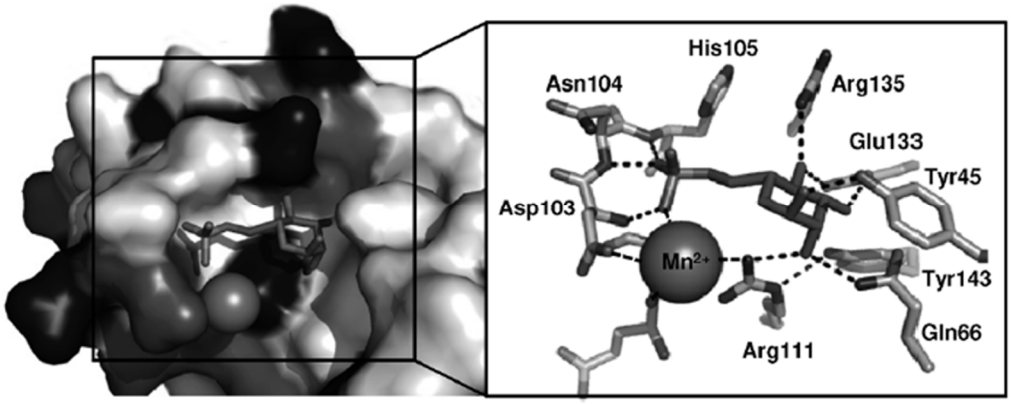

Figure 7: Carbohydrate hydroxyl and phosphate groups create hydrogen bonds with positively (black) or negatively charged (dark gray) residue side chains. The phosphate group also interacts with a Mn^{2+} cation found in the binding site.

The affinity of natural receptors for particular substrates has been exploited for applications in biological diagnostics since the 1950s. One example is ABO blood typing, in which several kind of lectins are used to recognise the characteristic sugar moieties present on the surface of different erythrocyte cell types.[29] Nonetheless, the use of proteins in biological diagnostics has several drawbacks such as non-specific substrate recognition, low protein stability with regard to temperature, and challenges in efficiently altering protein properties for several applications. The development of synthetic carbohydrates receptors can overcome these limitations to improve the applicability and use of them in fields such as biology, diagnostic or imaging.

1.2.2 Synthetic carbohydrate receptors: mimicking nature

Taking inspiration from the nature, chemists have focused on strategies to detect carbohydrates using synthetic lectins. The earlier work on carbohydrate recognition was typically carried out in non-competitive organic solvents.[4c] Receptors were developed in order to understand in detail the specific carbohydrate recognition via different architectural structures through hydrogen bonding and other kinds of interactions. The idea was that if an optimal architecture would be found, it could be used as a starting point for the design of new carbohydrate receptors able to detect carbohydrates in water.

1.2.2.1 Carbohydrate recognition in organic media

In non-polar solvents, the hydrogen bond is an effective noncovalent bond with sufficient strength, especially when multiple bonds occur in the same structure. Therefore, architectures in which the carbohydrate is surrounded by hydrogen bond donors and/or acceptors are likely to be successful. One example of the applicability of this concept was reported by Aoyama *et al.* in 1988 who developed the bowl-shaped octahydroxyresorcin[4]arene (Figure 8) which presented a cavity which was able to

extract certain monosaccharides, such as D-ribose, D-arabinose and L-fucose from water into organic media.[30]

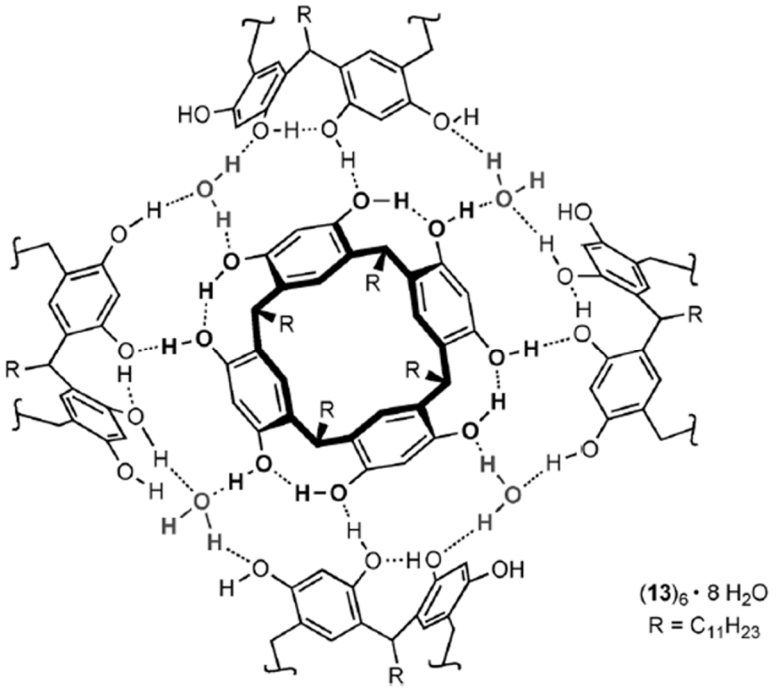

Figure 8: Side view of the self-assembled capsule formed by hydrogen bonding between six molecules of octahydroxyresorcin[4]arene 13 and eight structural water molecules (only half of the capsule is shown here). This supramolecular assembly can encapsulate up to three molecules of methyl β-D-glucoside.

Although earlier studies evidenced that this receptor could form a 2:1 sandwich complex to bind methyl-β-D-glucoside in an enantiomeric selective manner,[30] overall the receptor did not present excellent selectivity in 1:1 receptor-substrate complexes.

Another example was reported in the early 1990's by Bonar-Law and Davis in which they presented a covalent cyclic structure capable of fully encapsulating carbohydrates substituted with an aliphatic chains. The structure was derived from cholic acid and referred to as cholaphane (Figure 9). This receptor displayed clear enantioselectivity for octyl-β-D-glucoside [K_a ($CDCl_3$) = 3100 M^{-1}] over β-L-glucoside [K_a ($CDCl_3$) = 550 M^{-1}] and α-D-glucoside stereoisomers [K_a ($CDCl_3$) = 1000 M^{-1}].[31]

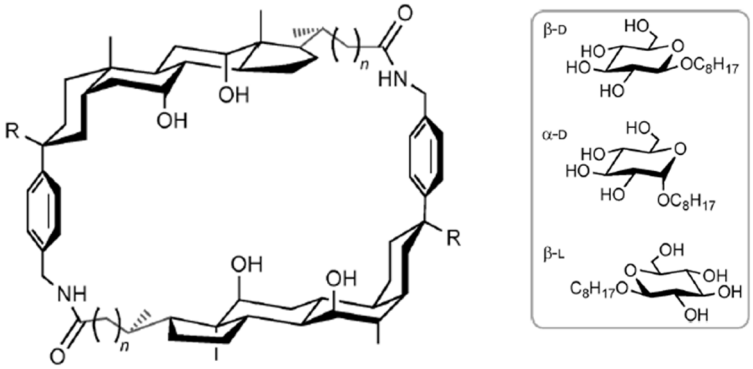

Figure 9: Cyclophane displays enantioselectivity towards different octyl glucosides (inset).

Taking inspiration from the strong interaction of mannose-6-phosphate with lectin through the formation of charge-reinforced H-bonds between the sugar's phosphate group and polar side chains of amino acid residues,[32] new classes of carbohydrate receptors were reported in which the phosphate groups were incorporated in the receptor. Such groups could act as a hydrogen bond acceptor for two vicinals hydroxyl groups in a carbohydrate. An example was reported by Diederich and co-workers who studied the tetraphosphate macrocyclic receptor shown in Figure 10. The cavity of the macrocyclic receptor is sufficiently large to favour the binding of disaccharides [K_a (CDCN/CD_3OD 44:6) = 10750-12500 M^{-1}] in the presence of a competitive solvents such as CD_3OD.[33] Regrettably, this receptor had a very low solubility in water.

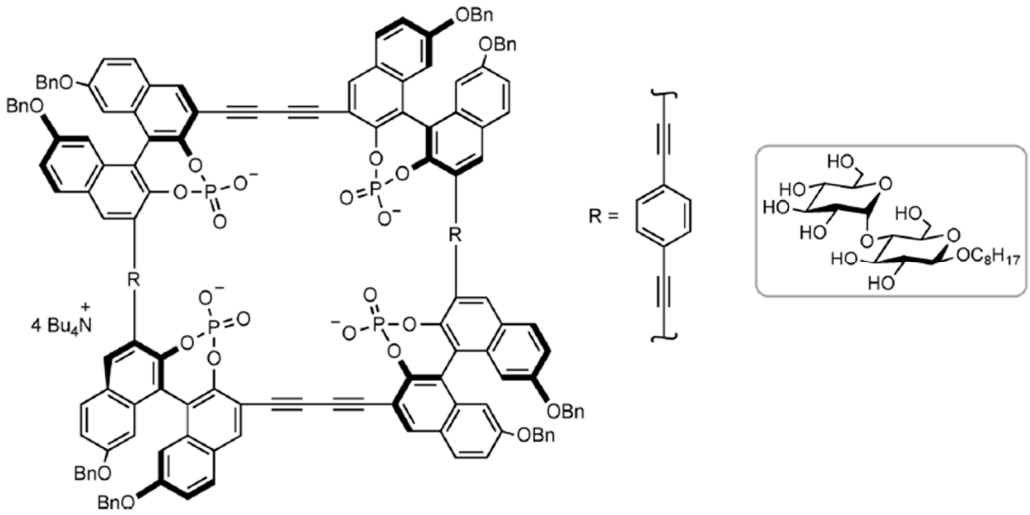

Figure 10: Tetraphosphate macrocycle. Octyl β-D-glucoside.

In the early 2000's Mazik *et al.* reported a new type of carbohydrate receptor containing multiple H-bonding recognition motifs. They observed that the change of a phenyl group in the amide receptor by a pyridine, the association constant for the binding of octyl-β-D-glycoside was improved by 1 order of magnitude [K_a ($CDCl_3$) = 700 and 8700 M^{-1} respectively].[34] This trend continued when the pyridine was replaced by napthyridine, which offers two H-bond acceptor sites for the same hydroxyl group [K_a ($CDCl_3$) = 26500 M^{-1}].[34] So just like in the case of lectins, the multivalency offered by H-bonding recognition motif with multiple adjacent interaction sites, it can remarkably improve the binding affinity of the artificial receptor for carbohydrate (Figure 11).

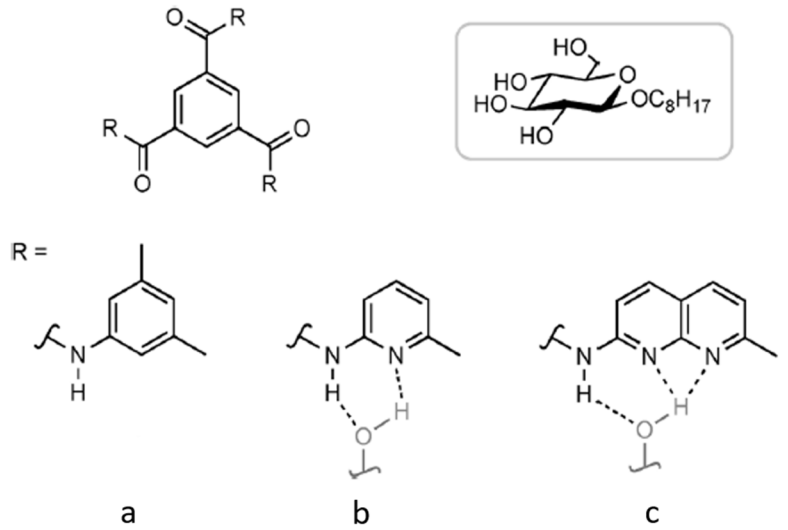

Figure 11: The binding of octyl β-D-glucoside (inset) by receptors a, b, and c illustrates the importance of multiple H-bond donors and acceptors in artificial receptors. Receptor c, which features H-bond acceptors able to form multiple long-range H-bonds with the same hydroxy group (gray), exhibits particularly strong binding.

The small list of examples mentioned above are able to operate in organic media and therefore the potential for application in a biological context is rather limited.

1.2.2.2 Carbohydrate recognition in water

Synthetic receptors for carbohydrate recognition in water can be divided into two main groups. The first group is based on dynamic covalent bonds complemented with weaker non-covalent interactions. The second group of receptors are able to recognize carbohydrates in water only through noncovalent interactions.

Boronic acid receptors are based on reversible covalent bond formation that occurs between hydroxyl groups of carbohydrates and boronic acids giving rise to boronic esters (Figure 12). The process is limited to high pH which may represent a drawback for certain biological applications.[35]

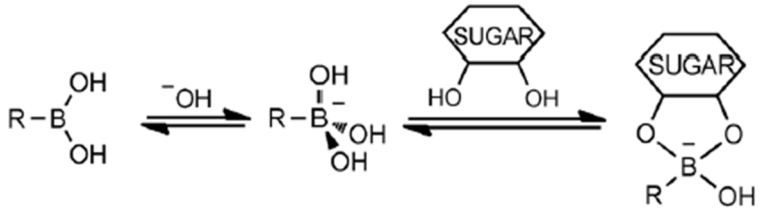

Figure 12: The reaction between boronic acid and carbohydrate hydroxyl groups used for carbohydrate recognition.

Shinkai and co-workers overcame this limitation and reported a boronic acid sensor in which they used basic tertiary amine groups to link boronic acid sites and a reporting fluorophore unit.[36] Due to the presence of the tertiary amine, which provide the electron density required to activate the hydroxyl exchange, it was possible that the process

occurred in physiological pH. The sensor was able to recognize D-glucose in a 1:2 methanol:water mixture with a good affinity $K_a = 4000\ M^{-1}$ (Figure 13).[37]

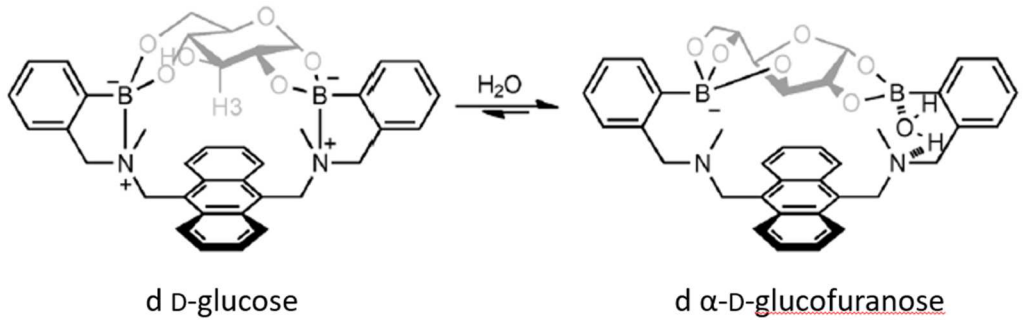

Figure 13: Receptor d binds D-glucose (gray), which undergoes isomerization in aqueous media to its α-D-glucofuranose form.

An example of how boronic acid sensors present a huge potential for glucose recognition and disease biomarkers is the semi-permanent "smart tattoo" for the continuous monitoring of the blood glucose levels in diabetics. This is composed of polymeric nanosensors containing the octylboronic acid receptor along with hydrophobic cores that are implanted under the skin (Figure 14).[38]

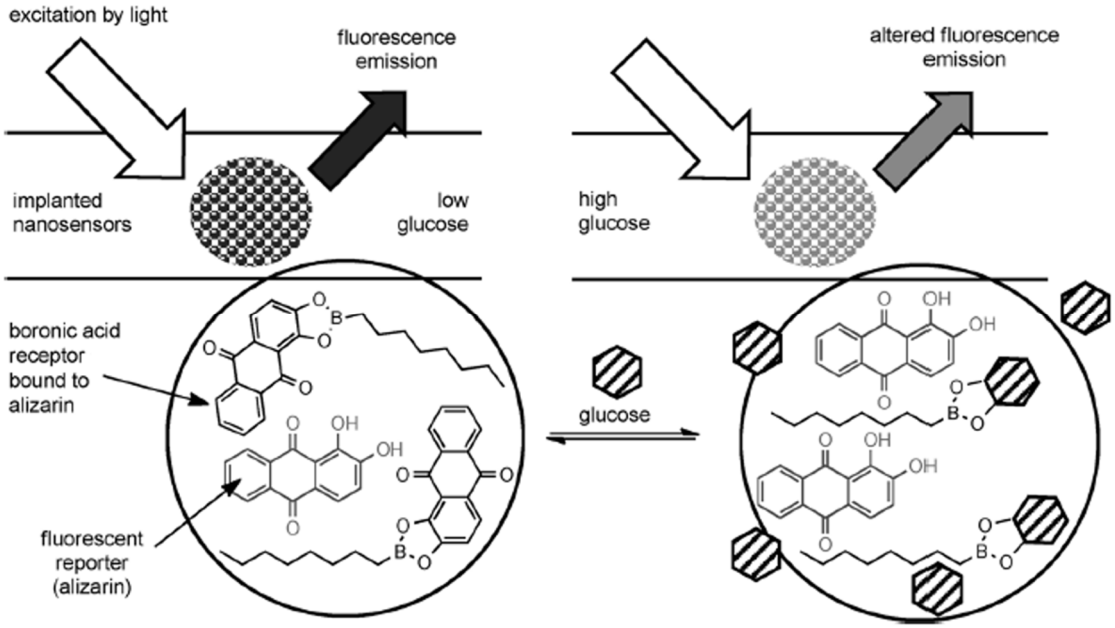

Figure 14:"Smart tattoos" with boronic acid receptors can be used to monitor blood glucose levels in diabetics.

Depending on the levels of glucose, the fluorescence reporter binds to the free receptor transmitting a coloured signal when the levels of glucose is low. On the other hand, when the levels of glucose are high the receptor binds to glucose and the fluorescence of the reporter is altered. This sensor reached the phase of *in vivo* studies with mice showing a positive monitoring of glucose at physiological pH.

The second group involves carbohydrate receptors based only on non-covalent interactions. One of the most famous example was reported in 2009 by Davis and co-workers who developed "The Temple" which is basically composed of polar and nonpolar regions (Figure 15 left).[4c] "The Temple" contains apolar anthracenes as "roof" and "floor", which can interact with the C-H bond of carbohydrates via CH-π interactions, and two polar isophthalamides as "pillars", which can interact with the hydroxyl groups of carbohydrates through hydrogen bonds. The receptors present a remarkable selectivity to D-glucose in water compared to other monosaccharides such as D-mannose, D-galactose or D-fructose, but with a modest overall binding affinity [K_a (D_2O) = 56 M^{-1}]. Therefore, this receptor shows a huge potential for biological diagnostics (Figure 15 right).[39]

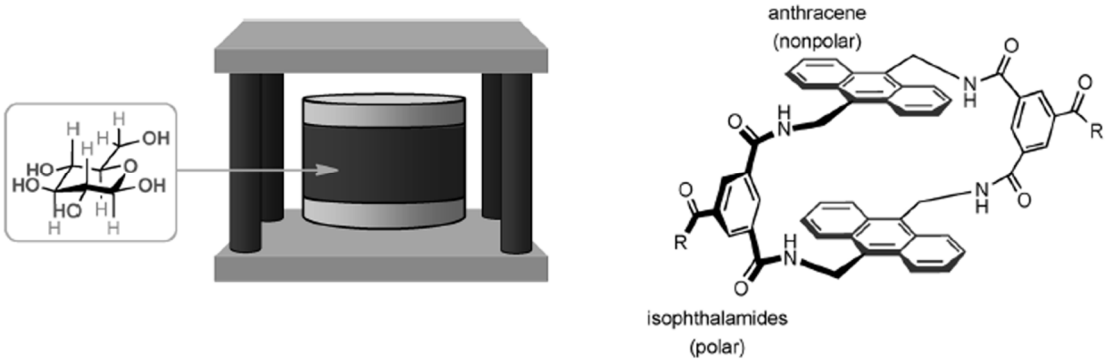

Figure 15: Representation of "the temple" receptor, designed to complement the polar (dark grey) and nonpolar regions (light grey) of D-glucose (inset) (left) and chemical structure of the carbohydrate receptor based on "the temple" structure (right).

Another example is the peptide-based receptor reported by Ravoo and co-workers who exploited dynamic combinatorial chemistry (DCC) as a tool for finding the optimal receptor structure. The reversible nature of disulfide bond formation (Figure 16a) allows a biorelevant sugar such as Neu5Ac to act as a temple for the spontaneous emergence of the optimal receptor from a dynamic library of Cys-X-Cys tripeptides in aqueous solution. The addition of the Neu5Ac target to the dynamic library caused the spontaneous amplification in 2-fold of macrocycle, composed of two units of Cys-His-Cys, in parallel and antiparallel orientation reporting 72.7 M^{-1} and 7.7 x 10^3 M^{-1} for K_{a1} and K_{a2} respectively (Figure 16b).[40] This study shows that DCC is a powerful tool for the discovery of new classes of receptors for carbohydrate recognition in water.

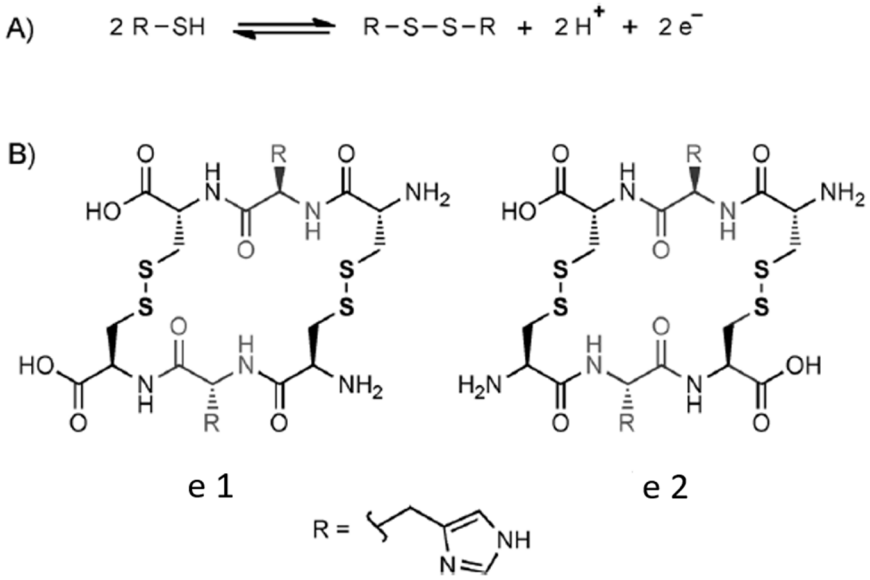

Figure 16: a) The reversible thiol/disulfide equilibrium allows tripeptides containing terminal cysteine residues to macrocyclize in the presence of atemplating substrate, to form b) histidine-containing (grey) receptors e1 and e2.

1.3 Monolayer protected gold nanoparticles as multivalent protein like receptors

Over the past decade, monolayer protected gold nanoparticles (AuNPs) have gained relevance owing to the emergence of the fields of nanoscience and nanotechnology.[41] Gold nanoparticles are attractive because they possess interesting physical and chemical properties. They show unique optoelectronic properties such as surface plasmon resonance, conductivity and redox activity (Figure 17).[42]

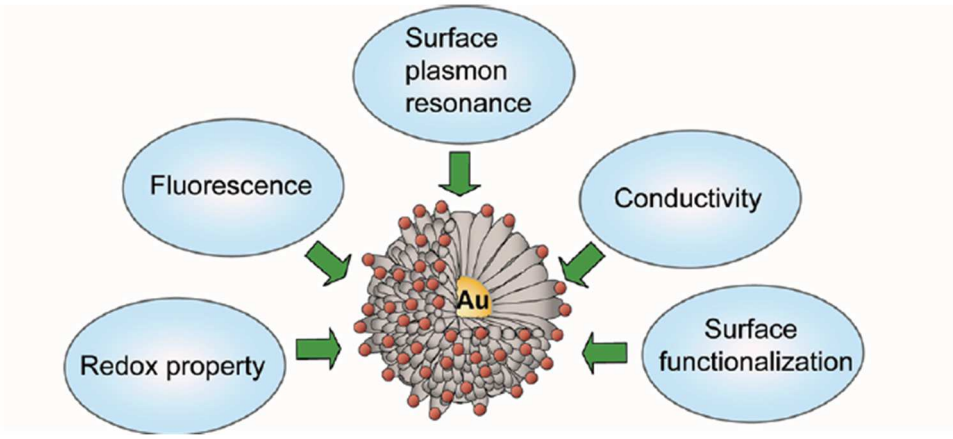

Figure 17: AuNPs properties.

Besides, AuNPs present a series of features that make them more suitable in biological application such as non-toxicity and biocompatibility.[43] Furthermore, AuNPs are able to quench the fluorescence of a fluorophore that is bound to the surface. These features of AuNPs make them an excellent component of biosensing systems.

AuNPs can be synthesized in a straightforward manner and are stable for long periods because of the organic monolayer of thiols, disulfides or phosphines.[44] In 1994, Brust and

Schiffrin reported a biphasic synthetic strategy in which the strong thiol-gold interaction was exploited. AuNPs were obtained with high stability under physiologically relevant conditions even at very low concentrations (Figure 18).[45]

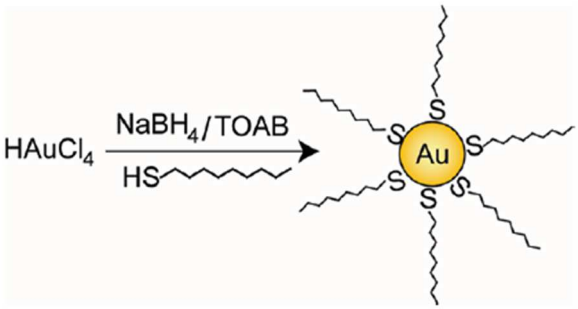

Figure 18: Brust-Schiffrin method for two-phases synthesis of AuNPs by reduction of gold salts in presence of external thiol ligands.

In 2008, Scrimin and co-workers reported the synthesis of water-soluble thiol-protected AuNPs.[46] Their strategy permits different thiols to be anchored to the gold nucleus creating a large variety of AuNPs.

AuNPs have become a promising scaffold for the creation of receptors mimicking the biomolecular surface and present important attributes for the development of these type of sensors. Firstly, the size of the nanoparticle can be tuned easily. Secondly, nanoparticles can be synthesized with a wide range of surface functionalities. Thirdly, the metal core presents electronic and fluorescence properties. Last but not least, they allow for self-templation to complementary surfaces which allows a spontaneous adaptation to the guest. These features give it an advantage compared to conventionally used synthetic receptors.[47]

1.4 Scope of the thesis

AuNPs present very interesting features which can be exploited for the design of novel chemical and biological sensors. In the Prins' group AuNP **1**, which are gold nanoparticles (d = 1.8 ± 0.4 nm) covered with hydrophobic C9-thiols terminating with a 1,4,7-triazacyclonone (TACN)·Zn^{2+}, have been extensively used for application in sensing, catalysis and system chemistry. In this thesis AuNP **1** have been used for the study of carbohydrate recognition. The studies aim at providing the initial bases for the development of innovative synthetic carbohydrate receptors that bind carbohydrates in water using non-covalent interactions.

Chapter 2 deals with the study of the interaction between phosphorylated carbohydrates and AuNP **1** covered with different fluorescent probes. A selective response is observed between slightly different carbohydrates, and this process appears to involve the fluorescent probe.

Chapter 3 deals with the study of binding interactions between AuNP **1** and small molecules by means of fluorescence correlation spectroscopy (FCS), isothermal titration calorimetry (ITC), diffusion-ordered spectroscopy (DOSY) and ^{31}P-NMR. The binding interactions amongst phosphorylated carbohydrates and AuNP **1** was taken as a reference

system in order to identify the strengths and weaknesses of the techniques in detecting weak interactions. The study provided relevant information about the role of the fluorescent probe in the recognition process.

Chapter 4 introduces an approach based on the combination of AuNP **1** and peptides in order to form binding pockets for carbohydrates on the surface of AuNP **1**. An improvement of the binding affinity of phosphorylated carbohydrates for AuNP **1** is shown in the presence of peptides containing multiple Trp-residues.

Chapter 5 introduce a new approach in order to increase the signal strength generated by the interactions between phosphorylated carbohydrates and AuNP **1** covered with a fluorescence probe. The idea relies on the dephosphorylation process of phosphorylated carbohydrates performed by enzyme. Several carbohydrates were studied observing modest selectivity for the signal output.

1.5 Bibliography

1. Dashty, M., A quick look at biochemistry: Carbohydrate metabolism. *Clin. Biochem.* **2013,** *46* (15), 1339-1352.
2. D. L. Nelson, M. M. C., *Principles of Biochemistry*. Freeman: New York, 2008.
3. Candy, D. J., *Biological Functions of Carbohydrates*. Springer Netherlands: 1980; p IX, 197.
4. (a) The Information-Storing Potential of the Sugar Code. In *Glycosciences*; (b) Laine, R. A., A calculation of all possible oligosaccharide isomers both branched and linear yields 1.05 x 10(12) structures for a reducing hexasaccharide: the Isomer Barrier to development of single-method saccharide sequencing or synthesis systems. *Glycobiology* **1994,** *4* (6), 759-67; (c) Davis, A. P., Synthetic lectins. *Org. Biomol. Chem.* **2009,** *7* (18), 3629-3638.
5. (a) Alavi, A.; Axford, J. S., Sweet and sour: the impact of sugars on disease. *Rheumatology* **2008,** *47* (6), 760-770; (b) Mendez-Huergo, S. P.; Maller, S. M.; Farez, M. F.; Mariño, K.; Correale, J.; Rabinovich, G. A., Integration of lectin–glycan recognition systems and immune cell networks in CNS inflammation. *Cytokine Growth Factor Rev.* **2014,** *25* (3), 247-255; (c) Yu, L.-G., The oncofetal Thomsen–Friedenreich carbohydrate antigen in cancer progression. *Glycoconj. J.* **2007,** *24* (8), 411-420.
6. Davidson, B.; Berner, A.; Nesland, J. M.; Risberg, B.; Kristensen, G. B.; Tropé, C. G.; Bryne, M., Carbohydrate antigen expression in primary tumors, metastatic lesions, and serous effusions from patients diagnosed with epithelial ovarian carcinoma: Evidence of up-regulated Tn and Sialyl Tn antigen expression in effusions. *Hum. Pathol.* **2000,** *31* (9), 1081-1087.
7. (a) Greene, N. M., Anaesthesia and carbohydrate transport across cell membranes. *Ann R Coll Surg Engl* **1971,** *48* (2), 68-70; (b) Simmons, R. A., 43 - Cell Glucose Transport and Glucose Handling During Fetal and Neonatal Development A2 - Polin, Richard A. In *Fetal and Neonatal Physiology (Fifth Edition)*, Abman, S. H.; Rowitch, D. H.; Benitz, W. E.; Fox, W. W., Eds. Elsevier: 2017; pp 428-435.e3.
8. (a) F. A. Quiocho, Protein-carbohydrate interactions: basic molecular features. *Pure Appl. Chem.* **1989,** *61*, 1293; (b) Johnson, Q.; Lindsay, R.; Petridis, L.; Shen, T., Investigation of Carbohydrate Recognition via Computer Simulation. *Molecules* **2015,** *20* (5), 7700.
9. Miron, C. E.; Petitjean, A., Sugar Recognition: Designing Artificial Receptors for Applications in Biological Diagnostics and Imaging. *ChemBioChem* **2015,** *16* (3), 365-379.
10. Vaillant, O.; Cheikh, K. E.; Warther, D.; Brevet, D.; Maynadier, M.; Bouffard, E.; Salgues, F.; Jeanjean, A.; Puche, P.; Mazerolles, C.; Maillard, P.; Mongin, O.; Blanchard-Desce, M.; Raehm, L.; Rébillard, X.; Durand, J.-O.; Gary-Bobo, M.; Morère, A.; Garcia, M., Mannose-6-Phosphate Receptor: A Target for Theranostics of Prostate Cancer. *Angew. Chem. Int. Ed.* **2015,** *54* (20), 5952-5956.
11. Danishefsky, S. J.; Shue, Y.-K.; Chang, M. N.; Wong, C.-H., Development of Globo-H Cancer Vaccine. *Acc. Chem. Res.* **2015,** *48* (3), 643-652.
12. Wang, C.-C.; Huang, Y.-L.; Ren, C.-T.; Lin, C.-W.; Hung, J.-T.; Yu, J.-C.; Yu, A. L.; Wu, C.-Y.; Wong, C.-H., Glycan microarray of Globo H and related structures for quantitative analysis of breast cancer. *Proc. Natl. Acad. Sci.* **2008,** *105* (33), 11661-11666.
13. Sun, X.; James, T. D., Glucose Sensing in Supramolecular Chemistry. *Chem. Rev.* **2015,** *115* (15), 8001-8037.
14. Lis, N. S. H., *Lectins*. 2 ed.; Springer Netherlands: 2007.
15. Goldstein, I. J.; Hayes, C. E., The Lectins: Carbohydrate-Binding Proteins of Plants and Animals**Writing of this article was supported, in part, by a grant (AM-10171) from the National Institutes of Health. The authors are grateful for the assistance of the Editors and of Paula Kane

and Peggy Rogers in the preparation of this Chapter. In *Advances in Carbohydrate Chemistry and Biochemistry*, Tipson, R. S.; Horton, D., Eds. Academic Press: 1978; Vol. 35, pp 127-340.

16. Sharon, N.; Lis, H., The structural basis for carbohydrate recognition by lectins. *Adv Exp Med Biol* **2001,** *491*, 1-16.

17. Bundle, D. R.; Young, N. M., Carbohydrate-protein interactions in antibodies and lectins. *Curr. Opin. Struct. Biol.* **1992,** *2* (5), 666-673.

18. Lemieux, R. U., How Water Provides the Impetus for Molecular Recognition in Aqueous Solution. *Acc. Chem. Res.* **1996,** *29* (8), 373-380.

19. Spiwok, V., CH/π Interactions in Carbohydrate Recognition. *Molecules* **2017,** *22* (7), 1038.

20. Goldstein, I. J.; Murphy, L. A.; Ebisu, S., LECTINS AS CARBOHYDRATE-BINDING PROTEINS. In *Carbohydrate Chemistry–8*, Onodera, K., Ed. Pergamon: 1977; pp 1095-1103.

21. Boggs, J. M.; Wang, H.; Gao, W.; Arvanitis, D. N.; Gong, Y.; Min, W., A glycosynapse in myelin? *Glycoconj. J.* **2004,** *21* (3), 97-110.

22. Kitov, P. I.; Sadowska, J. M.; Mulvey, G.; Armstrong, G. D.; Ling, H.; Pannu, N. S.; Read, R. J.; Bundle, D. R., Shiga-like toxins are neutralized by tailored multivalent carbohydrate ligands. *Nature* **2000,** *403*, 669.

23. (a) Mathai, M.; Seok-Ki, C.; M., W. G., Polyvalent Interactions in Biological Systems: Implications for Design and Use of Multivalent Ligands and Inhibitors. *Angew. Chem. Int. Ed.* **1998,** *37* (20), 2754-2794; (b) Shinohara, Y.; Hasegawa, Y.; Kaku, H.; Shibuya, N., Elucidation of the mechanism enhancing the avidity of lectin with oligosaccharides on the solid phase surface. *Glycobiology* **1997,** *7* (8), 1201-8.

24. (a) MacKenzie, C. R.; Hirama, T.; Lee, K. K.; Altman, E.; Young, N. M., Quantitative Analysis of Bacterial Toxin Affinity and Specificity for Glycolipid Receptors by Surface Plasmon Resonance. *J. Biol. Chem.* **1997,** *272* (9), 5533-5538; (b) Kuziemko, G. M.; Stroh, M.; Stevens, R. C., Cholera Toxin Binding Affinity and Specificity for Gangliosides Determined by Surface Plasmon Resonance. *Biochemistry* **1996,** *35* (20), 6375-6384.

25. (a) Herndon, M. E.; Stipp, C. S.; Lander, A. D., Interactions of neural glycosaminoglycans and proteoglycans with protein ligands: assessment of selectivity, heterogeneity and the participation of core proteins in binding. *Glycobiology* **1999,** *9* (2), 143-55; (b) Lookene, A.; Chevreuil, O.; Østergaard, P.; Olivecrona, G., Interaction of Lipoprotein Lipase with Heparin Fragments and with Heparan Sulfate: Stoichiometry, Stabilization, and Kinetics. *Biochemistry* **1996,** *35* (37), 12155-12163; (c) Lee, M. K.; Lander, A. D., Analysis of affinity and structural selectivity in the binding of proteins to glycosaminoglycans: development of a sensitive electrophoretic approach. *Proc. Natl. Acad. Sci. U.S.A.* **1991,** *88* (7), 2768-2772.

26. Lee, Y. C.; Lee, R. T., Carbohydrate-Protein Interactions: Basis of Glycobiology. *Acc. Chem. Res.* **1995,** *28* (8), 321-327.

27. Dennis, J.; Laferte, S.; Waghorne, C.; Breitman, M.; Kerbel, R., Beta 1-6 branching of Asn-linked oligosaccharides is directly associated with metastasis. *Science* **1987,** *236* (4801), 582-585.

28. Krześlak, A.; Pomorski, L.; Gaj, Z.; Lipińska, A., Differences in glycosylation of intracellular proteins between benign and malignant thyroid neoplasms. *Cancer Lett.* **2003,** *196* (1), 101-107.

29. Sharon, N.; Lis, H., History of lectins: from hemagglutinins to biological recognition molecules. *Glycobiology* **2004,** *14* (11), 53R-62R.

30. Aoyama, Y.; Tanaka, Y.; Toi, H.; Ogoshi, H., Polar host-guest interaction. Binding of nonionic polar compounds with a resorcinol-aldehyde cyclooligomer as a lipophilic polar host. *J. Am. Chem. Soc.* **1988,** *110* (2), 634-635.

31. Bonar-Law, R. P.; Davis, A. P., Synthesis of steroidal cyclodimers from cholic acid; a molecular framework with potential for recognition and catalysis. *J. Chem. Soc. Chem. Commun.* **1989,** (15), 1050-1052.
32. Dahms, N. M.; Olson, L. J.; Kim, J.-J. P., Strategies for carbohydrate recognition by the mannose 6-phosphate receptors. *Glycobiology* **2008,** *18* (9), 664-678.
33. Sally, A.; Ulf, N.; Volker, G.; François, D., A New Family of Chiral Binaphthyl-Derived Cyclophane Receptors: Complexation of Pyranosides. *Angew Chem. Int. Ed. Engl.* **1995,** *34* (15), 1596-1600.
34. Monika, M.; Willi, S., Molecular Recognition of Carbohydrates by Artificial Receptors: Systematic Studies towards Recognition Motifs for Carbohydrates. *Chem. Eur. J.* **2001,** *7* (3), 664-670.
35. Hall, D. G., Structure, Properties, and Preparation of Boronic Acid Derivatives. Overview of Their Reactions and Applications. In *Boronic Acids*, Wiley-VCH Verlag GmbH & Co. KGaA: 2006; pp 1-99.
36. D., J. T.; Samankumara, S. K. R. A.; Seiji, S., A Glucose-Selective Molecular Fluorescence Sensor. *Angew Chem. Int. Ed. Engl.* **1994,** *33* (21), 2207-2209.
37. James, T. D., Saccharide-Selective Boronic Acid Based Photoinduced Electron Transfer (PET) Fluorescent Sensors. In *Creative Chemical Sensor Systems*, Schrader, T., Ed. Springer Berlin Heidelberg: Berlin, Heidelberg, 2007; pp 107-152.
38. (a) Cash, K. J.; Clark, H. A., Nanosensors and nanomaterials for monitoring glucose in diabetes. *Trends Mol Med* **2010,** *16* (12), 584-593; (b) Billingsley, K.; Balaconis, M. K.; Dubach, J. M.; Zhang, N.; Lim, E.; Francis, K. P.; Clark, H. A., Fluorescent Nano-Optodes for Glucose Detection. *Anal. Chem.* **2010,** *82* (9), 3707-3713.
39. Ke, C.; Destecroix, H.; Crump, M. P.; Davis, A. P., A simple and accessible synthetic lectin for glucose recognition and sensing. *Nat Chem* **2012,** *4* (9), 718-723.
40. (a) Rauschenberg, M.; Bandaru, S.; Waller, M. P.; Ravoo, B. J., Peptide-Based Carbohydrate Receptors. *Chem. Eur. J.* **2014,** *20* (10), 2770-2782; (b) Rauschenberg, M.; Bomke, S.; Karst, U.; Ravoo, B. J., Dynamic Peptides as Biomimetic Carbohydrate Receptors. *Angew. Chem. Int. Ed.* **2010,** *49* (40), 7340-7345.
41. Daniel, M.-C.; Astruc, D., Gold Nanoparticles: Assembly, Supramolecular Chemistry, Quantum-Size-Related Properties, and Applications toward Biology, Catalysis, and Nanotechnology. *Chem. Rev.* **2004,** *104* (1), 293-346.
42. Eustis, S.; El-Sayed, M. A., Why gold nanoparticles are more precious than pretty gold: Noble metal surface plasmon resonance and its enhancement of the radiative and nonradiative properties of nanocrystals of different shapes. *Chem. Soc. Rev.* **2006,** *35* (3), 209-217.
43. Shah, M.; Badwaik, V. D.; Dakshinamurthy, R., Biological Applications of Gold Nanoparticles. *J Nanosci Nanotechnol* **2014,** *14* (1), 344-362.
44. You, C.-C.; Verma, A.; Rotello, V. M., Engineering the nanoparticle-biomacromolecule interface. *Soft Matter* **2006,** *2* (3), 190-204.
45. Brust, M.; Walker, M.; Bethell, D.; Schiffrin, D. J.; Whyman, R., Synthesis of thiol-derivatised gold nanoparticles in a two-phase Liquid-Liquid system. *J. Chem. Soc. Chem. Commun.* **1994,** (7), 801-802.
46. Manea, F.; Bindoli, C.; Polizzi, S.; Lay, L.; Scrimin, P., Expeditious Synthesis of Water-Soluble, Monolayer-Protected Gold Nanoparticles of Controlled Size and Monolayer Composition. *Langmuir* **2008,** *24* (8), 4120-4124.
47. Saha, K.; Agasti, S. S.; Kim, C.; Li, X.; Rotello, V. M., Gold Nanoparticles in Chemical and Biological Sensing. *Chem. Rev.* **2012,** *112* (5), 2739-2779.

Chapter 2: Carbohydrate recognition by monolayer protected gold nanoparticles

2.1 Summary

This chapter focuses on the study of phosphorylated carbohydrate recognition by monolayer protected gold nanoparticles using fluorescence spectroscopy. Exploiting the advantages of gold nanoparticles, such as multivalency, stability in physiological conditions and photochemical properties, a nanoparticle-based recognition system was developed. The system was composed of AuNP **1**, which are gold nanoparticles (d = 1.8 ± 0.4 nm) covered with hydrophobic C9-thiols terminating with a 1,4,7-triazacyclonone (TACN)·Zn^{2+}, and different fluorescent probes assembled on the monolayer surface. A selective response to carbohydrates with subtle structural differences was observed.

2.2 Carbohydrate recognition by gold nanoparticles

Carbohydrates are present in many types of important biological systems, playing key roles in various intercellular communication events such as immune system, cell adhesion or virus infection.[1] Therefore, carbohydrate recognition and detection are very important in the fields of medicine, either related to diagnosis or therapy.[2] Nonetheless, specific receptors for carbohydrates are not easy to obtain owing to the intrinsic complexity of carbohydrates as well as the strong similarities between them. Furthermore, carbohydrate recognition requires a delicate interplay of multiple weak interactions which increases the required complexity of the receptor from a structural point of view.

Monolayer protected gold nanoparticles (AuNPs) are in principle promising scaffolds for the formation of biomolecular receptors since they present a combination of attractive features. These include their ease of preparation, stability in physiological conditions and intrinsic optoelectronic properties that can be used for signal generation.[3] Because of these features, AuNPs have been extensively used for the development of synthetic carbohydrate receptors based on covalent and/or non-covalent interactions.

For example, in 2013 Sun *et.al.* reported a colorimetric carbohydrate recognition system based on gold nanoparticles covered with a copolymer, composed of 3-(acryloyl-thioureido)phenylboronic acid along with N-isopropylacrylamide, which was able to generate a differentiated response to different carbohydrates, such as glucose, ribose, fructose, xylose, galactose and mannose, in the µM to mM range. The recognition process occurs through reversible covalent bond formation between the hydroxyl groups of the carbohydrates and boronic acid moieties present in the polymer along with multiple H-bonding interactions between urea units, avoiding the aggregation of the polymer and consequently, aggregation of the AuNPs. In contrast, in the absence of carbohydrate aggregation takes place owing the formation of hydrophobic shells around the AuNPs (Figure 1).[4] However, the system presented some limitation due to the requirement for a

pH equal to or greater than 9 in order to permit boronic ester bond formation. For this reason, the applicability of the system in medical or diagnostic fields is dramatically reduced.

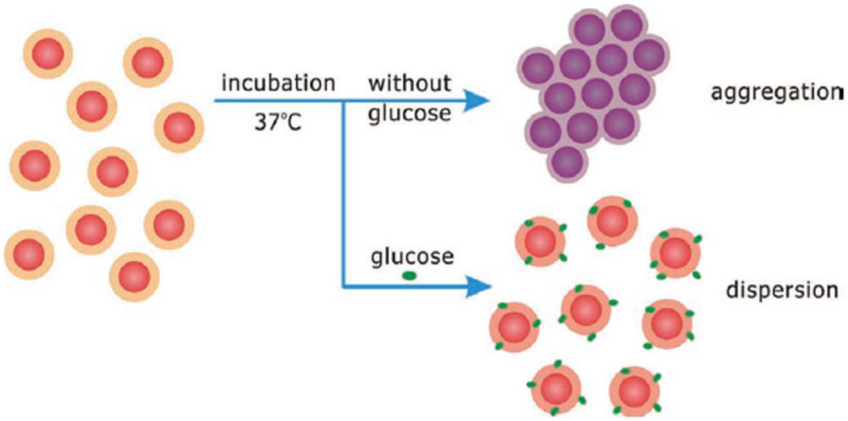

Figure 1: Working principle for colorimetric sensing of biomolecules using glucose-responsive AuNPs based on a dispersion-dominated chromogenic mechanism. The AuNPs are originally well dispersed at room temperature, but will aggregate after incubation at a higher temperature (e.g., 37 °C) due to the temperature responsiveness of the copolymer shell, inducing a significant colour change of solution from red to violet. However, when a certain amount of glucose is present, glucose molecules will interact with the copolymer. It results in a highly hydrophilic state of the polymer shell, which prevents the aggregation of AuNPs at high temperatures, and the solution will remain red.

Different alternative strategies were investigated in order to carry out carbohydrate recognition by AuNPs. In 2009, Mannino *et.al.* reported a new class of optical nanoprobes composed of electrospun polyamide meshes containing gold salts for carbohydrate sensing in water. The approach relies on the reaction of carbohydrates with these gold salts in basic media at room temperature generating AuNPs via a redox process in which the aldehyde group is oxidised while the gold salt is reduced to Au^0. This process leads to a red-colouring of the solution (Figure 2).[5] Several carbohydrates, such as galactose, glucose and fructose, had different efficiencies for gold salt reduction, which could be used as a distinguishing factor.

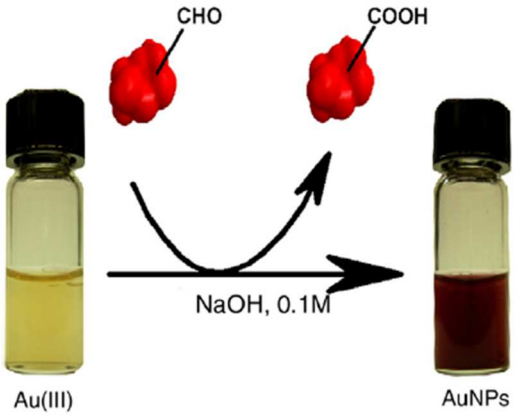

Figure 2: Reactions scheme of gold nanoparticles growth from reducing sugars.

Selective recognition of carbohydrates in aqueous media is a huge challenge. First of all, carbohydrates are hydrophilic molecules containing many hydroxyl groups and therefore they resemble the water surrounding them. The complexity further increases because of the subtle structural differences between different carbohydrates. For instance, the only difference among D-glucose and D-mannose in the configuration of a single stereocenter. Yet, in 2017 Linker and co-workers reported the binding of different carbohydrates, namely β-glucose, β-arabinose, α-galactose, α-mannose and β-maltose, to AuNPs (d = 13.4 ± 3 nm) studied by means of Surface Plasmon Resonance (SPR), X-ray photoelectron spectroscopy (XPS) and IR spectroscopy along with aggregation kinetics (Figure 3).[6] Clear differences in behaviour were observed since β-glucose caused precipitation of AuNPs on the second time scale, whereas β-arabinose required 3 h and β-maltose did not give any precipitation AuNPs even after 48 h. However, the functioning of this approach was limited to carbohydrates containing a thiol-moiety, required for interaction of the carbohydrate with the AuNPs surface.

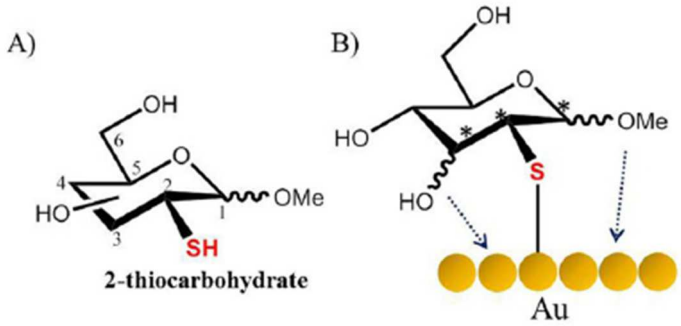

Figure 3: a) General structure of a 2-thiocarbohydrate with atom numbers. b) Possible interactions of the thiol group and the adjacent functional groups with the surface gold atoms. Asterisks indicate the three stereocenters most closely located to the surface.

We decided to develop a new class of carbohydrate receptors inspired by lectins which recognize carbohydrates exclusively using non-covalent interactions. A strategy was developed based on self-assembly processes involving AuNP **1**. Self-assembly is the spontaneous organization of molecule into ordered aggregates.[7] The driving forces are non-covalent interactions such as electrostatic interactions, hydrophobic effects, coordination bonds and hydrogen bonding. Non-covalent bond formation between the molecules makes self-assembly a reversible process, which creates a fundamental difference with structures relying on covalent bonds. AuNP **1** are gold nanoparticles covered with hydrophobic C9-thiols terminating with 1,4,7-triazacyclononane (TACN) coordinated with Zn^{2+} as head groups. Previous work in the Prins' group has shown that AuNP **1** is an attractive scaffold for the creation of multivalent supramolecular structures. AuNP **1** has been shown to catalyse chemical transformations of surface-bound molecules and to concentrate small anionic molecules on the monolayer surface.[8] Indeed, the polycationic nature of the AuNP **1** surface enhances the affinity for small negatively charged molecules, such as oligonucleotides, for instance ATP, ADP or AMP, and small peptides like Ac-Asp-Asp-Asp and $Coumarin_{343}$-Gly-Asp-Asp.[9] These kind of molecules spontaneously assembly on the AuNP **1** surface in aqueous buffer by means of a

combination of hydrophobic effects and electrostatic interactions (Figure 4). The strong interaction between AuNP **1** and small molecules could be the initial step of the development of a new class of carbohydrate receptors in water.

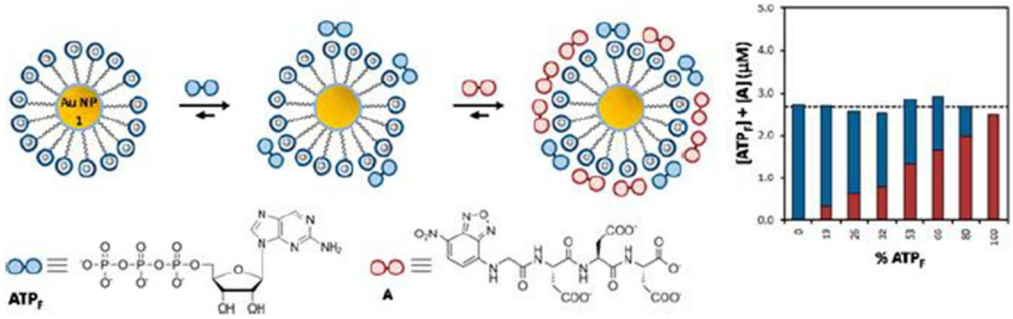

*Figure 4: Co-assembly of ATP$_F$ and peptide A on AuNP **1** leads to heterogeneous surface composition.*

2.3 Methodology for the study of carbohydrate recognition by monolayer protected gold nanoparticles

The synthesis of the starting materials and AuNP **1** were carried out following procedures described by the Prins' group.[9-10] AuNP **1** was characterized by means of ^{1}H-NMR spectroscopy, UV-Vis spectroscopy, thermogravimetric analysis (TGA), transmission electron microscopy (TEM) and dynamic light scattering (DLS) (Figure 5).

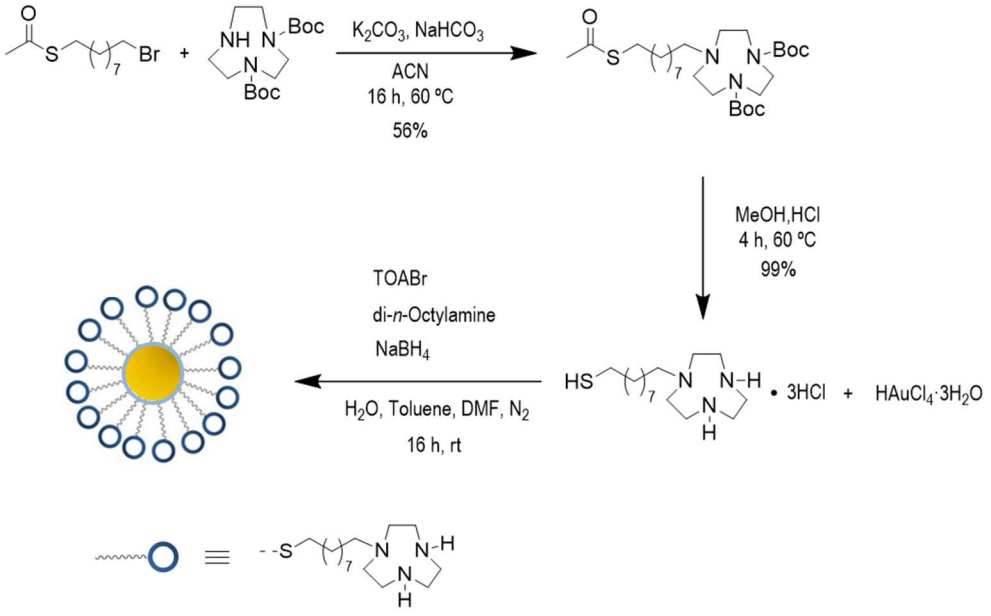

*Figure 5: Synthesis of AuNP **1** initiating from the starting materials.*

Binding interactions between AuNP **1** and small negatively charged molecules can been studied in two different ways: either by using direct fluorescence titrations – in case the molecules are fluorescent - or by means of fluorescence displacement assays – in case the molecule of interest is not fluorescent.

The affinity of a fluorescence probe for the surface of AuNP **1** can be studied by measuring the fluorescence intensity (F.I.) as a function of the amount of probe added to a solution of AuNP **1** (Figure 6). This titration relies on the capacity of gold nanoparticles to efficiently quench the fluorescence of bound fluorophores.[11] The probes are quantitatively bound to the surface up to the surface saturation concentration (SSC) if they present a high binding affinity for AuNP **1**. Once the SSC is reached, the additional amount of fluorescent compound remains free in solution and, consequently, the F.I. starts to increase linearly as a function of the amount of probe added.

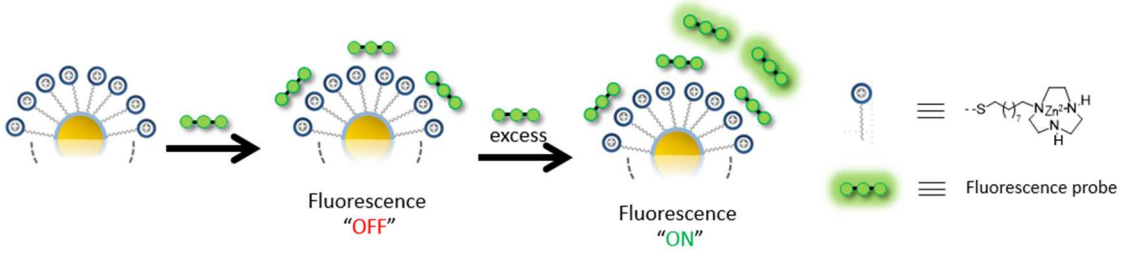

Figure 6: Schematic representation of binding assay.

On the other hand, displacement assays rely on the dynamic nature of the system, which causes the displacement of a fluorescent probe from the AuNP **1** surface upon the addition of increasing amount of a (non-fluorescent) competitor (Figure 7). The displacement can be easily monitored by measuring the F.I. of displaced fluorescent probe as a function of the concentration of added competitor. Displacement experiments of different probes by the same competitor provide information of the relative affinities of the probes for AuNP **1**.

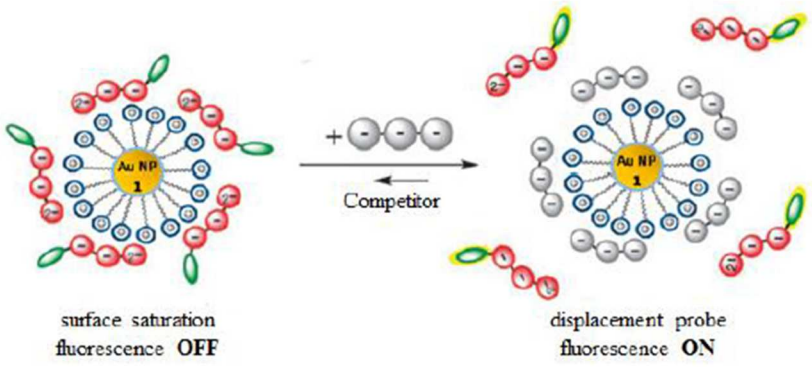

Figure 7: Schematic representation of the displacement experiments.

The displacement experiments in the presence of carbohydrates were performed working with a concentration of fluoresce probe equal to 100% of the SSC, in order to detect even a minimal amount of carbohydrate.

All the carbohydrates selected possessed a phosphate group which is negatively charged and thereby were expected to interact with the polycationic AuNP **1** surface. D-Glucose-6P, D-mannose-6P and D-galacose-6P were selected in order to study the selectivity of

AuNP **1** for carbohydrates. In addition, α-D-glucose-1P, α-D-mannose-1P and α-D-galactose-1P were selected in order to study whether the position of the phosphate group relative to the pyranose ring would make a difference. The affinity of α-D-glucose-1P and β-D-glucose-1P was compared to study the difference between anomers of the same carbohydrate. Finally, D-fructose-6P and D-fructose-1,6-bisphosphate were studied in order to determine how the number of negative charges in the carbohydrate affect to the binding affinity for AuNP **1** (Figure 8).

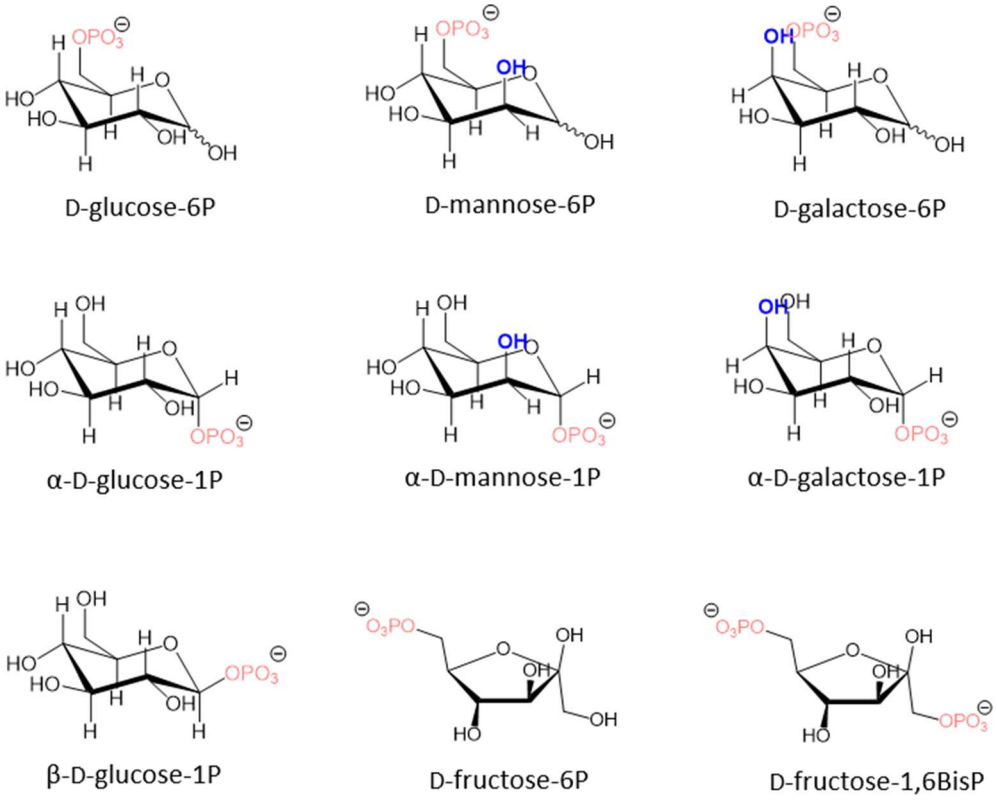

Figure 8: The selected phosphorylated carbohydrates.

The following fluorescent probes were selected for the displacement assays: Coumarin$_{343}$-Gly-Asp-Asp (Probe **A**; λ_{ex} = 450 nm, λ_{em} = 493 nm), 1-pyrenesulfonate (**MSP**; λ_{ex} = 346 nm, λ_{em} = 376 nm), 6,8-Dihydroxy-1,3-pyrene disulfonic acid (**BSP**; λ_{ex} = 407 nm, λ_{em} = 489 nm) and 2-aminopurine-riboside-5'-triphosphate (**ATP$_F$**; λ_{ex} = 305 nm, λ_{em} = 370 nm) (Figure 9).

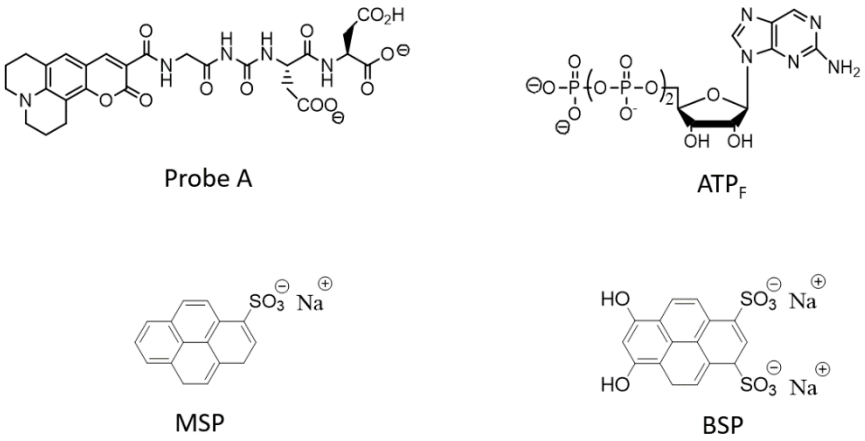

Figure 9: The selected fluorescence probes.

Probe **A** contains a fluorogenic moiety, coumarin 343, attached to tripeptide Gly-Asp-Asp, which interacts with the AuNP **1** surface mainly through electrostatic interactions. **MSP** is a monosulfonate substituted fluorogenic pyrene, whereas **BSP** is a pyrene with two sulfonate groups. ATP_F is a fluorescent analogue of ATP and possess a high affinity for AuNP **1** because of the presence of three phosphate groups.

2.4 Results and discussion

2.4.1 Carbohydrate affinity for AuNP 1

Initially, the SSCs of the fluorescence probes were determined through titration experiments adding the stock solution of the probe to a mixture of AuNP **1**, at 10 μM, in buffered water. Then, the linear part of the curve was extrapolated to F.I. = 0 to obtain the SSC.[9]

To test the working principle of the system, the interaction of D-glucose-6P with AuNP **1** was studied through displacement experiments using the four fluorescent probes. The titrations were performed up to 1 mM of carbohydrate (Figure 10a).

Comparison of the amount of probe displaced after the addition of 1 mM of carbohydrate – quantified by comparing the observed F.I. with the expected F.I. for a full displacement of probe – yielded values of 3, 6, 11 and 22% for the probes ATP_F, **A**, BSP and MSP, respectively. These values reflect the relative affinities of the probes for the surface of AuNP **1** (Figure 10b).

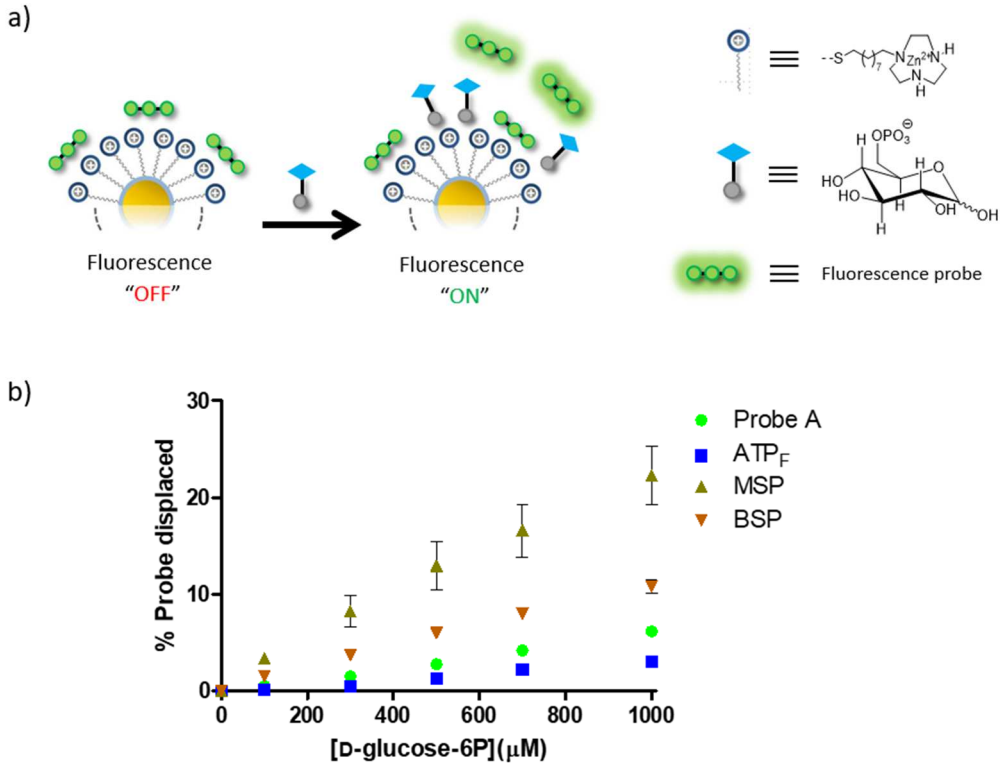

Figure 10: a) Schematic representation of displacement experiments. b) Displacement of fluorescence probes in the presence of increasing amount of D-glucose-6P. Experimental conditions: [HEPES] = 10 mM, pH 7.0, [TACN·Zn^{2+}] = 10 μM, [Probe] = 100 % SSC, 37 °C, slits = 5.0/5.0 nm. Averaged values from two independent measurements.

2.4.2 Affinity of C6-phosphorylated carbohydrates for AuNP 1

A small set of C6-phosphorylated carbohydrates, namely D-glucose-6-phosphate, D-mannose-6-phosphate and D-galactose-6-phosphate, was then studied for their capacity to induce a differentiated response (Figure 11).

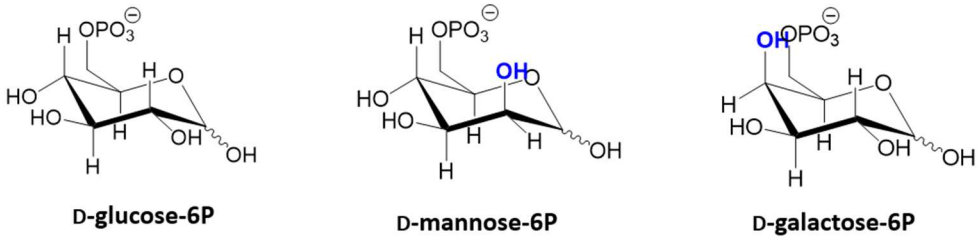

Figure 11: Studied phosphorylated carbohydrates in C6-position in which the structural difference between them is the configuration of single stereocenter.

First, the C6-phosphorylated carbohydrates were assayed using probe **A** as fluorescence probe in aqueous buffer at pH 7.0. Although the absolute observed difference between these carbohydrates is rather modest, the results nonetheless showed that the system has a minimal discriminatory capacity. Comparison of the amount of probe **A** displaced by the three carbohydrates at 1 mM (6 ± 0.5, 7 ± 0.6 and 9 ± 0.8% for D-glucose-6P, D-

mannose-6P and D-galactose-6P, respectively) revealed a slightly higher affinity of D-galactose-6P for AuNP **1**, just within the experimental error (Figure 12).

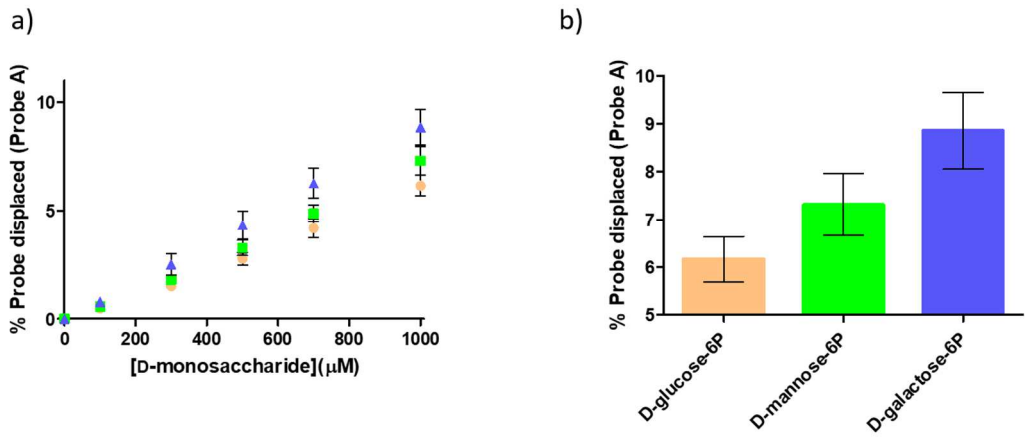

*Figure 12: a) Percentage of probe **A** displaced by phosphorylated carbohydrates in C6 position. b) Histogram of the percentage of probe **A** displaced at 1 mM concentration of carbohydrate. Experimental conditions: [HEPES] = 10 mM, pH 7.0, [TACN·Zn^{2+}] = 10 μM, [probe **A**] = 100% SSC, 37 °C, $\lambda_{ex,\ Probe\ A}$ = 450nm $\lambda_{em,\ Probe\ A}$ = 493nm slits = 5.0/5.0 nm. Averaged values from two independent measurements.*

Afterwards, the carbohydrates phosphorylated in C6 position were studied using MSP as fluorescence probe, observing displacement of 28% for D-mannose-6P and D-galactose-6P and 22% for D-glucose-6P at 1 mM concentration. The higher probe displacement was a result of the lower binding affinity of the probe for AuNP **1**. A modest discrimination was observed between glucose, having the lowest affinity, and mannose and galactose, which have the same binding affinity (Figure 13a and b).

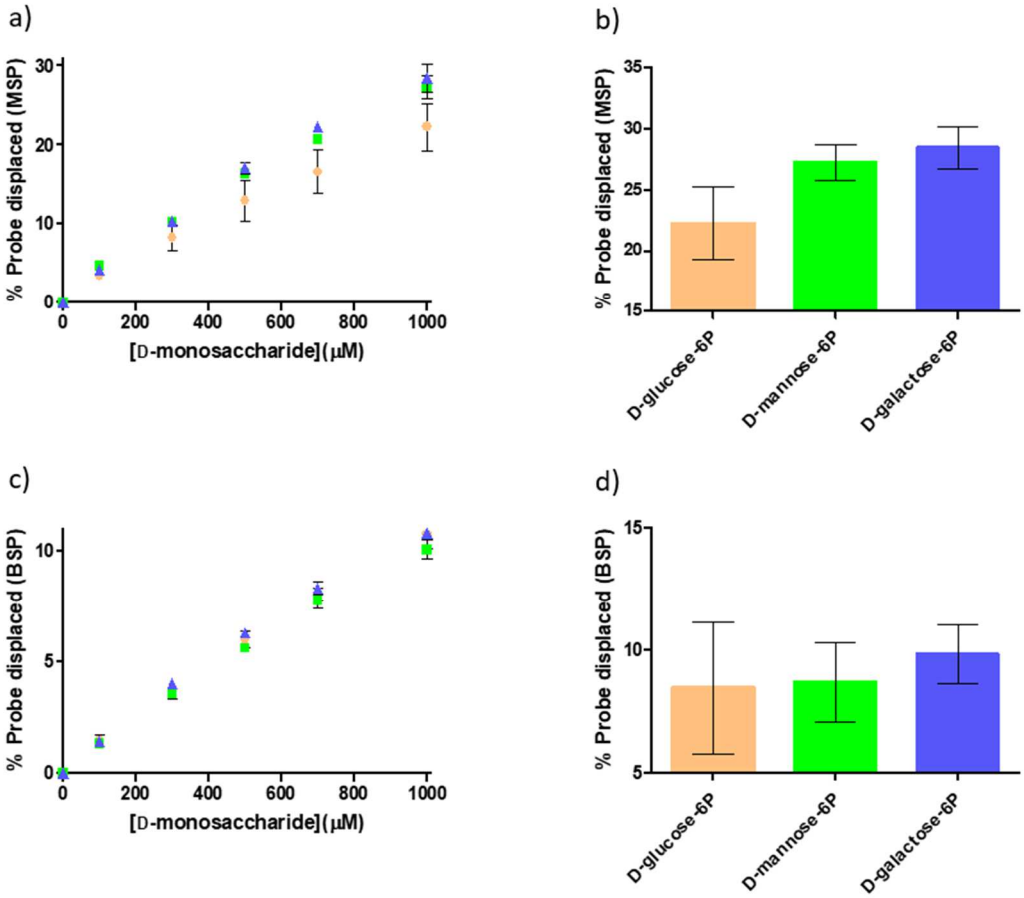

Figure 13: a) Percentage of MSP displaced by phosphorylated carbohydrates in C6 position b) Histogram of the percentage of MSP displaced at 1 mM concentration of carbohydrate c) Percentage of BSP displaced by phosphorylated carbohydrates in C6 position. d) Histogram of the percentage of BSP displaced at 1 mM concentration of carbohydrate. Experimental conditions: [HEPES] = 10 mM, pH 7.0, [TACN·Zn^{2+}] = 10 μM, [Probe] = 100% SSC, 37 °C, slits = 5.0/5.0 nm. *Averaged values from two independent measurements.*

Then, the C6-phosphorylated carbohydrates were assayed using BSP as fluorescence probe. In this case, no difference was observed for these carbohydrates, at 1 mM concentration, since just 10% of the probe was displaced in all the cases (Figure 13c and d).

The results showed that AuNP **1** coated with either one of the fluorescent probes has a very limited capacity to discriminate between the tested carbohydrates.

2.4.3 Affinity of C1-phosphorylated carbohydrates for AuNP 1

Next, the same set of carbohydrates was studied but phosphorylated in the C1. In this set, the phosphate group is closer to the pyranose ring compared to the C6-phosphorylated carbohydrates (Figure 14). It was hoped that this would increase the possibility that the different alignment of hydroxyl groups on the pyranose-ring would affect the binding affinity for AuNP **1**.

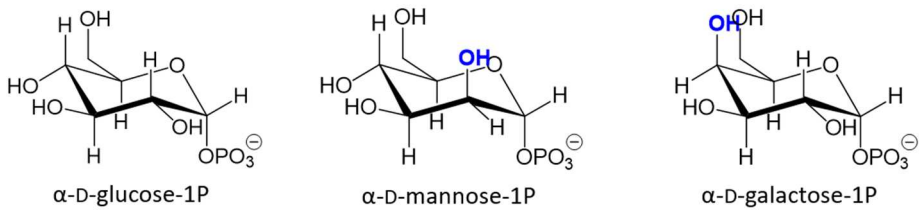

Figure 14: Set of phosphorylated carbohydrates in C1-position.

The obtained data for the three probes tested are given in Figure 15. Whereas for MSP and BSP no significant difference in displacement could be detected, an increased displacement of probe **A** was observed for α-D-glucose-1P (9 ± 0.2%) compared to α-D-mannose-1P and α-D-galactose-1P (5 ± 0.9% and 7 ± 0.5%, respectively). Although the differences are not very large, two important conclusions can be drawn from these results. First, the system AuNP **1**·**A** can discriminate between structurally very similar carbohydrates. Second, and more important, the difference is only observed for probe **A**, which suggests that the chemical structure of the probe may play a role in the recognition process.

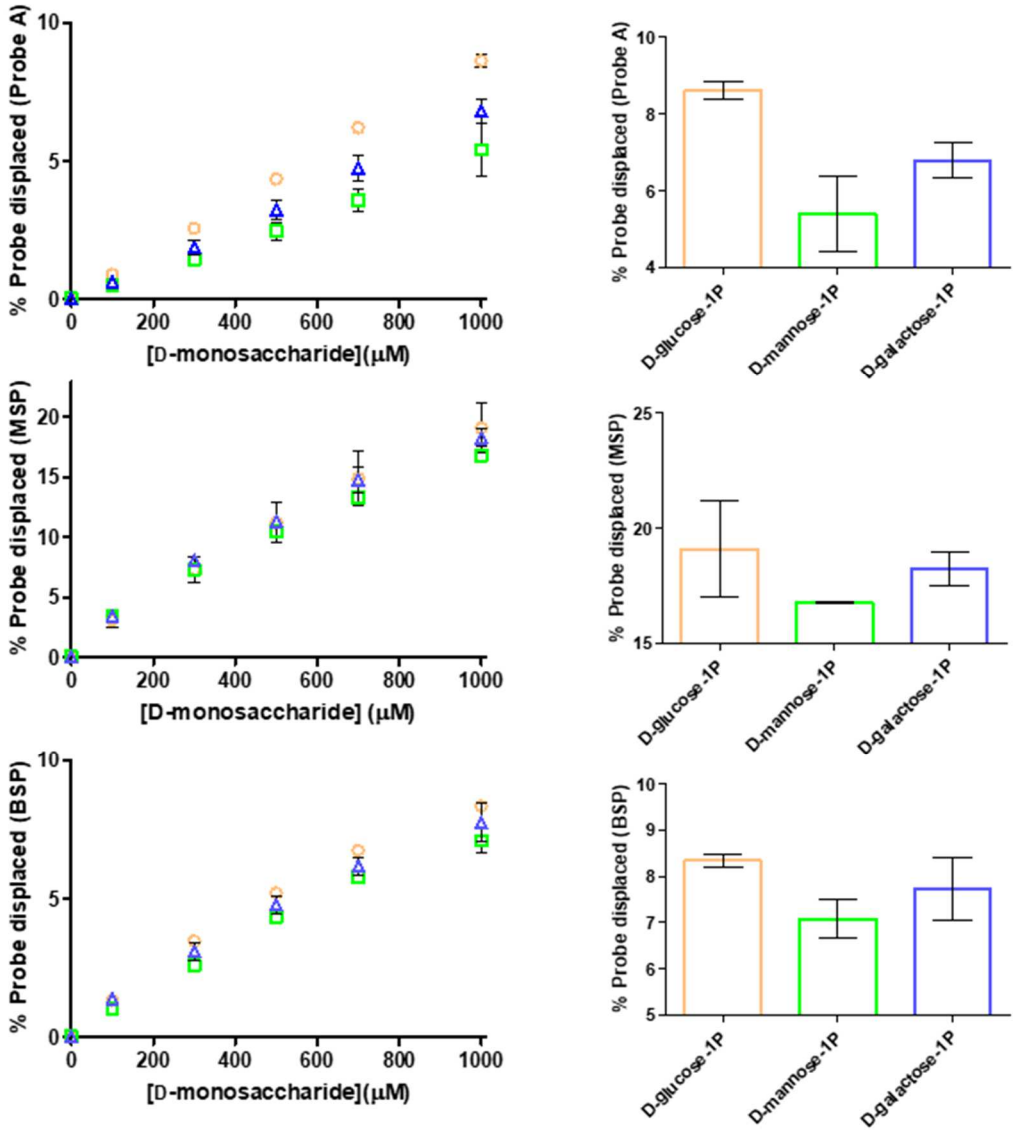

Figure 15: Percentage of fluorescence probes displaced by phosphorylated carbohydrates in C1 position along with the histogram of percentage of probe displaced at 1mM concentration of carbohydrate. Experimental conditions: [HEPES] = 10 mM, pH 7.0, [TACN·Zn^{2+}] = 10 μM, [Probe] = 100% SSC, 37 °C, slits = 5.0/5.0 nm. Averaged values from two independent measurements.

2.4.4 Carbohydrate isomer discrimination by AuNP 1

The data obtained above was then analysed to see whether AuNP **1** in combination with either one of the three probes **A**, MSP or BSP could discriminate between carbohydrates that are identical apart from the phosphorylation site (C6 *vs* C1).

For each probe studied, the obtained data were plotted for each couple α-D-glucose-1P/6P, α-D-mannose-1P/6P and α-D-galactose-1P/6P.

In order to quantify the affinity of the selected carbohydrates for AuNP **1** in this study, the amount of carbohydrate required to displace a fixed amount of probe from AuNP **1** was taken as reference. Then, for graphical reason 1/[monosaccharide] (μM) was plotted to ensure that the highest value corresponds to a major affinity of the carbohydrate for AuNP **1**.

In presence of MSP, the C6-phosphorylated carbohydrates showed 1.2, 1.9 and 1.7 times better binding affinity compared to the C1-phosphorylated carbohydrates for glucose, mannose and galactose respectively. In the case of BSP, glucose, mannose and galactose phosphorylated in C6 positions showed 1.3, 1.4 and 1.5 folds stronger binding affinity with regard to their isomers phosphorylated at C1 positions. On the other hand using probe **A**, D-mannose-6P and D-galactose-6P presented 1.2 and 1.3 times better binding affinity compared to α-D-mannose-1P and α-D-galactose-1P. However, α-D-glucose-1P showed 1.5 stronger binding affinity with regard to D-glucose-6P.

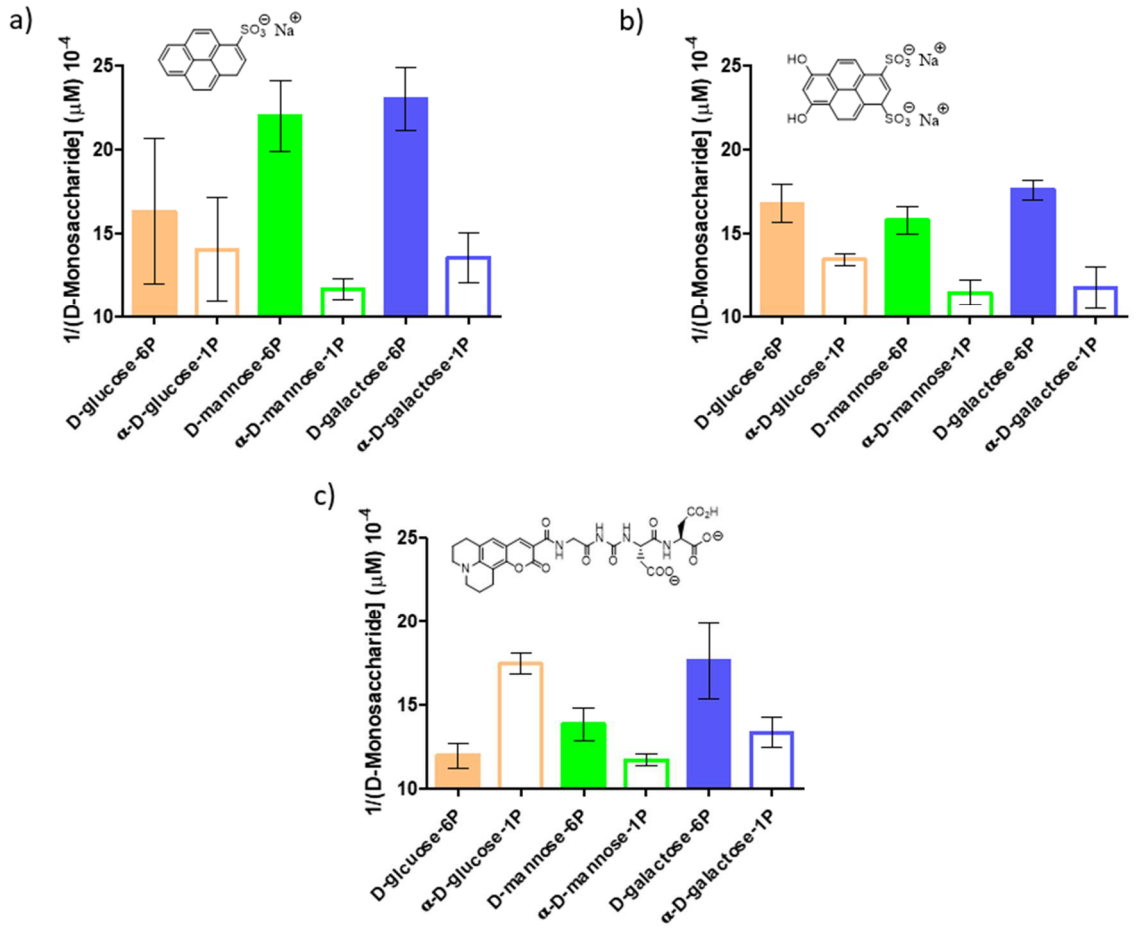

*Figure 16: a) 1/Concentration of phosphorylated isomers carbohydrates necessary in order to displace 15% of MSP. b) 1/Concentration of phosphorylated isomers carbohydrates necessary in order to displace 7% of BSP. c) 1/Concentration of phosphorylated isomers carbohydrates necessary in order to displace 5% of Probe **A**. Averaged values from two independent measurements.*

A general trend can be observed. In nearly all cases the 6P-isomer has a higher affinity compared to the 1P-isomer. This can be rationalized by the fact that the phosphate group in the C6-position is more distanced from the polar hydroxyl groups, permitting thus more efficient binding to the TACN·Zn^{2+} head groups without negative interference by the hydroxyl groups. For all couples and all probes studied the C6-isomer has a higher affinity compared to the C1-isomer with preferences ranging from 1.2-fold to 1.9-fold and from 1.3-fold to 1.7-fold (for mannose, and galactose, respectively). There is only one notable exception, which marks the most interesting observation in this study. In the presence of probe **A** – and only for this probe - the selectivity is inverted and the affinity for the C1-isomer was higher compared to the C6-isomer. The observation that the relative affinities change only for probe **A** strongly suggests that the probe plays a direct role in the carbohydrate recognition process (Figure 16).

2.4.5 Recognition of anomers of C1-phosphorylated by AuNP 1

Encouraged by the results obtained for the C1-phosphorylated carbohydrates, further studies were performed to determine the response of the system towards the α- and β-anomers of C1-phosphorylated D-glucose.

The response was measured for the three systems comprising probe **A**, MSP and BSP respectively. The results are given in Figure 17 as 1/concentration needed to displace 5% of the fluorescent probe. For MSP no reliable data could be obtained, whereas for BSP a slight selectivity in favour of the β-anomer could be detected (1.1-fold). Surprisingly, for probe **A** the selectivity was inverted and also slightly enhanced (1.3-fold) (Figure 17). It is true that the observed selectivities are relatively small, but are nonetheless significant compared to the error.

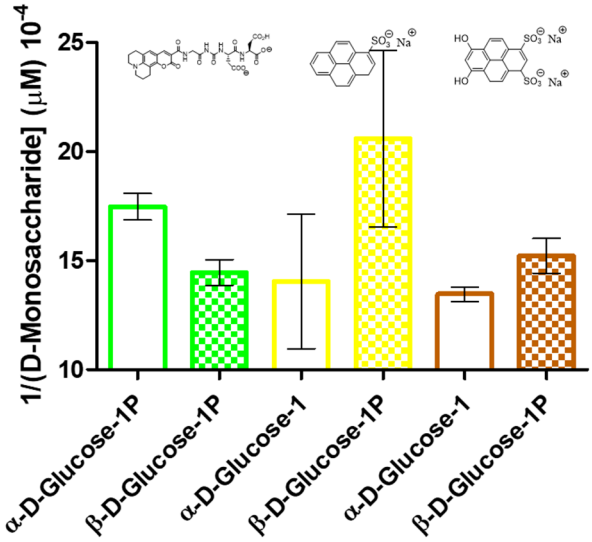

Figure 17: 1/Concentration of anomers of phosphorylated glucose in C1 necessary in order to displace fix amount of fluorescence probe. Averaged values from two independent measurements.

2.4.6 Affinity of carbohydrates with multiple phosphate groups

In order to determine how the affinity of the carbohydrates was correlated to the number of phosphate groups present in the carbohydrates, it was performed displacement studies of probe **A** by D-glucose, D-fructose-6P and D-fructose-1,6-bisP (Figure 18a).

D-Fructose-1,6-bisP displaced 90% of the probe at a 1 mM concentration while only 9% of the probe was displaced by D-fructose-6P at the same concentration (Figure 18b). The relative binding affinities of the carbohydrates were calculated as above observing that D-fructose-1,6-bisP presented 268 times better binding affinity compared to D-fructose-6P for AuNP **1**. D-Glucose showed no displacement at all in the concentration regime studied. Similar relative affinities were obtained for the probes MSP and BSP (93 times and 105 times, respectively).

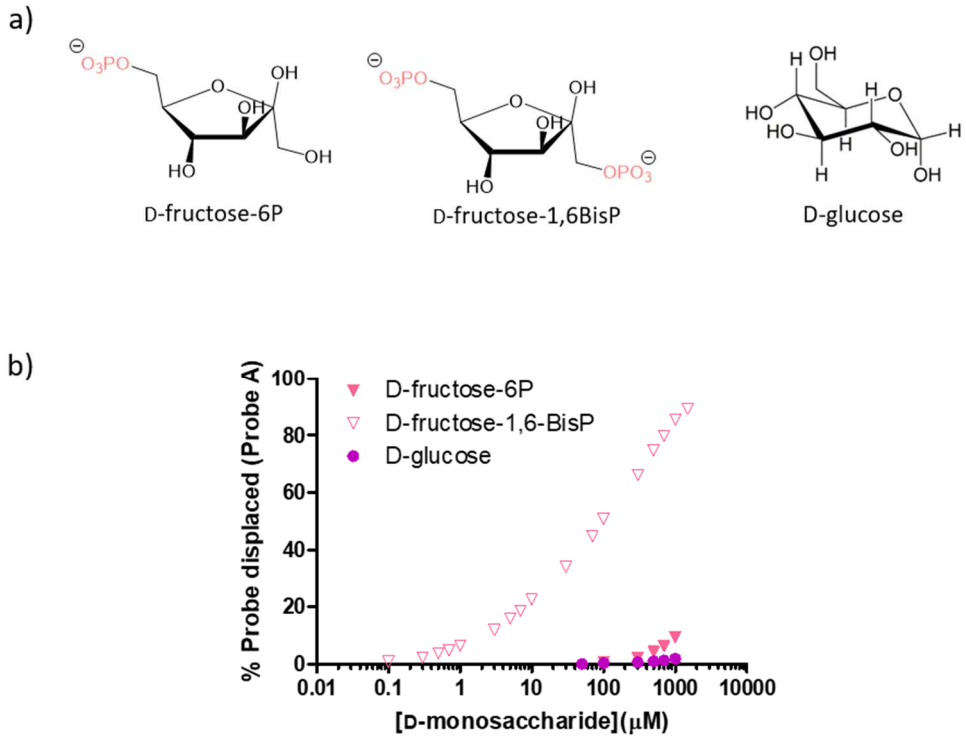

*Figure 18: a) chemical structure of the fructose with different number of phosphate groups and D-glucose. b) Percentage of fluorescence probe **A** displaced as a function of carbohydrate. Experimental conditions: [HEPES] = 10 mM, pH 7.0, [TACN·Zn^{2+}] = 10 μM, [probe **A**] = 100% SSC, 37 °C, $\lambda_{ex,\ Probe\ A}$= 450 nm $\lambda_{em,\ Probe\ A}$= 493 nm. Averaged values from two independent measurements.*

In line with previous data obtained in Prins' group, an increase in phosphate-groups in the carbohydrate – and thus an increase in negative charge – causes a significant increase in the affinity for AuNP **1**. This is important as it permits a design strategy of a sensing system relying on the formation of a high-affinity complex between a single phosphorylated carbohydrate and an additional negatively charged recognition unit. This information was used for the development of an alternative sensing system relying on dephosphorylation described in Chapter 5.

2.5 Conclusions

In conclusion, the studies of phosphorylated carbohydrates demonstrated that AuNP **1** binds phosphorylated carbohydrates. The driving force of the recognition process is the electrostatic interaction between the phosphate group of the carbohydrate and the polycationic surface of AuNP **1**. This was confirmed by the observed increase in affinity when the number of phosphate-groups was increased from 0 – 2. In the absence of phosphate groups no probe displacement was observed even at 1 mM carbohydrate concentration whereas D-fructose-1,6-bisphospahate started to displace the probe already at low μM concentrations.

The system composed of AuNP **1** covered with probe **A** showed a modest discrimination between the set of carbohydrates phosphorylated in C6 position while in the case of BSP

and MSP that discrimination was not observed. Similar results were observed for the set of carbohydrates phosphorylated in C1 position. In addition, modest selectivity was observed for C6-isomers compared to C1-isomers in presence of MSP and BSP for glucose, mannose and galactose. However, in presence of probe **A** an inversion of the selectivity was observed for glucose but it was not observed for mannose and galactose. Therefore, the system composed of AuNP **1** saturated with probe **A** is able to discriminate between epimers of carbohydrates in a discrete manner. In addition, only in presence of probe **A** the discrimination was observed. This suggests that the chemical structure of the probe could play a role in the recognition process.

Likewise, the study of the α- and β- anomers demonstrated that AuNP **1**, covered with a fluorescence probe is able to discriminate between anomers of carbohydrates. The selectivity between α/β could be modified just changing the fluorescence probe. α-Anomer showed better binding affinity for AuNP **1** compared to β-anomer in the presence of probe **A** while in the presence of BSP an opposite selectivity was observed.

These studies demonstrated that AuNP **1** may be a promising scaffold for the development of synthetic carbohydrates receptors in water.

2.6 Experimental section

2.6.1 Instrumentation

NMR Analysis

^{1}H-NMR spectra were recorded using a Bruker spectrometers operating at 300, 400 and 500 MHz for ^{1}H. Chemical shifts (δ) are reported in ppm using D_2O or $CDCl_3$ residual solvent value as internal reference.[13] Diffusion-ordered ^{1}H-NMR spectra were recorded using the "longitudinal-eddy-current-delay" (LED) pulse sequence.[14]

TEM Analysis

TEM images were recorded on a Jeol 300 PX electron microscope. One drop of sample was placed on the sample grid and the solvent was allowed to evaporate. TEM images were elaborated using the freeware software ImageJ (http://rsb.info.nih.gov/ij/).

DLS Analysis

Dynamic light scattering measurements were recorded on a Zetasizer Nano-S (Malvern, Malvern, Worcestershire, UK) equipped with a thermostatted cell holder and an Ar laser operating at 633 nm.

TGA Analysis

Thermogravimetric analysis (TGA) was run on 1-2 mg nanoparticle samples using a Q5000 IR model TA instrument from 30 to 1000 °C under a continuous air flow.

pH measurements

The pH of buffer solutions was determined at room temperature using a pH-meter Metrohm-632 equipped with a Ag/AgCl/KCl reference electrode.

UV-Vis and Fluorescence spectroscopy

UV-Vis measurements were recorded on a Varian Cary 50 spectrophotometer, while fluorescence measurements were recorded on a Varian Cary Eclipse fluorescence spectrophotometer. Both the spectrophotometers were equipped with thermostatted cell holders.

ESI-MS Analysis

ESI-MS measurements were performed on an Agilent Technologies 1100 Series LC/MSD Trap-SL spectrometer equipped with an ESI source, hexapole filter and ionic trap.

2.6.2 Materials

$Zn(NO_3)_2$ was analytical grade product. 4-(2-hydroxyethyl)-1-piperazineethanesulfonic acid (HEPES) was purchased from Sigma Aldrich and used without further purification. 2-Aminopurine riboside-5'-O-triphosphate (ATP_F) was obtained from Biolog Life Science Institute and used as received. 1-Pyrenesulfonate (MSP), 6,8-dihydroxy-1,3-pyrene disulfonic acid (BSP) were purchased from Sigma Aldrich and were used without further purifications. $Coumarin_{343}$-Gly-Asp-Asp (probe **A**) was synthesised previously in the group. D-Glucose-6-phosphate, D-mannose-6-phosphate, D-galactose-6-phosphate, α-D-mannose-1-phosphate, α-D-galactose-1-phosphate and D-fructose-1,6-bisphosphate were purchased from Sigma Aldrich. D-Fructose-6-phosphate, α-D-glucose-1-phosphate, β-D-glucose-1-phosphate were purchased from CarboSynth. In all cases, stock solutions were prepared using deionized water filtered with a milliQ-water-purifier (Millipore) and stored at 4 °C or -20 ºC.

2.6.3 Synthesis and characterization of AuNP 1

2.6.3.1 Synthesis of S-(9-bromonyl) ethanethiote[15]

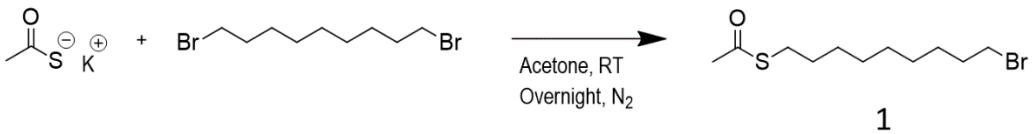

1

1,9-Dibromononane (4 mL, 19.4 mmol) was dissolved in acetone (50 mL). Potassium thioacetate was added (2.24 g, 19.22 mmol) and the resulting mixture was kept at room temperature under nitrogen overnight. The resulting suspension was then filtered and after solvent evaporation, the crude product was purified by flash chromatography (silica gel,

eluent Ether Petrolium (EP)/CH_2Cl_2: 70/30) 2.1 g (39% yield) of **1** was obtained as colourless oil.

^{1}H-NMR (δ ppm, 400 MHz, $CDCl_3$, 300K): 3.40 (t, *J* = 6.8 Hz, 2H), 2.86 (t, *J* = 7.3 Hz, 2H), 2.32 (s, 3H), 1.91 – 1.76 (m, 2H), 1.64 – 1.49 (m, 2H), 1.48 – 1.19 (m, 10H).

MS (ESI,+, MeOH): *m/z* [M(^{79}Br)+H]$^+$, 281.2 ([M(^{79}Br)+H]$^+$, cal. 281.05), *m/z* [M(^{81}Br)+H]$^+$, 283.2 ([M(^{81}Br)+H]$^+$, cal. 283.05).

2.6.3.2 Synthesis of di-tert-butyl 1,4,7-triazonane-1,4-dicarboxylate[16]

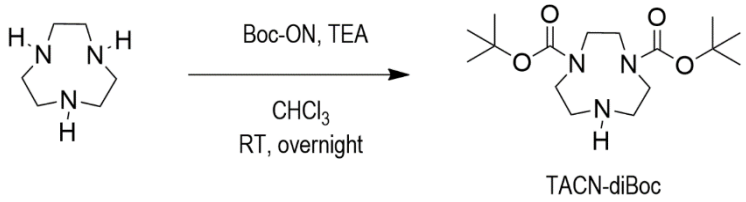

A solution of 2-(Boc-oxyimino)-2-phenylacetonitrile (3.05 g, 12.38 mmol, 2 equiv.) in anhydrous $CHCl_3$ (10.66 mL) was added with a syringe pump (1 mL/h, 15 h, rt.) to a solution of 1,4,7-triazacyclonone (800 mg, 6.19 mmol, 1 equiv.) and Et_3N (2.56 mL, 18.39 mmol, 2.97 equiv.) in $CHCl_3$ (26.68 mL). The reaction mixture was stirred for 24 h at r.t., after the addition. Then, the solvent was removed under reduced pressure. Afterwards, $CHCl_3$ was added and then it was washed with 5% aqueous Na_2CO_3 (3 x 10 mL), brine (2 x 20 mL), and 10% aqueous citric acid (3 x 10 mL). The aqueous citric acid solution was then basified with 2 M NaOH solution until pH 11 and extracted with $CHCl_3$ (3 x 20 mL). The combined organic layers were dried over $MgSO_4$ and the solvent was removed under reduced pressure. Pure compound TACN-diBoc (1.4 g, 69% yield) was obtained as pale yellow oil.

^{1}H-NMR (δ ppm, 400 MHz, $CDCl_3$, 300K): 3.55 – 3.40 (m, 4H), 3.34 – 3.16 (m, 4H), 2.98 – 2.86 (m, 4H), 1.48 (s, 18H).

Data in accordance with the literature [*J. Med. Chem. 2008, **51**, 118*].

2.6.3.3 Synthesis of di-tert-butyl 7-(9-(acetylthio)nonyl)-1,4,7-triazanone-1,4-dicarboxylate[15]

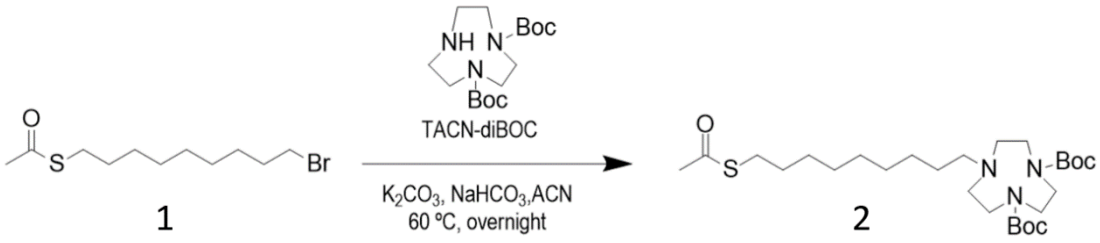

Compound **1** (151 mg, 0.536 mmol, 1.2 equiv.) and TACN-diBOC (160 mg, 0.446 mmol, 1 equiv.) were added to a suspension of K_2CO_3 (183 mg, 1.33 mmol, 2.97 equiv.) and $NaHCO_3$ (111.5 mg, 1.33 mmol, 2.97 equiv.) in ACN (4.38 mL). The suspension was stirred overnight at 60 ºC. Then, the suspension was filtered under a gooch filter and the organic layer was saved. Later on, the solvent was removed under reduced pressure and the crude product was purified by flash chromatography (silica gel, eluent: DCM/MeOH 97/3 v/v). The compound **2** (133 mg, 56% yield) was obtained such a colourless oil.

^{1}H-NMR (δ ppm, 400 MHz, $CDCl_3$, 300K): 3.51 – 3.40 (m, 4H), 3.22 (m_{br}, 4H), 2.84 (t, J = 7.3 Hz, 2H), 2.63 – 2.55 (m, 4H), 2.49 – 2.39 (m, 2H), 2.30 (s, 3H), 1.58 – 1.50 (m, 2H), 1.45 (s, 18H), 1.33 (s_{br}, 12H).

MS (ESI,+, MeOH): *m/z* $[M+H]^+$, 530.6 ($[M+H]^+$, cal. 530.35)

2.6.3.4 Synthesis of 9-(1,4,7-triazanone-1-yl)nonane-1-thiol[17]

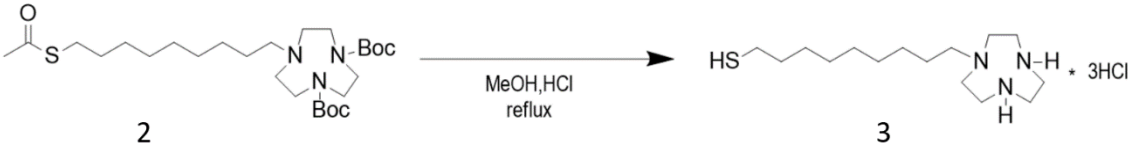

2 3

Compound **2** (48.54 mg, 91.62 µmol) was solubilized in MeOH (4.09 mL) and HCl (6 M) (4.08 mL) was added. The resulting solution was stirred for 4 hours at 60 ºC and after evaporation of the solvent under reduced pressure, the compound **3** (37.5 mg, 99% yield) was obtained as a pink solid.

^{1}H-NMR: (δ ppm, 300 MHz, $CDCl_3$, 300K): 3.42 (s, 4H), 3.24 (m, 4H), 3.09 (m, 4H), 2.74 (m, 2H), 2.28 (t, J = 7 Hz, 2H), 1.42 (m, 4H), 1.33 (s_{br}, 12H).

MS (ESI,+, H_2O): *m/z* $[M+H]^+$, 288.3 ($[M+H]^+$, cal. 287.2)

2.6.3.5 Synthesis of gold nanoparticles

$HAuCl_4 \cdot 3H_2O$ (40 mg, 0.101 mmol, 1 equiv.), weighted in a dry-box, was dissolved in H_2O (mQ, 2.53 mL). Separately, a solution of TOABr (665 mg, 1.19 mmol, 11.73 equiv.) in degassed toluene (99.16 mL) was prepared (sonication for 1h). The aqueous solution of Au(III) was extracted with the TOAbr-solution (3 x 5.9 mL) causing the transfer of $[AuCl_4]^-$ ions into the organic phase (red-orange colour). The organic phase was brought together with the remaining amount of the TOABr solution in a 250 mL round bottom flask and di-n-octylamine (1.64 mL, 5.32 mmol, 52.40 equiv.) was added (with plastic syringe). The solution was vigorously stirred for 30 minutes under N_2 atmosphere, resulting in a progressive decoloration (red, yellow, green; few minutes). Subsequently, $NaBH_4$ (17.81 mg, 0.45 mmol, 4.4 equiv.) dissolved in H_2O (mQ; 0760 mL) was added under vigorous stirring, resulting in the formation of the gold nanoparticles (brown colouring). The solution was stirred for an additional 3 h under N_2 atmosphere, after which the aqueous phase was removed with a separating funnel. Then, the deprotected the compound **3** (36 mg, 0.09 mmol, 1 equiv.) solubilized in a minimum quantity of DMF

(0.33 mL) was added quickly. The solution became colourless and after several minutes a brown precipitate was formed. The obtained suspension was stored under inert atmosphere overnight. Then, H_2O (mQ, 1.96 mL) was added and the solution was stirred during 30 minutes under N_2 atmosphere. Finally, the aqueous phase was separated and washed with diethyl ether (2 x 5.9 mL), toluene (2 x 5.9 mL), ethyl acetate (2 x 5.9 mL) and again diethyl ether (2 x 5.9 mL). The resulting dark brown aqueous phase was concentrated and passed through a Sephadex G-25 (mQ water). Finally, the collected brown fraction was concentrated and passed through a Sephadex LH-20 using MeOH.

AuNP **1** was characterized by several technique such as ^{1}H-NMR, TEM, DSL and TGA. Usually, the ^{1}H-NMR experiments using "longitudinal-eddy-current-delay" (LED) pulse sequence allows to differentiate molecules based on their diffusion coefficients. This provide a clear proof that thiols are bound to the AuNP surface (broad signals) as well as a manner to control the purity of the samples. The obtained NMR spectra without (a) and with (b) the diffusion filter showed that only minimal amounts of unbound additives were presents in the final sample (Figure 22).

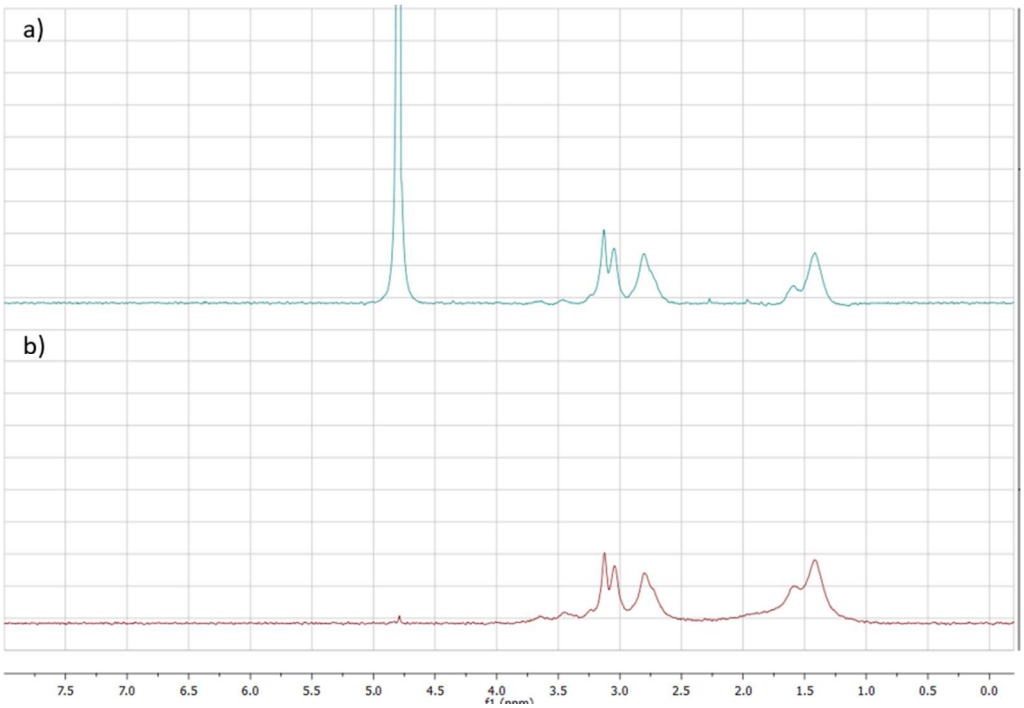

*Figure 22: ^{1}H-NMR spectra of a solution of AuNP **1** in D_2O. a) ^{1}H-NMR without the diffusion filter. b) ^{1}H-NMR with the diffusion filter.*

TEM, DSL and TGA techniques provide information about the size and morphology of functionalized gold nanoparticles. TEM analysis proved that the synthesized nanoparticles were nicely mono-dispersed, with a gold core diameter = 1.65 ± 0.36 nm (Figure 22a). The hydrodynamic radius observed by DLS was 5.6 ± 1.2 nm (Figure 22b).

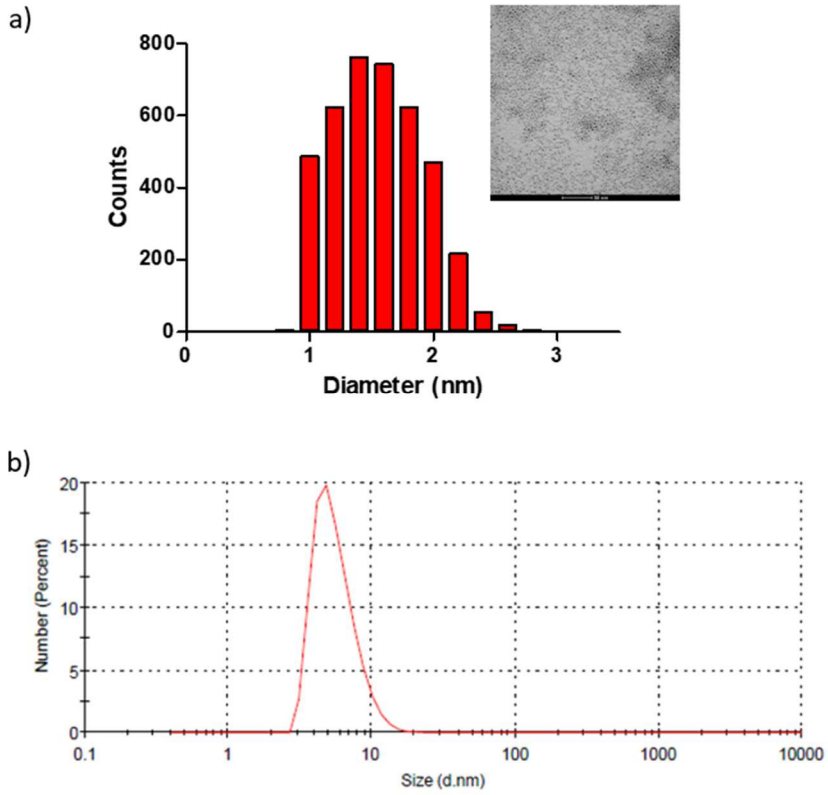

Figure 22: a) TEM image (scale bar = 20 nm) together with the corresponding ImageJ elaboration. b) DLS analysis.

Finally, the weight loss measured by means of TGA was 54% (Figure 23a). In addition, the absence of the surface plasmon resonance band at 520 nm in the UV/Vis spectrum (Figure 23b) provides additional information confirming the presence of sub 3 nm sized AuNP **1**.

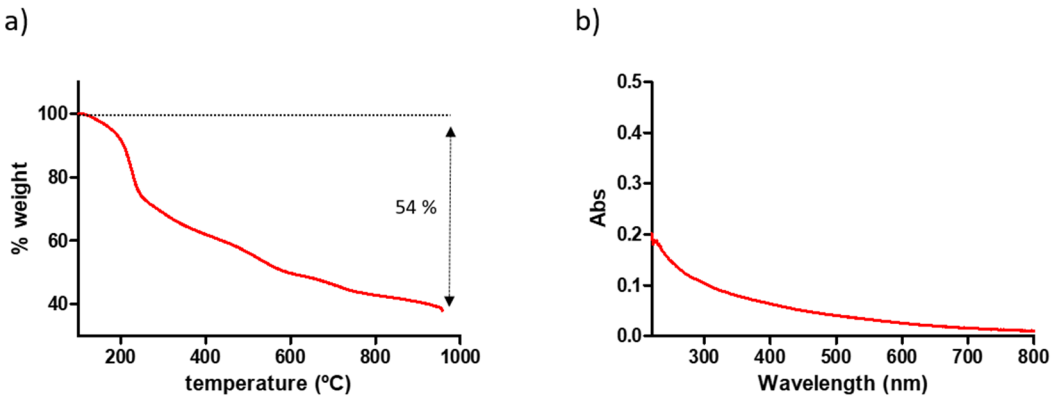

*Figure 23: a) TGA analysis b) UV/Vis absorption spectrum of AuNP **1**. Experimental conditions: [HEPES] = 10mM, pH: 7, [TACN·Zn^{2+}] = 10 μM.*

2.6.4 Determination of the stock solution concentrations

The concentration of $Zn(NO_3)_2$ solution was determined by atomic absorption spectroscopy. The concentration of the selected fluorescence probe were determined by

UV spectroscopy at pH 7.0. The concentration of phosphorylated carbohydrate solution were determined by ^{1}H-NMR using a coaxial tube along with pyrazine as internal standard how previously was reported in the group.[18] The concentration of TACN head groups was determined by kinetic titration using $Zn(NO_3)_2$.[19]

Probe	Molar extinction coefficient (M^{-1} cm^{-1}) pH:7.0	Wavelength (nm)
probe **A**	45000	450
ATP_F	8000	243
MSP	27700	346
BSP	16300	408

2.6.4.1 Determination of concentration of head groups of AuNP 1

In order to obtain a quick estimation of the head group concentration, a titration of the mother solution of AuNP **1** was performed in the presence of 2.5 µM of 2-aminopurine riboside-5'-O-triphosphate (ATP_F). An increasing amount of the stock solution was added to a solution of [ATP_F] = 2.5 µM dissolved in [HEPES] = 10 mM at pH: 7.0. Once the addition of a volume of stock solution leading to a 10 µM concentration of head group in the cuvette, the fluorescence is totally quenched (Figure 24).

In this example after the addition of 12 µL of the AuNP **1** solution the fluorescence was quenched. As the saturation concentration of ATP_F at this pH is around 2.5 µM for 10 µM of TACN that means [headgroup] = $\frac{1*10^{-3}(Vol.cubet)L\ x\ 10*10^{-6}(Vol.\ Zn(NO3)2)M}{12*10^{-6}(Vol\ AuNP\ add)L}$*10^3 = 0.83 mM. Usually this approach leads to the obtainment of a value slightly lower than the one obtained by the zinc titration (20% lower).[9]

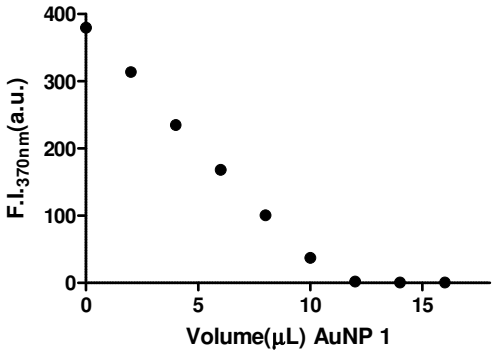

*Figure 24: AuNP **1** titration in the presence of ATP_F.*

2.6.5 Surface Saturation Concentration

The fluorescence titration were performed by adding consecutive amounts of a stock solution of fluorescence probe in milliQ water to a 1 mL buffered aqueous solution ([HEPES] = 10 mM, pH 7.0) containing a [AuNP **1**] = 10 µM, in terms of head group, at

37 or 25 ºC. Then, the fluorescence intensity is plotted as function of the concentration of probe (Figure 25).

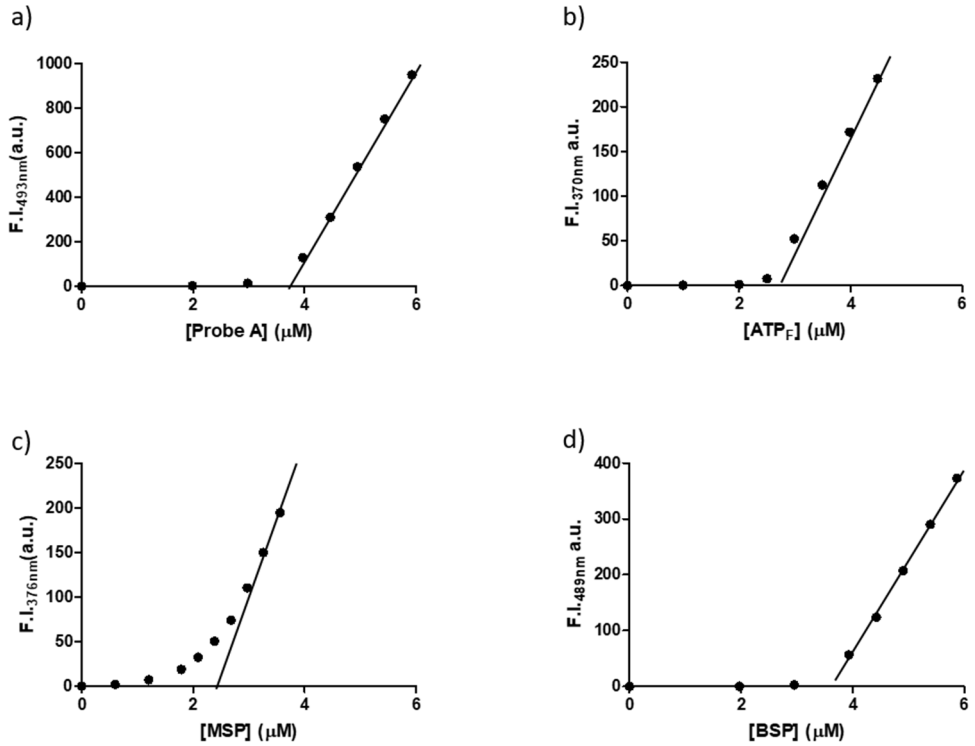

*Figure 25: Fluorescence intensity as a function of the amount of fluorescence probe add to a solution of AuNP **1**. Experimental conditions: a) [HEPES] = 10 mM, pH 7.0, [TACN·Zn^{2+}] = 10 μM, 37 ºC, $\lambda_{ex,\ Probe\ A}$= 450 nm $\lambda_{em,\ ProbeA}$= 493 nm slits = 5.0/5.0 nm. b) [HEPES] = 10 mM, pH 7.0, [TACN·Zn^{2+}] = 10 μM, 37 ºC, $\lambda_{ex,\ ATPF}$= 305 nm $\lambda_{em,\ ATPF}$= 370 nm slits = 5.0/5.0 nm. c) [HEPES] = 10 mM, pH 7.0, [TACN·Zn^{2+}] = 10 μM, 37 ºC, $\lambda_{ex,\ MSP}$= 346 nm $\lambda_{em,\ MSP}$= 376 nm slits = 5.0/5.0 nm. d) [[HEPES] = 10 mM, pH 7.0, [TACN·Zn^{2+}] = 10 μM, [BSP] = 4.13 μM, 37 ºC, $\lambda_{ex,\ BSP}$= 407 nm $\lambda_{em,\ BSP}$= 489 nm slits = 5.0/5.0 nm.*

The Surface Saturation Concentration (SSC) was determined by the extrapolation of the linear part of the curve, in which the fluorescence intensity increased linearly as a function of the amount of probe ($y = mx + q$). Since in the absence of binding the hypothetical increase in fluorescence would be $y = mx$, it follows that the amount of probe bound to the surface correspond to $x = -q/m$ (Table 1).

Fluorescence probe	SSC value (μM)
Probe **A**	3.60
ATP_F	2.55
MSP	2.20
BSP	3.69

*Table 1: SSC values obtained from the titration of the probe to AuNP **1** solution at pH 7. Experimental conditions: a) [HEPES] = 10 mM, pH 7.0, [TACN·Zn^{2+}] = 10 μM, 37 ºC, $\lambda_{ex,\ Probe\ A}$= 450 nm $\lambda_{em,\ ProbeA}$= 493 nm slits = 5.0/5.0 nm. b) [HEPES] = 10 mM, pH 7.0, [TACN·Zn^{2+}] = 10 μM, 37 ºC, $\lambda_{ex,\ ATPF}$= 305 nm $\lambda_{em,\ ATPF}$= 370 nm slits = 5.0/5.0 nm. c) [HEPES] = 10 mM, pH 7.0, [TACN·Zn^{2+}] = 10 μM, 37 ºC, $\lambda_{ex,\ MSP}$= 346 nm $\lambda_{em,\ MSP}$= 376 nm slits = 5.0/5.0 nm. d) [[HEPES] = 10 mM, pH 7.0, [TACN·Zn^{2+}] = 10 μM, [BSP] = 4.13 μM, 37 ºC, $\lambda_{ex,\ BSP}$= 407 nm $\lambda_{em,\ BSP}$= 489 nm slits = 5.0/5.0 nm.*

In order to avoid any kinetic problems, the first fluorescence titration with a new probe were always performed by following the evolution of the F.I. after each addition of the probe (between 8 and 10 minutes between each additions).

The slope of the linear part of the SSC curve allows an estimation of F.I. in function of the concentration of the free probe in solution of the AuNP **1**. This value can be used in order to verify the maximum of F.I. that should be expected for a full displacement of the probe from the AuNP **1** surface in a displacement experiment in presence of the competitor.

2.6.6 Displacement experiments

The displacement experiments were performed by adding consecutive amount of a stock solution of phosphorylated carbohydrate in milliQ water to a 1 mL aqueous solution ([HEPES] = 10 mM , pH 7.0) containing the AuNP **1** coated with the fluorescence probe at 100% of the surface saturation concentration at 37 ºC.

At the end of the displacement, it was verified that the maximum value was close to the value obtained by the extrapolation of the linear part of the titration curve (see above). Then this value was used to normalize the F.I. and to plot the percentage of probe displaced in function of the concentration of the competitor. However it was not possible to observe a full displacement of the probe, in almost all the cases. Therefore, it was assumed that the maximum value of F.I. was the value obtained from the intercept value of the equation obtained from the SSC experiment ($y = mx + \boldsymbol{q}$).

To ensure that a stable signal was obtained, the displacement studies were performed by measuring the fluorescence intensity in time after each addition until a constant value was observed.

2.7 Bibliography

1. Zeng, X.; Andrade, C. S.; Oliveira, M. L.; Sun, X.-L., Carbohydrate–protein interactions and their biosensing applications. *Anal. Bioanal. Chem.* **2012,** *402* (10), 3161-3176.
2. Wang, S.-K.; Cheng, C.-M., Glycan-based diagnostic devices: current progress, challenges and perspectives. *Chem. Commun.* **2015,** *51* (94), 16750-16762.
3. Pezzato, C.; Maiti, S.; Chen, J. L. Y.; Cazzolaro, A.; Gobbo, C.; Prins, L. J., Monolayer protected gold nanoparticles with metal-ion binding sites: functional systems for chemosensing applications. *Chem. Commun.* **2015,** *51* (49), 9922-9931.
4. Mingxi, Z.; Guangyan, Q.; Chenling, X.; Ran, C.; Dai-Wen, P.; Taolei, S., Dual-Responsive Gold Nanoparticles for Colorimetric Recognition and Testing of Carbohydrates with a Dispersion-Dominated Chromogenic Process. *Adv. Mater.* **2013,** *25* (5), 749-754.
5. Matteo, S.; Alessandra, A.; Saverio, M., Optical nanoprobes based on gold nanoparticles for sugar sensing. *Nanotechnology* **2009,** *20* (13), 135501.
6. Fudickar, W.; Pavashe, P.; Linker, T., Thiocarbohydrates on Gold Nanoparticles: Strong Influence of Stereocenters on Binding Affinity and Interparticle Forces. *Chem. Eur. J.* **2017,** *23* (36), 8685-8693.
7. (a) Whitesides, G.; Mathias, J.; Seto, C., Molecular self-assembly and nanochemistry: a chemical strategy for the synthesis of nanostructures. *Science* **1991,** *254* (5036), 1312-1319; (b) Whitesides, G. M.; Grzybowski, B., Self-Assembly at All Scales. *Science* **2002,** *295* (5564), 2418-2421.
8. Prins, L. J., Emergence of Complex Chemistry on an Organic Monolayer. *Acc. Chem. Res.* **2015,** *48* (7), 1920-1928.
9. Pieters, G.; Cazzolaro, A.; Bonomi, R.; Prins, L. J., Self-assembly and selective exchange of oligoanions on the surface of monolayer protected Au nanoparticles in water. *Chem. Commun.* **2012,** *48* (13), 1916-1918.
10. Zaupa, G.; Mora, C.; Bonomi, R.; Prins, L. J.; Scrimin, P., Catalytic Self-Assembled Monolayers on Au Nanoparticles: The Source of Catalysis of a Transphosphorylation Reaction. *Chem. Eur. J.* **2011,** *17* (17), 4879-4889.
11. Sapsford, K. E.; Berti, L.; Medintz, I. L., Materials for Fluorescence Resonance Energy Transfer Analysis: Beyond Traditional Donor–Acceptor Combinations. *Angew. Chem. Int. Ed.* **2006,** *45* (28), 4562-4589.
12. Klein, E.; Crump, M. P.; Davis, A. P., Carbohydrate Recognition in Water by a Tricyclic Polyamide Receptor. *Angew. Chem. Int. Ed.* **2004,** *44* (2), 298-302.
13. Gottlieb, H. E.; Kotlyar, V.; Nudelman, A., NMR Chemical Shifts of Common Laboratory Solvents as Trace Impurities. *J. Org. Chem.* **1997,** *62* (21), 7512-7515.
14. Wu, D. H.; Chen, A. D.; Johnson, C. S., An Improved Diffusion-Ordered Spectroscopy Experiment Incorporating Bipolar-Gradient Pulses. *J. Magn. Reson. A* **1995,** *115* (2), 260-264.
15. Zaramella, D.; Scrimin, P.; Prins, L. J., Self-Assembly of a Catalytic Multivalent Peptide–Nanoparticle Complex. *J. Am. Chem. Soc.* **2012,** *134* (20), 8396-8399.
16. Diez-Castellnou, M.; Mancin, F.; Scrimin, P., Efficient Phosphodiester Cleaving Nanozymes Resulting from Multivalency and Local Medium Polarity Control. *J. Am. Chem. Soc.* **2014,** *136* (4), 1158-1161.
17. Pieters, G.; Pezzato, C.; Prins, L. J., Reversible Control over the Valency of a Nanoparticle-Based Supramolecular System. *J. Am. Chem. Soc.* **2012,** *134* (37), 15289-15292.
18. Neri, S.; Pinalli, R.; Dalcanale, E.; Prins, L. J., Orthogonal Sensing of Small Molecules Using a Modular Nanoparticle-Based Assay. *ChemNanoMat* **2016,** *2* (6), 489-493.

19. Bonomi, R.; Cazzolaro, A.; Sansone, A.; Scrimin, P.; Prins, L. J., Detection of Enzyme Activity through Catalytic Signal Amplification with Functionalized Gold Nanoparticles. *Angew. Chem. Int. Ed.* **2011,** *50* (10), 2307-2312.

Chapter 3: Analytical techniques for studying recognition processes on 3D monolayers

3.1 Summary

As observed in the previous chapter, interesting recognition phenomena may take place between AuNPs and carbohydrates which involve not only the head groups and the target, but also additional molecules. Elucidation of the role of these additives requires the use of analytical techniques that permit the binding interaction between the AuNP **1** and small molecules to be studied directly. The aim of this Chapter is to identify the strengths and weaknesses of different techniques. The interaction between phosphorylated carbohydrates and AuNP **1** is used as an ideal system to probe the pros and cons of each technique, because of the relatively weak affinities and the subtle changes between different carbohydrates. The availability of other techniques that would provide information on the carbohydrate affinities also in the absence of fluorescence probe could affirm the role of the fluorescent probe in creating binding sites. The analytical techniques that will be explored are fluorescence correlation spectroscopy (FCS), isothermal calorimetry (ITC), Diffusion-Ordered Spectroscopy (DOSY), and ^{31}P-NMR.

3.2 Results and discussion

3.2.1 Fluorescence Correlation Spectroscopy

3.2.1.1 Introduction

Fluorescence correlation spectroscopy (FCS) employs correlation analysis of temporal fluctuations of fluorescence intensity to yield an autocorrelation curve from which the number of molecules, rates of diffusion, convection or chemical reactions can be extracted. FCS is a highly sensitive analytical tool that yields information about a very small number of molecules, even down to the single-molecule level, both in solution and in complex biological environments like cells.[1]

The high sensitivity of FCS was exploited to study more in detail the interaction between AuNP **1** and phosphorylated carbohydrates (Figure 1).

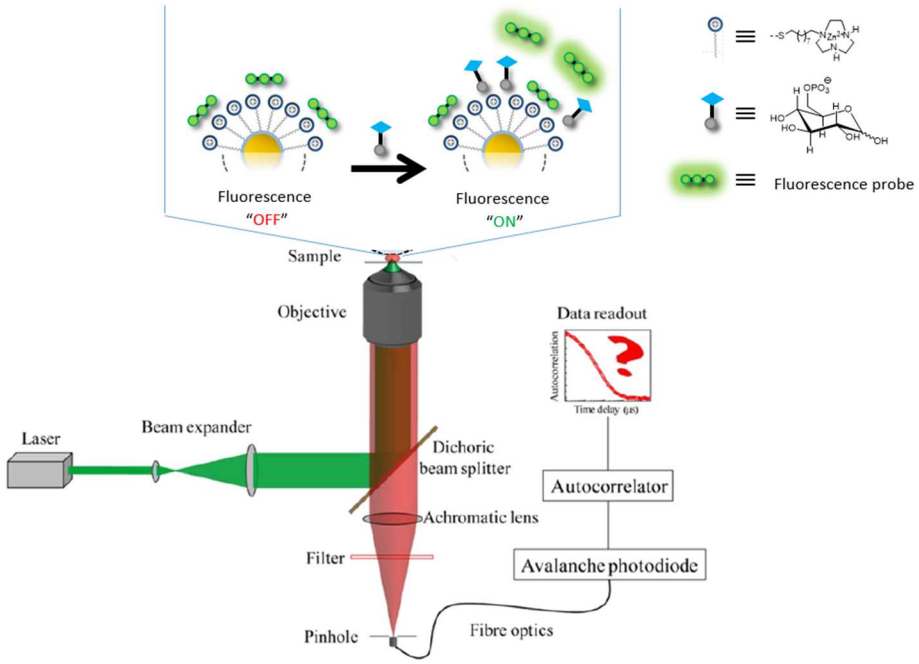

Figure 1: Schematic representation of displacement experiment by means of FCS technique.

3.2.1.2 Determination of Surface Saturation Concentration

The high sensitivity of the technique did not allow us to work under the same concentrations as used during the experiments described in Chapter 2. The SSC was determined adding consecutive amount of a stock solution of probe **A** to an aqueous buffered solution containing AuNP **1** at room temperature. After each addition the recorded fluctuations of fluorescence intensity were processed to give the corresponding autocorrelation function G(t) (Figure 2a). The local concentration of fluorescence probe molecules were determined from the amplitude G(0) of the autocorrelation curve (Equation 1)

$$\text{Equation 1: } G(0) = \frac{1}{N} = \frac{1}{Veff*C} \rightarrow N = Veff * C = \frac{1}{G(0)} \text{ α [Probe A]}_{\text{Free}}$$

Consequently, the concentration of free probe **A** (nm = 1/G(0) * 10) was then plotted against the total concentration (Figure 2b).

After additions of 0.2 μM and 0.4 μM, it was possible to detect a low and constant level of free probe **A**, which is consistent with an efficient quenching of its fluorescence by AuNP **1**. Afterwards, the titration was continued up to 1.2 μM observing that the concentrations of free probe **A** increased exponentially. This shows that FCS is in principle suitable for performing competition experiments. It is noted that the obtained SSC values (700 μM for a head group concentration of 10 μM) were significantly lower compared to the value obtained previously with regular fluorescence spectroscopy. This is a result of the much higher sensitivity of FCS, which causes saturation of the detector even at very low concentrations of probe **A**.

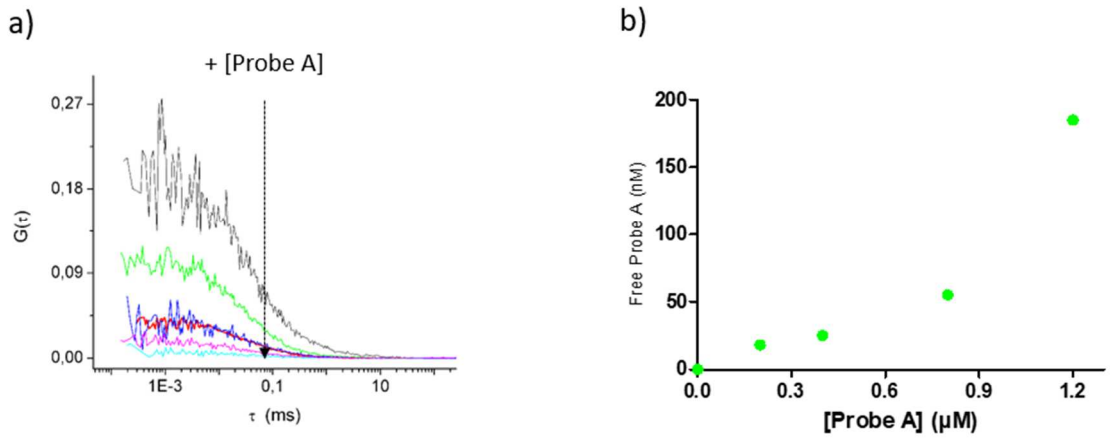

*Figure 2: a) Autocorrelation curves obtained after consecutive addition of probe **A** into a buffered solution containing AuNP **1**. The decrease in autocorrelation curve amplitude shows that the concentration of free probe **A** increases with its addition. b) Extrapolated concentrations of free probe **A**. Experimental conditions: [HEPES] = 10 mM, pH 7.0, [TACN·Zn^{2+}] = 10 µM, [probe **A**] = 100% SSC, r.t.*

3.2.1.3 Study of the selectivity of AuNP 1 for C6-phosphorylated carbohydrates

Once the experimental conditions were determined, the study of phosphorylated carbohydrate recognition by monolayer protected gold nanoparticles was performed through displacement experiments. A stock solution of the selected carbohydrate was added to an aqueous buffered solution of AuNP **1** saturated with probe **A** at room temperature. After each addition the recorded fluctuations of fluorescence intensity were processed to give the corresponding autocorrelation function G(t). The local concentration of fluorescence probe molecules, displaced from the AuNP **1** by the phosphorylated carbohydrate, were determined from the amplitude G(0) of the autocorrelation curve (Equation 1). Consequently, the concentration of free probe **A** (nm = 1/G(0) * 10) was determined and then normalized, taking as a reference the maximum concentration of free probe **A** in solution.

D-Glucose-6P, D-mannose-6P and D-galactose-6P were tested. Although in all cases the interaction between phosphorylated carbohydrate and AuNP **1** could be confirmed by an observed increase in fluorescence, it was immediately clear from these measurements that the error margins were far too large to detect a possible selective interaction with AuNP **1** (Figure 3). Based on these results it was concluded that FCS is not a suitable technique for studying accurately the relative affinities of carbohydrates for AuNP **1**.

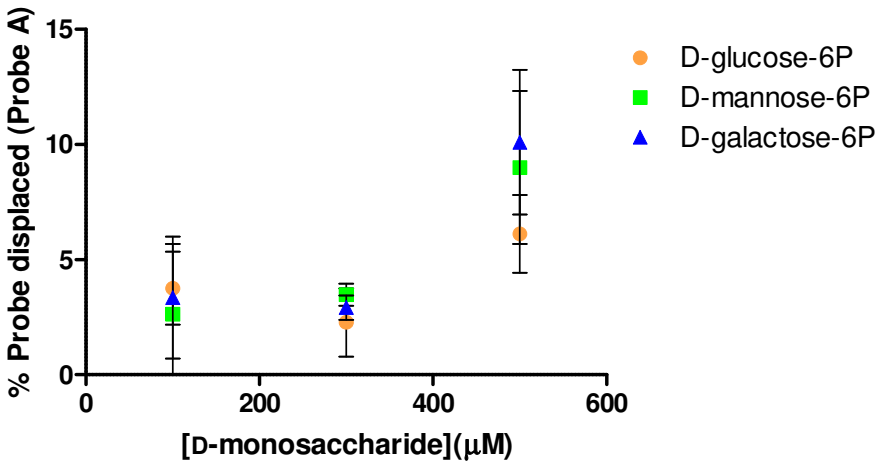

*Figure 3: Percentage of probe **A** displaced by phosphorylated carbohydrates in C6 position. Experimental conditions: [HEPES] = 10 mM, pH 7.0, [TACN·Zn^{2+}] = 10 μM, [probe **A**] = 100% SSC, r.t. Averaged values from two independent measurements.*

3.2.2 Isothermal Titration Calorimetry

3.2.2.1 Introduction

Isothermal titration calorimetry (ITC) is a technique developed during the 1960's to study chemical reactions.[2] Since then, the technique has been continuously improved in terms of sensitivity. During the 1980's, the sensitivity of the technique reached the μJ range, which enabled the first studies in biology, biochemistry and physical chemistry.[3] Nowadays the technique is commonly used to study in detail the interactions between proteins and other proteins, small molecules, metal ions, lipids, nucleic acids and carbohydrates. The strength of ITC is that a single experiment provides information about the binding affinity, stoichiometry, entropy and enthalpy of the binding process.[4]

An isothermal titration calorimeter is composed of an adiabatic shield containing two cells (reference and sample cells), which are connected to the outside through access tubes. The sample cell is loaded with the solution of the desired compound while the reference cell is usually filled with the solvent, generally water, used for the analysis at fix temperature for both cells. The substrate solution is titrated to the sample cell, through a syringe, provoking a temperature fluctuation. This creates a difference of temperature between the cells which is measured by thermoelectric device. Through a "cell feedback network" the calorimeter keeps the difference between the cells at zero by adding or subtracting heat.[5]

ITC can be considered a universal technique for measuring complex formation, since almost all molecular recognition processes are accompanied by a change in enthalpy. A measure of the heat released to the surroundings (for an exothermic process) or heat absorbed from the surroundings (for an endothermic process) is related to the amount of

formed complex. For a simple 1:1 binding model this relation is given by $Q = \Delta H_{HG}V[HG]$ in which Q (J) is the measured heat, ΔH_{HG} (J/mol) is the change in enthalphy for quantitative complex formation, and V (L) is the volume of the cell.

Unlike optical methods, calorimetric measurements can be performed with reactants that are spectroscopically silent (a fluorogenic or chromogenic tag is not necessary), can be done on opaque, turbid or heterogeneous solutions (for instance protein suspensions), and can be performed over a range of biologically relevant conditions (pH, temperature, ion strength, etc).[6] Obviously, the only condition is that the free energy of the reaction (ΔG) contains an enthalpy component (ΔH). This excludes the study of complexes that are entirely entropy-driven.

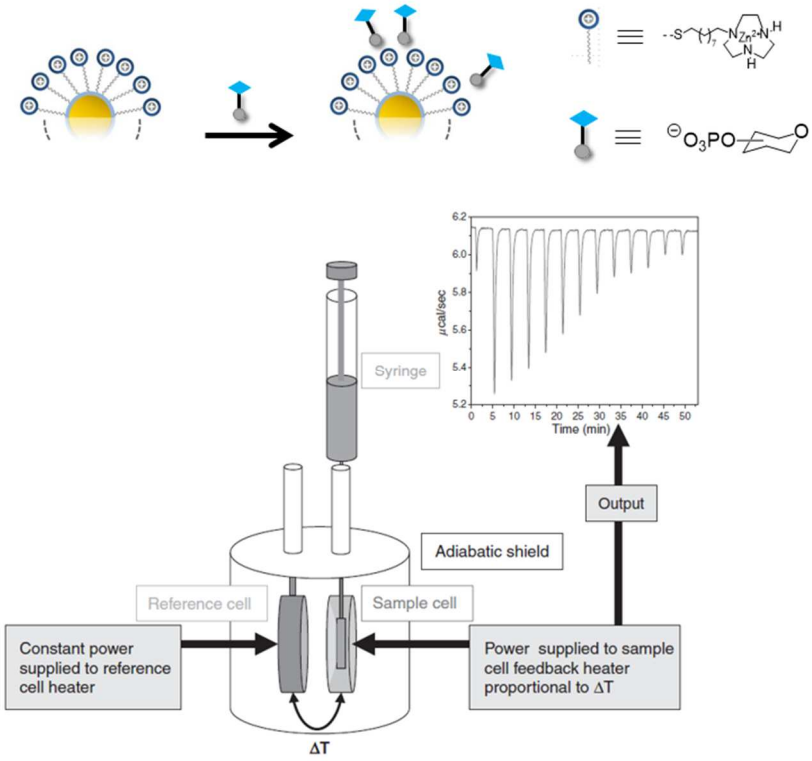

*Figure 4: Schematic representation of ITC experiments in which the carbohydrate is added to AuNP **1** solution along with representative diagram of a typical ITC showing how the power applied by the instrument to maintain constant temperature amongst the sample and reference cell is measured resulting in the instrument signal.*

ITC has been used widely in the study of carbohydrate recognition by synthetic receptors. In 2016, Davis and co-workers reported a synthetic receptor composed of pyrenyl tetraamine along with isophthaloyl spacers lead to new carbohydrate receptor that work in water. The receptor showed an impressive binding constant for derivatives of N-acetylglucosamine presenting K_a = 2 x 10^4 M^{-1}. The recognition of the carbohydrates occurs via CH-π interactions with the pyrene moieties and C-H bonds of carbohydrate and hydrogen bonding between the hydroxyl group of carbohydrates and the spacers. The interactions were confirmed by means of ^{1}H-NMR spectroscopy.[7] Ravoo *et. al.* reported a synthetic carbohydrate receptor based on covalent bond formation with the carbohydrates functionalizing tripeptides with boronic acids (Cys-X-Cys (X= aminoacids

containing boronic acid moiety)). Several carbohydrates such as fructose, glucose and mannose were assayed in presence of the peptides observing binding constants from 2 x 10^1 M^{-1} to 3 x 10^3 M^{-1} confirmed by means of fluorescence spectroscopy.[8] Therefore, we were strongly motivated to exploit ITC for studying carbohydrate recognition by AuNP **1** in water (Figure 4).

3.2.2.2 Optimization of the experimental conditions

To carry out ITC experiments for the study of carbohydrate recognition by AuNP **1** it was necessary to determine the optimal experimental conditions. A critical point in ITC is to ensure that the heat effect originates exclusively from the binding interaction. The sensitivity of ITC is so high that even simple dilutions will be detected. Therefore, solutions need to be prepared in such a way to minimize artefacts. In addition, a series of control experiments (buffer-to-buffer, analyte-to-buffer) need to be carried out in order to detect the quantity of heat that originates from secondary events.

The concentration of the carbohydrate stock solutions were determined by ^{1}H-NMR as described in the experimental section. After freeze-drying, the samples were diluted in buffer solution up to the desired concentration. The AuNP **1** stock solution was prepared in milliQ water and then concentrated under reduced pressure, after which the AuNP **1** was taken up in the same buffer solution up to the desired concentration.

Several initial experimental conditions were explored to determine the appropriate concentration regime for AuNP **1** and phosphorylated carbohydrates. In order to detect the interactions with the carbohydrates, it was required to increase the AuNP **1** concentration up to 500 μM, in terms of head group. In addition, the titrations with carbohydrates were carried out up to 3 mM in order to form a sufficient amount of complex.

3.2.2.3 ITC-binding study of phosphorylated glucose isomers

Once the experimental conditions were optimized, the first set of ITC experiments were performed using three isomers of mono-phosphorylated glucose: α/β-D-glucose-6P, α-D-glucose-1P and β-D-glucose-1P (Figure 5a). Our particular interest in the glucose carbohydrates originated from the interesting observation that the displacement experiments had shown that the selectivity of binding was affected by the nature of the chemical probe. ITC-data could provide information on the intrinsic affinity of each isomer in the absence of probe and, thus, could strengthen the hypothesis that the fluorescent probe played indeed a role in determining the selectivity.

The calorimetric output for α/β-D-glucose-6P, α-D-glucose-1P and β-D-glucose-1P titrated to 0.5 mM concentration of AuNP **1** solution in buffered water (pH 7.0, 37 ºC) is shown in the Figure 5b. It represents typical differential molar enthalpy as a function of the amount of titrant added. In all the cases, the output represents an endothermic process.

In order to calculate the binding constants and the other parameters from the ITC experiments, the values obtained for the carbohydrates were fitted to 1:1 binding site model. The enthalpy of binding process (ΔH), the molar ratio of phosphorylated carbohydrate to AuNP **1** (0.5 mM concentration)(N) and the binding constant for the binding process amongst the carbohydrate and the AuNP **1** were obtained. In addition, the ΔG and ΔS are calculated knowing the temperature (Figure 5b).

In the case of α/β-D-glucose-6P a single binding event was observed with a stoichiometric ratio of 1.2 ± 0.1:1 for α/β-D-glucose-6P:AuNP **1**, and a binding constant, K_a, of 4.3 ± 1.3 x 10^3 M^{-1}. The values obtained for ΔH and ΔS were 1822 ± 185 cal/mol and 22.5 cal/mol*K, respectively, indicating that the binding process of α/β-D-glucose-6P to AuNP **1** is enthalpically unfavourable, but entropically favourable. On the other hand, α-D-glucose-1P and β-D-glucose-1P showed binding constants of 2.2 x 10^3 M^{-1} and 4.6 x 10^3 M^{-1} respectively. Therefore, α/β-D-glucose-6P presented a 1.95 times better binding affinity for AuNP **1** with regard to α-D-glucose-1P. In addition, from the point of view of enthalpy 6-isomer was 1.1-fold enthapically disfavoured and 1.1 times favoured in terms of entropy compared to the α-D-glucose-1P. β-D-Glucose-1P presented a comparable binding affinity compared to α/β-D-glucose-6P. In terms of enthalpy and entropy was 1.1-fold disfavoured and 1.0-fold favoured, respectively (Figure 5c).

a)

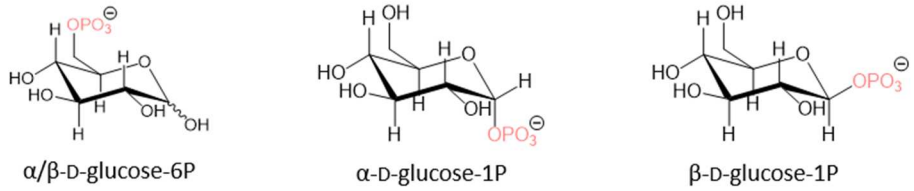

b)

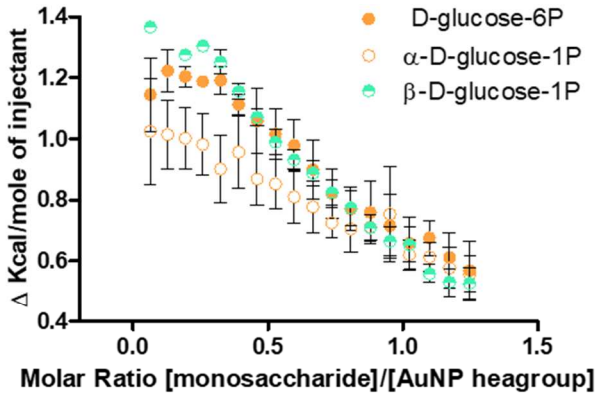

c)

monosaccharide	N	K_a(M^{-1})	ΔG(cal/mol)	ΔH(cal/mol)	T*ΔS(cal/mol)
α/β-D-glucose-6P	1.2 (±0.1)	4.3 (± 1.3) x 10^3	-5153	1822 (± 185)	6975
α-D-glucose-1P	1.6 (± 0.1)	2.2 (± 0.8) x 10^3	-4732	1654 (± 203)	6386
β-D-glucose-1P	1.0 (±0.1)	4.6 (± 1.0) x 10^3	-5197	2088 (± 176)	7285

Figure 5: a) Phosphorylated glucose isomers. b) ITC data, after the subtraction of heat dilution, of phosphorylated glucose isomers. c) Thermodynamic data of ITC experiments. Experimental conditions:

[HEPES] = 10 mM, pH 7.0, [TACN·Zn^{2+}] = 0.5 mM, [monosaccharide] = 3 mM, 37 °C. Averaged values from two independent measurements.

β-D-Glucose-1P presented a 2.1-fold better binding affinity for the AuNP **1** with regard to α-D-glucose-1P despite the only difference being the disposition of the phosphate group. However, in the fluorescence studies α-D-glucose-1P showed 1.3 better binding affinity regarding β-D-glucose-1P in presence of probe **A** (see chapter 2). Therefore, an inversion of selectivity is observed for α-D-glucose-1P and β-D-glucose-1P when the probe **A** is on the AuNP **1** surface. This provides support for the hypothesis that the probe plays a role in the selectivity for carbohydrates by AuNP **1**.

3.2.2.4 ITC-binding study of C6-phosphorylated carbohydrates

Then, the set of carbohydrates phosphorylated in the C6-position were studied, *i.e.* α/β-D-glucose-6P, α/β-D-mannose-6P *and* α/β-D-galactose-6P (Figure 6a). For this series significant differences were observed. For galactose no significant heat effects could be detected and determination of the binding constant was not possible. The binding isotherm of glucose was already discussed in the previous section and it was shown that the curve could be fitted to a 1:1 binding model with a constant of 4.3 x 10^3 M^{-1}. Yet, a clearly distinct isotherm was measured for mannose and fitting to a 1:1 binding model yielded a value for K_a of 10.9 x 10^3 M^{-1}, but with a large error (Figure 6b and c).

In order to obtain a consistent data, the binding isotherm of α/β-D-mannose-6P was fitted to 1:2 binding site model obtaining 1.1 ± 2.8 x 10^5 M^{-1} and 1.2 ± 3.6 x 10^3 M^{-1} for K_{a1} and K_{a2} respectively. It was observed that K_{a1} is 2 order of magnitude higher regarding K_a, obtained from 1:1 binding model, but the large errors indicate that the obtained values need to be interpreted with caution.

a)

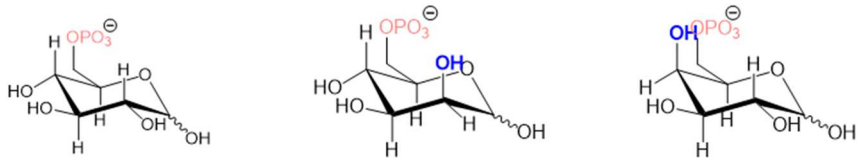

α/β-D-glucose-6P α/β-D-mannose-6P α/β-D-galactose-6P

b)

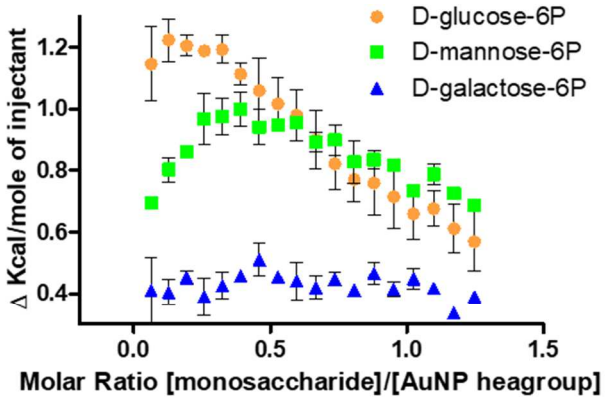

c)

monosaccharide	N	K_a(M^{-1})	ΔG(cal/mol)	ΔH(cal/mol)	T*ΔS(cal/mol)
α/β-D-glucose-6P	1.2 (±0.1)	4.3 (± 1.3) x 10^3	-5153	1822 (± 186)	6975
α/β-D-mannose-6P	1.8 (±0.2)	10.9 (± 7.5) x 10^3	-5720	1131 (± 81)	6851
α/β-D-galactose-6P	N/A	N/A	N/A	N/A	N/A

Figure 6: a) Phosphorylated carbohydrates in C6-position. b) ITC data, after the subtraction of heat dilution, of phosphorylated carbohydrates in C6-position. c) Thermodynamic data of ITC experiments. Experimental conditions: [HEPES] = 10 mM, pH 7.0, [TACN·Zn^{2+}] = 0.5 mM, [monosaccharide] = 3 mM, 37 °C. Averaged values from two independent measurements.

3.2.2.5 ITC-binding study of C1-phosphorylated carbohydrates

Finally, α-D-glucose-1P, α-D-mannose-1P and α-D-galactose-1P were assayed (Figure 7a). Significant differences were observed also for this set of carbohydrates. The binding isotherm of glucose was discussed above in the previous section and it was shown that the curve obtained could be fitted to a 1:1 binding model obtaining binding constant of 2.2 x 10^3 M^{-1}. Distinct binding isotherms were obtained for mannose and galactose and both were fitted to a 1:1 binding model yielded a value for K_a of 6.1 ± 7.9 x 10^3 M^{-1} and 95 ± 72 x 10^3 M^{-1}, respectively, but also in this case with large errors (Figure 7b and c).

Thus, the binding isotherms of mannose and galactose were fitted to a 1:2 binding model. In the case of mannose, values of 1.8 ± 25.3 x 10^5 M^{-1} and 0.1 ± 5.6 x 10^3 M^{-1} were obtained for K_{a1} and K_{a2} respectively. For galactose, these values 6.1 ± 5.3 x 10^5 M^{-1} and 4.8 ± 2.7 x 10^3 M^{-1}, respectively. In this case, galactose presents 3.38 and 48 fold better binding affinity regarding mannose for K_{a1} and K_{a2}, respectively. Yet, also in this case the errors were too large to permit a reliable interpretation of the data.

a)

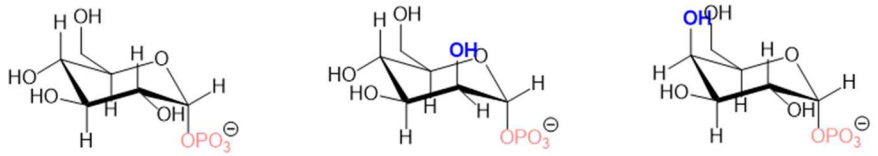

b)

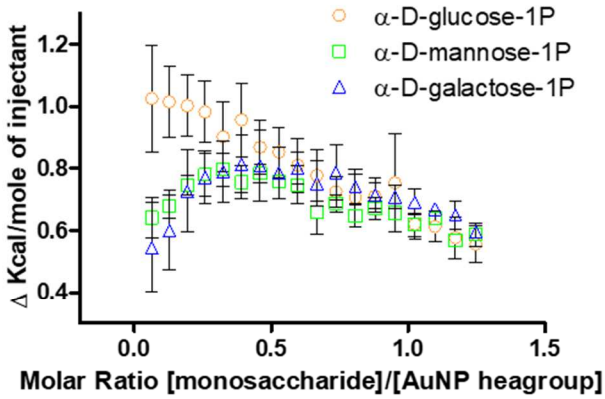

c)

monosaccharide	N	K_a(M^{-1})	ΔG(cal/mol)	ΔH(cal/mol)	T*ΔS(cal/mol)
α-D-glucose-1P	1.6 (± 0.1)	2.2 (± 0.8) x 10^3	-4732	1654 (± 203)	6386
α-D-mannose-1P	2.2 (±0.7)	6.1 (± 7.9) x 10^3	-5363	929.4 (± 140)	6293
α-D-galactose-1P	1.5 (±0.2)	95 (± 72) x 10^3	-7068	805.9 (± 19)	7874

Figure 7: a) Phosphorylated carbohydrates in C1-position. b) ITC data, after the subtraction of heat dilution, of phosphorylated carbohydrates in C1-position. c) Thermodynamic data of ITC experiments. Experimental conditions: [HEPES] = 10 mM, pH 7.0, [TACN·Zn^{2+}] = 0.5 mM, [monosaccharide] = 3 mM, 37 °C. Averaged values from two independent measurements.

In conclusion, the ITC-studies have provided valuable additional information on the affinity between phosphorylated carbohydrates and AuNP **1**. In particular, binding studies of the glucose-isomers illustrated a higher affinity of the β-isomer compared to the α-isomer, which is in line with the observations made in Chapter 2 when using displacement experiments in the presence of the MSP and BSP-probes. Importantly, these data now confirm that the increased affinity of the α-isomer when probe **A** was used, must be a result of additional interactions between the α-isomer and probe **A**. Overall, it was noted though that the heat effects were generally not high, which induced large errors. Although this hampered a quantitative interpretation of the data, the qualitative inspection of the binding isotherms indicate that it is very likely that the same carbohydrate can bind with different affinities to AuNP **1**. This indicates that different binding pockets may be present on the monolayer.

3.2.3 Diffusion-Ordered Spectroscopy

3.2.3.1 Introduction

Diffusion-ordered spectroscopy (DOSY) is a mixture of NMR experiments based on pulsed field gradient spin (PFGSE) or stimulated (PFGSTE) echo measurements.[9] In these experiments, the measured signal intensity depends on timing, diffusion coefficient and gradient pulse. Therefore, the measurements made with a range of gradient strengths allow determination of the diffusion coefficients for different signals. Considering that the diffusion coefficient is a characteristic of a molecule, the NMR signals from species of different sizes can be differentiated.[10] The name DOSY refers to the use of a set of diffusion-attenuated spectra to build up a multidimensional spectrum in which signal are separate according to diffusion coefficient in one of the dimensions. Therefore, in an ideal 2-D DOSY spectrum, all the signal from the same specie appear at the same diffusion coefficient, allowing the analysis of the NMR spectra of complex mixture (Figure 8).

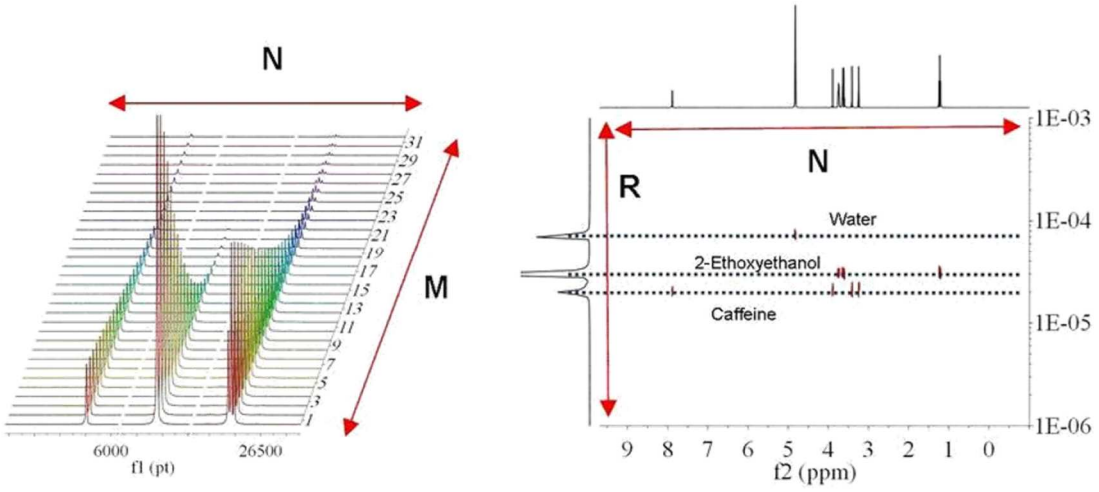

Figure 8: (Left) array of ^{1}H PFGSTE spectra measured with linearly increasing field gradient, (right) the resultant DOSY spectrum.

In 2015, Mancin and co-workers exploited DOSY in the context of chromatographic NMR. A set of gold nanoparticles, with an 1.8 nm core diameter, passivated with different thiols, including also the C9-thiols terminating with a 1,4,7-triazacyclonone (TACN)·Zn^{2+} (AuNP **1**) were investigated. Using DOSY it was found that AuNP **1** presented an affinity for hydrophilic organic anions and also showed a stronger interaction with phosphorylated molecules compared to molecules with carboxylate groups.[11] This result were perfectly in line with the results previously obtained by Prins and co-workers using fluorescence spectroscopy measurements.[12]

The attractiveness of AuNPs for DOSY experiments relies on two important features. Relatively small AuNPs, with diameters up to 2 nm are still small enough to not perturb the magnetic field homogeneity across the sample. This allows the use of solution NMR

without significant line broadening. On the other hand, their size is large enough to have significantly different diffusion rates compared to small molecules. It is important to consider that the signals obtained in DOSY NMR depend on the diffusion of the molecules and, in the case of complex formation under rapid exchange, the signal is an average of the diffusion coefficient of the free and bound molecules. The large difference in diffusion coefficient between free and bound molecules ensures that even a relatively small fraction of bound molecules will significantly affect the average diffusion coefficient. This makes DOSY in principle suited for detecting also relatively weak interactions. Therefore, we thought that DOSY would be an attractive technique for studying the interaction between phosphorylated carbohydrates and AuNP **1**. This was further motivated by the fact that also in this case, the interaction can be studied without the need for auxiliary (fluorogenice) molecules (Figure 9).

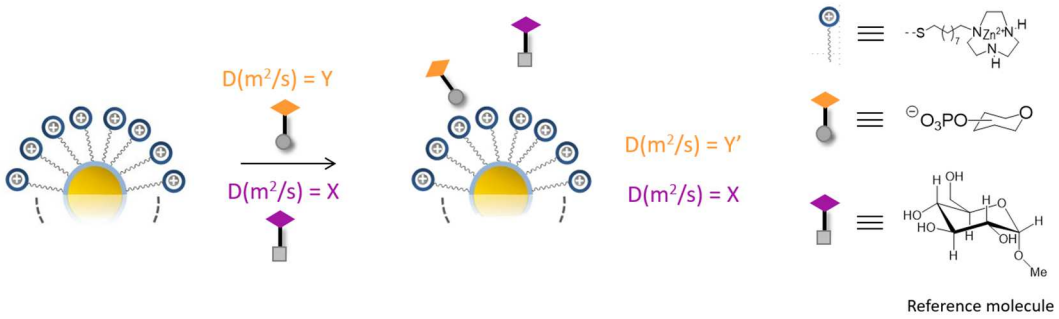

*Figure 9: Schematic representation of DOSY experiment in which the diffusion coefficient of phosphorylated carbohydrates is altered by the presence of AuNP **1** while the diffusion coefficient for the reference molecule was not perturbed.*

3.2.3.2 Optimization of the experimental conditions

In order to carry out the DOSY experiments, it was necessary to determine the experimental conditions. First of all, the concentrations of the stock solutions of phosphorylated carbohydrates and methyl α-D-glucopyranoside, as a reference molecule, were determined as reported in the experimental section.[13]

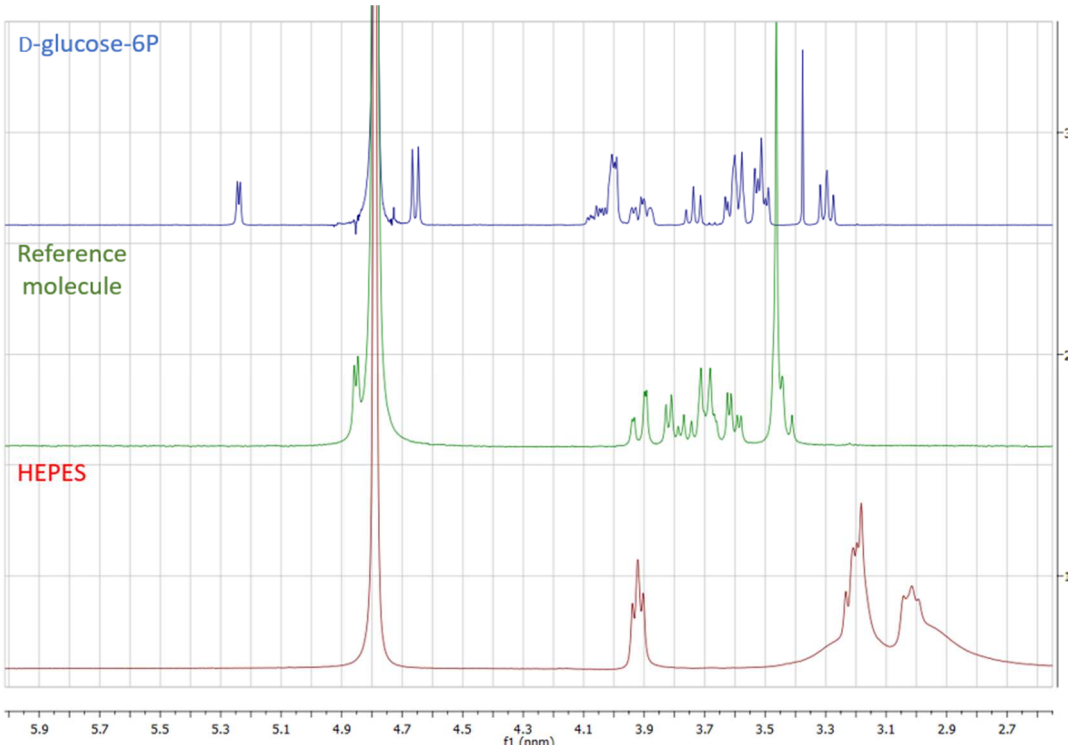

Figure 10 Partial ^{1}H-NMR spectra of D-glucose-6P, methyl α-D-glucopyranoside as reference molecule and HEPES.

For determination of the diffusion coefficient of a molecule it is necessary to identify a characteristic NMR signal of the molecule. Therefore, the ^{1}H-NMR spectra of HEPES, the reference molecule, and each carbohydrate were measured (Figure 10). It was found that the characteristic signals for HEPES and reference molecule appeared at 2.98 ppm and 4.81 ppm, respectively. On the other hand, for D-glucose-6P, D-mannose-6P and D-fructose-6P characteristic peaks were found at 5.24 ppm, 5.09 ppm and 4.13, ppm respectively.

Next, several experimental conditions were investigated to detect the interaction among AuNP **1** and the phosphorylated carbohydrate. Owing to the lower sensitivity of DOSY compared to fluorescence spectroscopy, concentrations of AuNP **1** in the mM range were required. In addition, the carbohydrate concentrations were increased up to 3 mM in order to shift the equilibrium towards the complex formation between carbohydrate and AuNP **1**.

3.2.3.3 DOSY experiments

DOSY experiments were performed in the absence and in presence of AuNP **1** using a set of phosphorylated carbohydrates, *i.e.* D-glucose-6P, D-mannose-6P and D-fructose-6P. All experiments were carried out in buffered water (pH = 7.0). In addition, methyl α-D-glucopyranoside was used as a reference molecule with a chemical structure similar to the target analytes but without any affinity for AuNP **1**.

First, DOSY experiments were carried out in the absence of AuNP **1** to determine the diffusion coefficients of the carbohydrates by themselves (Figure 11).

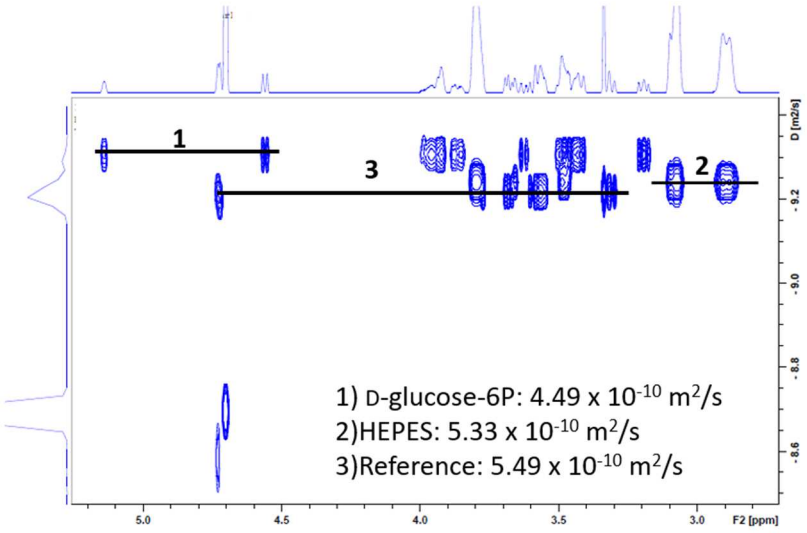

Figure 11: DOSY spectrum including the diffusion coefficients values. Experimental conditions: [HEPES]= 10 mM, pD 7.0, [Reference molecule]= 3 mM, [Phosphorylated carbohydrate]= 3 mM.

For all carbohydrates similar diffusion coefficients were obtained, which is not surprising considering their similar size and structure (Table 1).

Carbohydrate	D (m^2/s)$_{\text{in absence of AuNP 1}}$	D (m^2/s)$_{\text{in presence of AuNP 1}}$
D-glucose-6P	4.51 x 10^{-10}	3.57 x 10^{-10}
D-mannose-6P	4.46 x 10^{-10}	3.08 x 10^{-10}
D-fructose-6P	4.49 x 10^{-10}	3.35 x 10^{-10}

*Table 1: Diffusion coefficients values of DOSY experiments in the absence and in the presence of AuNP **1**. Experimental conditions: [HEPES]= 10 mM, pD 7.0, [TACN·Zn^{2+}]= 2 mM, [Reference molecule]= 3 mM, [phosphorylated carbohydrate]= 3 mM.*

Next, the diffusion coefficients were determined in the presence of AuNP **1** (Table 1). For all phosphorylated carbohydrates a significant reduction in the diffusion coefficient was observed, which unambiguously demonstrates that the phosphorylated carbohydrates interact with the AuNP **1**. Lower diffusion coefficient values indicate higher interaction with AuNP **1**. It is important to note that the diffusion coefficients of the reference compound was not affected at all (5.43 x 10^{-10} m^2/s and 5.49 x 10^{-10} m^2/s in absence and presence of AuNP **1** respectively).

Comparing the previous results with the results obtained by fluorescence technique, D-mannose-6P presented higher binding affinity than D-glucose-6P for AuNP **1** in presence of fluorescence probe **A** (1.16-fold) and MSP (1.27-fold) while in presence of BSP both carbohydrates presented similar results. Therefore, mannose presented higher binding affinity than glucose for AuNP **1** in presence and in absence of fluorescence probe.

In conclusion, DOSY experiments allowed to detect the interaction between AuNP **1** and C6-phosphorylated carbohydrate. Because of the sensitivity of the technique, it was required to increase the concentration of AuNP **1** and carbohydrates to mM ranges for the detection of AuNP **1**·C6-phosphorylated carbohydrate complex. The results showed that mannose presented a higher binding affinity, observing the strongest decrease in diffusion coefficient. On the other hand, in the presence of fluorescence probe **A** and MSP a similar selectivity was observed by fluorescence (see Chapter 2). This again confirms that probe **A** plays a role in the recognition process.

3.2.4 Study of carbohydrate recognition by means of ^{31}P-NMR

3.2.4.1 Introduction

^{31}P-NMR spectroscopy can be used to study chemical compounds that contain phosphorus. Phosphorus has a medium sensitive nucleus, compared to ^{1}H and ^{13}C, for NMR spectroscopy. Phosphorus presents a 100% of natural abundance compared to 99.9844% and 1.108% for ^{1}H and ^{13}C, respectively. The relative receptivity of ^{31}P: 0.0665, which makes it 16 times less sensitive than ^{1}H, but 370-fold more sensitive than ^{13}C. Usually, the experiment is acquired with ^{1}H decoupling to facilitate interpretation of the spectra. The resonances can be found in large chemical shift window, which is from 1400 ppm to -500 ppm.

^{31}P-NMR has been widely used for the study of phosphor-containing compounds in complex biological media.[14] Considering that in our systems the phosphate-groups constitutes the main driving force for the interaction between carbohydrate and AuNP **1**, we decided to explore the interaction with ^{31}P-NMR spectroscopy.

3.2.4.2 Optimization of the experimental conditions

In order to study the interaction between the AuNP **1** and the phosphorylated carbohydrates by ^{31}P-NMR spectroscopy it was necessary to determine suitable experimental conditions. The stock solutions of different carbohydrates, AuNP **1** and HEPES were prepared as reported in the experimental section. Titration experiments were carried out by adding AuNP **1** to a solution of phosphorylated carbohydrate in buffered water with 10% of D_2O (v/v) solution, such as to keep the intensity of the ^{13}P-signal constant. Experiments were performed in NMR tubes in which a co-axial tube was inserted containing a solution of H_3PO_4 (15 mM) as reference. The use of a co-axial tube was preferred to avoid the contamination of sample solution by the reference compound. In order to quantify the interaction between AuNP **1** and phosphorylated carbohydrates, variation in chemical shifts were measured taking as a reference the value observed for the carbohydrate in absence of AuNP **1**. Afterwards, the values were plotted as function of concentration of AuNP **1** and the resulting curve was fitted to a 2:1 binding site model obtaining the corresponding K_{a1} and K_{a2} for the binding process.

Several experimental conditions were investigated in order to detect the interaction between the AuNP **1** and the phosphorylated carbohydrates. A compromise on the carbohydrate concentration was made between a concentration as high as possible to observe a detectable signal within short acquisition times and a concentration as low as possible to maximize complex formation with AuNP **1**. The titration of AuNP **1** was performed up to 1.2 mM, in terms of head group concentration.

3.2.4.3 ^{31}P-NMR studies of the interaction between phosphorylated carbohydrates and AuNP 1

The interaction between AuNP **1** and D-glucose-6P, as a model carbohydrate, was studied by means of ^{31}P-NMR. The AuNP **1** solution was added to D-glucose-6P solution in buffered water with 10% D_2O (v/v).

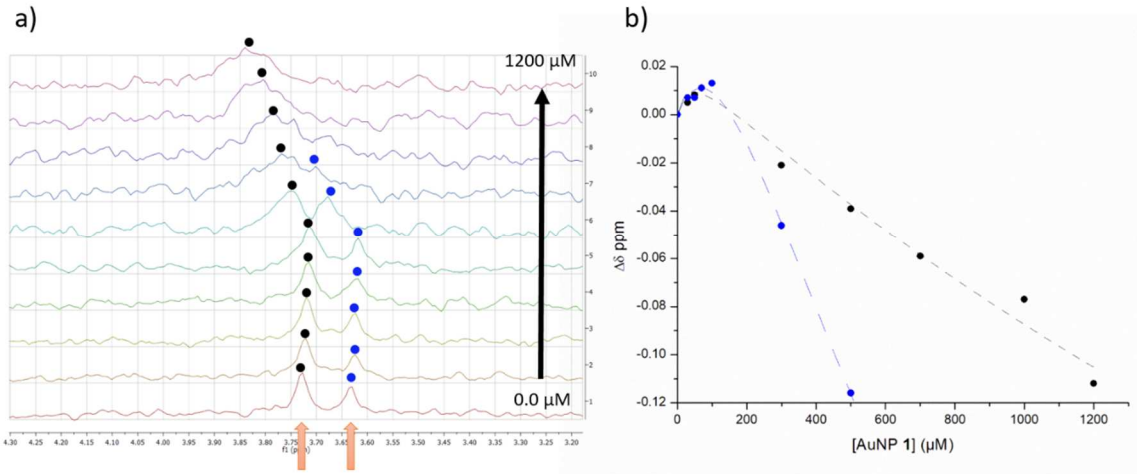

Figure 12: a) Partial ^{31}P-NMR spectra from the titration experiments. b) Observed and calculated binding curve for ^{31}P-NMR.

In the absence of AuNP **1**, two signals were observed at 3.728 ppm and 3.632 ppm, corresponding to the β- and α-anomers of D-glucose-6P, respectively.[15]

The addition of AuNP **1** affected both peaks in terms of chemical shift and also in terms line broadening. The change in chemical shift was plotted as a function of AuNP **1** concentration for both the β- and α-anomers. It is noted that only the signal for the β-anomer could be detected up to 1.2 mM of AuNP **1**. The line broadening of the signal corresponding to the α-anomer and the overlap with the β-anomer signal limited the study of this interaction up to a concentration of 0.5 mM of AuNP **1**. Nevertheless, for both anomers an interesting behaviour was observed. Focusing on the β-anomer it was observed that the addition of initial amounts of AuNP **1** resulted in an upfield chemical shift reaching a maximum Δδ of 0.014 ppm for 100 µM of AuNP **1**. However, at higher concentrations the signal started to shift downfield and continued to do so up till the maximum concentration of AuNP **1** studied (1200 µM). These results seem to confirm the observations made during the ITC experiments that multiple binding modes exist for the complex AuNP **1** and the C6-phosphorylated glucose. Tentative fitting of the curve

to a 2:1 binding model gave a curve that visually showed a good agreement. It was found, though, that the low degree of saturation and the small number of signal for the first binding event provided quantitatively poor data for K_{a1} and K_{a2} (Figure 12).

In conclusion, ^{31}P-NMR technique proved additional direct evidence for the interaction between AuNP **1** and both the α- and β-anomers of D-glucose-6P and evidence that suggests the presence of multiple binding sites on the multivalent surface of AuNP **1** was obtained. However, a thorough study of all carbohydrates was not performed because of the request for large amounts of material. It is noted that the synthesis of AuNP **1** typically produces a couple of ml of a mM solution and the cost of phosphorylated carbohydrates is significant. These initial results did not seem to justify an enormous investment in terms of energy and money.

3.3 Conclusions

Several techniques were investigated in order to detect the interaction between small molecules and AuNPs. It was taken as reference system the interactions amongst phosphorylated carbohydrates and AuNP **1**.

FCS is a highly sensitive fluorescence technique which allows detection of the interactions between C6-phosphorylated carbohydrates and AuNP **1**. The high sensitivity permits the reduction of substrate concentrations to the low μM or nM regime. Applied to the study of carbohydrate recognition by AuNP **1** covered with probe **A**, glucose mannose and galactose phosphorylated in the C6-positon were assayed. However, a difference between the carbohydrates could not be observed because of large errors. Despite the sensitivity of the technique it is less accurate for quantitative studies of our system.

ITC is highly sensitive technique allowing the detection of weak interactions between substrates even at low concentration. However for this system it was required to increase in the near of mM regime for AuNP **1**, in term of head group, and in the mM range for carbohydrate in order to detect complex formation. ITC was used to study the recognition process of phosphorylated glucose isomers by AuNP **1**. The results showed that the carbohydrates present similar binding affinities for AuNP **1** surface in absence of fluorescence probe. Comparison with the results obtained in presence of fluorescence probe **A**, a clear preference for α-D-glucose-1P was observed with regard to D-glucose-6P and β-D-glucose-1P (see chapter 2). This fact strongly suggest that the probe plays a role in the recognition process. Mannose and galactose phosphorylated in C6 and C1 positions were studied and the isotherms obtained were not possible to fit neither in 1:1 binding model and neither 1:2 properly providing values with large errors. Therefore, the data obtained about the process was not of high quality.

DOSY presented the lowest sensitivity of the techniques used and AuNP **1** and phosphorylated carbohydrates concentrations in the mM range were required. C6-phosphorylated carbohydrates were studied in the presence of AuNP **1**. It was observed

that D-mannose-6P had a higher binding affinity compared to D-glucose-6P. A similar selectivity trend was observed in the fluorescence studies, performed in Chapter 2, using fluorescence probe **A** and MSP while in presence of BSP the selectivity was not appreciate. Therefore, the results indicate that AuNP **1** present a modest selectivity for D-mannose-6P than D-glucose-6P however the selectivity can be affected depending on the probe used, such as BSP, and therefore indicating that the presence of fluorescence probe plays a role.

Finally, the interactions between α/β-D-glucose-6P and AuNP **1** were studied by ^{31}P-NMR through titration experiments. A variation in the chemical shift was observed as the concentration of AuNP **1** was increased showing complex formation between carbohydrate and AuNP **1.** The binding isotherms confirmed the results from ITC that the binding process cannot accurately be described by a 1:1 binding model.

3.4 Experimental section

3.4.1 Instrumentations

Fluorescence Correlation Spectroscopy measurements

FCS was performed on a commercial system consisting of an inverted Confocal Laser Scanning Microscope (CLSM; Mod. LSM510, Zeiss, Jena, Germany) and a ConfoCor3 system (Zeis, Jenna, Germany).

NMR Analysis

^{1}H-NMR spectra were recorded using a Bruker 400 Avance III spectrometer operating at 400 MHz for ^{1}H. Chemical shifts (δ) are reported in ppm using D_2O residual solvent value as internal reference.[16] ^{31}P-NMR experiments were performed using a Bruker 400 Avance III spectrometer operating at 162 MHz for ^{31}P using a solution of H_3PO_4 (15 mM) as external standard for calibration.

DOSY Analysis

DOSY experiments were performed using a Bruker spectrometers operating at 500 MHz. Chemical shifts (δ) are reported in ppm using D_2O residual solvent value as internal reference.[16] Then, the data was analysed using Dynamic Center software (Bruker) yielding the diffusion coefficients values (m^2/s).

pH measurements

The pH of buffer solutions was determined at room temperature using a pH-meter Metrohm-632 equipped with a Ag/AgCl/KCl reference electrode.

LIO5P freeze dryer

Lyophilisation was performed by the DiSC LIO-5P at minimum condensing temperature of -55 ºC under reduced pressure.

MicroCAL VP-ITC

Isothermal titration Calorimetry experiments were performed using MicroCAL VP-ITC composed by adiabatic cell of 1.4 mL and automatic syringe of 300 µL. The ITC data was analysed with MicroCal Origin software.

3.4.2 Materials

$Zn(NO_3)_2$ was of analytical grade. 4-(2-hydroxyethyl)-1-piperazineethanesulfonic acid (HEPES) was purchased from Sigma Aldrich and used without further purification. $Coumarin_{343}$-Gly-Asp-Asp (probe **A**) was synthesised previously in the group. D-Glucose-6-phosphate, D-mannose-6-phosphate, D-galactose-6-phosphate, α-D-Mannose-1-phosphate and α-D-galactose-1-phosphate were purchased from Sigma Aldrich. α-D-Glucose-1-phosphate, β-D-glucose-1-phosphate were purchased from CarboSynth. In all cases, stock solutions were prepared using deionized water filtered with a MilliQ-water-purifier (Millipore) and stored at 4 °C or -20 ºC.

3.4.3 Determination of the stock solutions

The concentration of $Zn(NO_3)_2$ solution was determined by atomic absorption spectroscopy. The concentration of the fluorescence probe **A** solution was determined by UV spectroscopy at pH 7.0 as was reported previously. The concentration of phosphorylated carbohydrate solutions were determined by ^{1}H-NMR using a coaxial tube along with pyrazine as an internal standard as previously reported in the group.[13] The concentration of TACN head group was determined as reported in chapter 2.

3.4.4 Fluorescence Correlation Spectroscopy

3.4.4.1 Surface Saturation Concentration

The SSC was determined adding consecutive amount of a stock solution of probe **A** in milliQ water to aqueous solution ([HEPES] = 10 mM, pH 7.0) containing [AuNP **1**] = 10 µM, in terms of head groups, at room temperature. After each addition the recorded fluctuations of fluorescence intensity were processed to give the corresponding autocorrelation function G(t). The local concentration of fluorescence probe molecules were determined from the amplitude G(0) of the autocorrelation curve (Equation 1).

$$G(0) = \frac{1}{N} = \frac{1}{Veff * C} \rightarrow N = Veff * C = \frac{1}{G(0)} \alpha \text{ [Probe A]}_{\text{Free}}$$

Consequently, the concentration of free probe **A** (nm = 1/G(0) * 10) was then plotted against the total concentration.

3.4.4.2 Displacement experiments

The displacement experiments were performed adding a consecutive amount of a stock solution of phosphorylated carbohydrate in milliQ water to aqueous solution ([HEPES] = 10 mM, pH 7.0) containing [TACN·Zn^{2+}] = 10 μM in terms of head groups coated with [probe **A**] = 100% SSC at room temperature. After each addition the recorded fluctuations of fluorescence intensity were processed to give the corresponding autocorrelation function G(t). The local concentration of fluorescence probe molecules, displaced from the AuNP **1** by the phosphorylated carbohydrate, were determined from the amplitude G(0) of the autocorrelation curve (Equation 1). Consequently, the concentration of free probe **A** (nm = 1/G(0) * 10) was determined and then normalized, taking as a reference the maximum concentration of free probe **A** in solution.

3.4.5 Isothermal titration calorimetry

Sample preparation

Once the concentration of carbohydrate stock solutions were determined by ^{1}H-NMR, the carbohydrate samples were prepared by dissolving the appropriate amount of carbohydrate stock solution in milliQ water to reach a concentration of 3 mM. After the samples were freeze-dried overnight, then were dissolved in HEPES buffer (10 mM, pH 7.0) until a 3 mM concentration.

The concentration of AuNP **1** and $Zn(NO_3)_2$ solutions were determined previously. After which, a mixture of 0.5 mM of AuNP **1** and $Zn(NO_3)_2$, in equimolar proportion, diluted in milliQ water was prepared. Then the solvent was removed under reduce pressure and the sample was placed in a vacuum line for 3 h. After which, the solid residue of AuNP **1**·Zn was dissolved in HEPES buffer (10 mM, pH 7.0) to obtain a concentration of 0.5 mM.

ITC experiments

Once the sample was prepared, before filling the cell, the solutions were degassed for 30 minutes. The phosphorylated carbohydrate sample solutions (3 mM) were titrated with AuNP **1**·Zn (0.5 mM) solution for 145 minutes. All the measurements were performed at 37 ºC using a stirring rate of 264 rpm and a 480 seconds interval between each injection. To determine the heat of dilution of each carbohydrate, it was titrated into HEPES buffer (10 mM, pH 7.0). The heat dilution was subtracted from the raw heat data. The data was fitted to a 1:1 or 1:2 binding model by using the ITC software.

3.4.6 Diffusion-ordered spectroscopy

Sample Preparation

Stock solution of phosphorylated carbohydrates, AuNP **1** and HEPES buffer (200 mM, pD 7.0) were prepared in D_2O. NMR tubes were prepared by mixing the required amounts of the stock solutions in the NMR tube and adjusting the volume to 600 µL with D_2O obtaining a final concentration of 2 mM, 3mM and 10 mM of AuNP **1**, carbohydrates and HEPES (pD 7.0) respectively.

DOSY experiments

The pulse sequence used for Diffusion Ordered Spectroscopy (DOSY) experiments was STE-LEDBPP, with the little delta and the big delta set as 0.003 s and 0.100 s respectively. The data were all analysed using the Dynamics Center 2.4.5 software package (Bruker Biospin) and the spectra were exported from TopSpin 3.5 software (Bruker Biospin). The reported diffusion coefficients are those related to isolated signals of the carbohydrates. Hydrodynamic diameters of the nanoparticles were estimated by means of the Stokes-Einstein equation.

3.4.7 ^{31}P-NMR

Sample Preparation

Stock solution of phosphorylated carbohydrates, AuNP **1**, HEPES buffer (100 mM, pH 7.0) were prepared in milliQ water. NMR tubes were prepared by mixing the required amounts of the stock solutions in the NMR tube and adjusting the volume to 500 µL with milliQ water (10% D_2O v/v) reaching a concentration of 0.45 mM and 10 mM of carbohydrates and HEPES (pH 7.0) respectively. A stock solution of 15 mM of H_3PO_4 was used as a reference inside the coaxial tube, fitted inside the NMR tube.

^{31}P-NMR experiments

The ^{31}P-NMR spectra (512 scan, delay time: 3 s) were recorded using a coaxial tube: an aqueous solution of 15 mM H_3PO_4 was placed inside and employed as a chemical shift reference (H_3PO_4 give δ= 0.0 ppm as a single), whereas the carbohydrate solution was placed in the external tube. The first spectrum was acquired for a solution of D-glucose-6P at 0.5 mM concentration in HEPES (10 mM, pH 7) with 10% of D_2O (v/v) (employed as a locking signal). Then, progressive additions of AuNP **1** stock solution to carbohydrate solution were performed and in each addition the spectra was acquired under the conditions mentioned above. The data was analysed with Origin software and the binding constant were determined fitting the data in 2:1 binding model implemented by the program.

3.5 Bibliography

1. Elson, E. L., Fluorescence Correlation Spectroscopy Measures Molecular Transport in Cells. *Traffic* **2001,** *2* (11), 789-796.
2. Christensen, J. J.; Izatt, R. M.; Hansen, L. D.; Partridge, J. A., Entropy Titration. A Calorimetric Method for the Determination of ΔG, ΔH, and ΔS from a Single Thermometric Titration1a,b. *J. Phys. Chem.* **1966,** *70* (6), 2003-2010.
3. Ramsay, G.; Prabhu, R.; Freire, E., Direct measurement of the energetics of association between myelin basic protein and phosphatidylserine vesicles. *Biochemistry* **1986,** *25* (8), 2265-2270.
4. Duff, M. R.; Grubbs, J.; Howell, E. E., Isothermal Titration Calorimetry for Measuring Macromolecule-Ligand Affinity. *J Vis Exp* **2011,** (55), 2796.
5. Freyer, M. W.; Lewis, E. A., Isothermal Titration Calorimetry: Experimental Design, Data Analysis, and Probing Macromolecule/Ligand Binding and Kinetic Interactions. In *Methods in Cell Biology*, Academic Press: 2008; Vol. 84, pp 79-113.
6. Martinez, J. C.; Murciano-Calles, J.; Cobos, E. S.; Iglesias-Bexiga, M.; Luque, I.; Ruiz-Sanz, J., Isothermal Titration Calorimetry: Thermodynamic Analysis of the Binding Thermograms of Molecular Recognition Events by Using Equilibrium Models. In *Applications of Calorimetry in a Wide Context - Differential Scanning Calorimetry, Isothermal Titration Calorimetry and Microcalorimetry*, Elkordy, A. A., Ed. InTech: Rijeka, 2013; p Ch. 04.
7. Rios, P.; Carter, T. S.; Mooibroek, T. J.; Crump, M. P.; Lisbjerg, M.; Pittelkow, M.; Supekar, N. T.; Boons, G.-J.; Davis, A. P., Synthetic Receptors for the High-Affinity Recognition of O-GlcNAc Derivatives. *Angew. Chem. Int. Ed.* **2016,** *55* (10), 3387-3392.
8. Otremba, T.; Ravoo, B. J., Linear and Cyclic Carbohydrate Receptors Based on Peptides Modified with Boronic Acids. *ChemistrySelect* **2016,** *1* (9), 2079-2084.
9. Johnson, C. S., Diffusion ordered nuclear magnetic resonance spectroscopy: principles and applications. *Prog Nucl Magn Reson Spectrosc* **1999,** *34* (3), 203-256.
10. Antalek, B., Using pulsed gradient spin echo NMR for chemical mixture analysis: How to obtain optimum results. *Concepts Magn Reson* **2002,** *14* (4), 225-258.
11. Salvia, M.-V.; Ramadori, F.; Springhetti, S.; Diez-Castellnou, M.; Perrone, B.; Rastrelli, F.; Mancin, F., Nanoparticle-Assisted NMR Detection of Organic Anions: From Chemosensing to Chromatography. *J. Am. Chem. Soc.* **2015,** *137* (2), 886-892.
12. Pezzato, C.; Scrimin, P.; Prins, L. J., Zn2+-Regulated Self-Sorting and Mixing of Phosphates and Carboxylates on the Surface of Functionalized Gold Nanoparticles. *Angew. Chem. Int. Ed.* **2014,** *53* (8), 2104-2109.
13. Neri, S.; Pinalli, R.; Dalcanale, E.; Prins, L. J., Orthogonal Sensing of Small Molecules Using a Modular Nanoparticle-Based Assay. *ChemNanoMat* **2016,** *2* (6), 489-493.
14. Bentley, J. D.; Jentoft, J. E.; Foreman, D.; Ambrose, D., 31P nuclear magnetic resonance (NMR) identification of sugar phosphates in isolated rat ovarian follicular granulosa cells and the effects of follicle-stimulating hormone. *Mol. Cell. Endocrinol.* **1990,** *73* (2), 179-185.
15. Jarori, G. K.; Maitra, P. K., Nature of primary product(s) of D-glucose 6-phosphate dehydrogenase reaction 13C and 31P NMR study. *FEBS Lett.* **1991,** *278* (2), 247-251.
16. Gottlieb, H. E.; Kotlyar, V.; Nudelman, A., NMR Chemical Shifts of Common Laboratory Solvents as Trace Impurities. *J. Org. Chem.* **1997,** *62* (21), 7512-7515.

Chapter 4: Peptide-assisted recognition of carbohydrates by monolayer protected gold nanoparticles

4.1 Summary

In Chapters 2 and 3 it was observed that a fluorescent probe, co-localized on the monolayer surface, affected the interaction between phosphorylated carbohydrates and AuNP **1**. In this Chapter this concept is exploited for the design of multivalent systems based on a combination of AuNP **1** and small peptides for carbohydrate recognition. The idea was to create binding pockets on AuNP **1** using peptides containing recognition elements for interaction with carbohydrate targets. The approach is inspired by lectins - natural carbohydrate receptors - which bind carbohydrates owing to the multiple interactions with functional groups of amino acid residues lined up in the binding pocket. A series of peptides were synthesised containing residues that could potentially interact with carbohydrates. These were then combined with AuNP **1** and fluorescent probe to yield a synthetic receptor capable of recognizing carbohydrates.

4.2 Introduction

Carbohydrates are involved in many biological process such as cell-cell recognition, virus infection or immune processes.[1] In addition, carbohydrates are biomarkers for several pathologies such as cancer.[2] Therefore, the development of strategies for carbohydrate recognition is important for a number of applications that can be employed in several fields like medical,[3] diagnostic[4] or sensing.[5]

However, carbohydrate recognition in water is not trivial.[6] Carbohydrates are highly hydrophilic species with an impressive line-up of hydroxyl groups resembling a cluster of water molecules and therefore making it especially difficult to distinguish them from the competing solvent. In addition, the structural differences among many carbohydrates are often very subtle (for instance, the configuration of a single stereocentre). Therefore, the development of carbohydrate receptors present a tremendous challenge for supramolecular chemists.

In nature, carbohydrates are recognized by a class of proteins called lectins.[7] The recognition process occurs in binding pockets containing multiple recognition units for carbohydrates which are involved in a variety of non-covalent interactions (Figure 1a). Primarily, the interaction between lectins and carbohydrates occurs via hydrogen bonding amongst the hydroxyl groups of carbohydrates and amino acids containing hydroxyl, amine and/or carboxyl groups in the side chain (for instance Arg, Ser, Asp or Asn).[8] In addition, the protein-carbohydrate complex is often stabilized by hydrophobic effects, CH-π interactions and/or coordination bonds with metal ions such as Ca^{2+} and Mg^{2+}.[9]

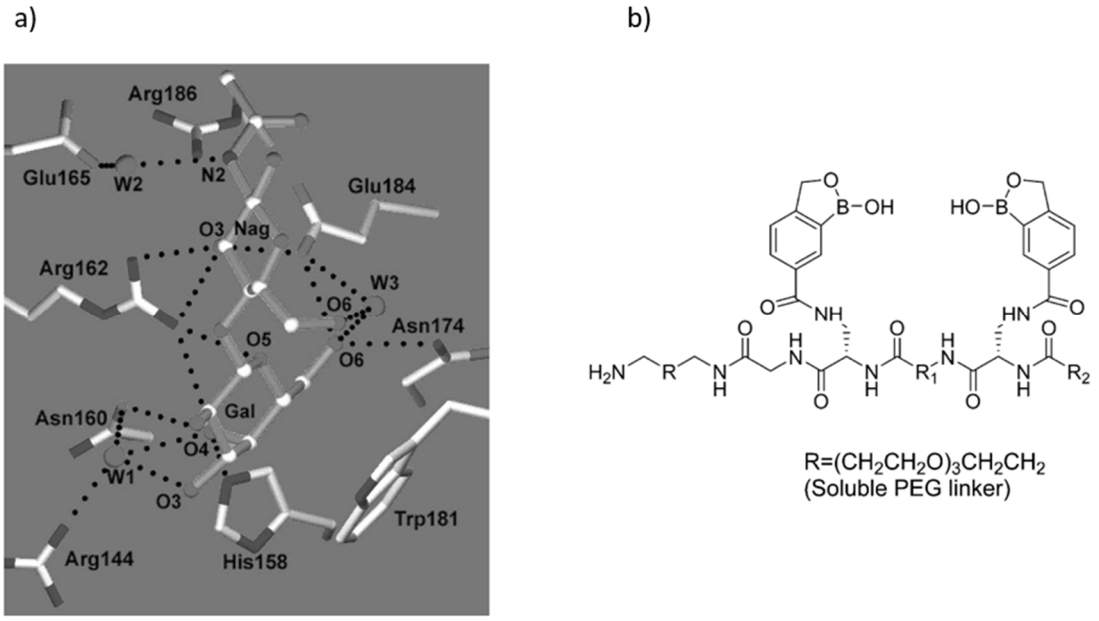

Figure 1: a) The human galactin-3 carbohydrate binding site. b) Peptide functionalized with boronic acids for carbohydrate recognition designed by Hall and co-workers.

Inspired by lectins, chemists have designed different synthetic receptors for carbohydrates.[10] The design of these receptors is cumbersome because carbohydrate recognition requires a delicate interplay of non-covalent interactions. The majority of developed synthetic receptors are operative in organic solvents, such as dichloromethane and acetonitrile.[10] In the absence of water, this allows the use of H-bonds as the main driving force for complex formation. Receptors have been developed with impressive binding constants (K_a > 2 x 10^7 M^{-1})[11] and high levels of selectivities, even for epimers, have been observed.[6b, 12] Yet, nearly all these receptors are unable to bind carbohydrates in water with a significant binding constant. This limits the applicability of these receptors in medical or diagnostic fields. Recently, the attention has shifted towards the design of synthetic carbohydrate receptors that function in water. A versatile approach is based on the formation of boronic esters between boronic acids and vicinal diols of carbohydrates.[13] Receptor structures included also peptides functionalized with boronic acids (Figure 1b).[14] These systems rely on (reversible) covalent bond formation, which marks a difference with carbohydrate recognition, which relies exclusively on noncovalent interactions.

Given that lectins are proteins,[15] it is appealing to use peptide sequences to construct synthetic carbohydrate receptors. In fact, a number of reports on medium-length carbohydrate-binding peptides have appeared. These peptide sequences were discovered by studying fragments of lectins in phage-displayed combinatorial libraries (Figure 2a).[16] Mimicking the "sandwiching" of saccharides between aromatic surfaces, which is well known to occur in protein-carbohydrate interactions,[9c, 9d, 17] a new class of peptide-based carbohydrate receptors were designed. In 2000, a library of small peptides, composed of 5 amino acid residues, were studied by Sugimoto *et. al.* for their ability to bind monosaccharides, such as erythrose and galactose, by means of fluorescence spectroscopy. The peptide with the sequence Trp-Gly-Asp-Glu-Tyr showed a remarkable

affinity of 3.5 x 10^5 and 5.2 x 10^4 M^{-1} for erythrose and galactose respectively in aqueous buffer at pH 7 (Figure 2b).[18] On the other hand, Davis and co-workers developed a synthetic receptor for carbohydrates operative in water composed of byphenyl surfaces and isopthalamides. The recognition process occurs through CH-π interactions, between the C-H bond of carbohydrates and the aromatic units of byphenyl, in which the carbohydrates is situated in between them. At the same time, hydrogen bonding amongst the hydroxyl groups of carbohydrates and amides moieties of isopthalamides occurs. The receptor showed a K_a of 60 M^{-1} for glucose in water. Besides, selectivity for glucose recognition was observed compared to galactose (20:1) and mannose (60:1) (Figure 2c).[19]

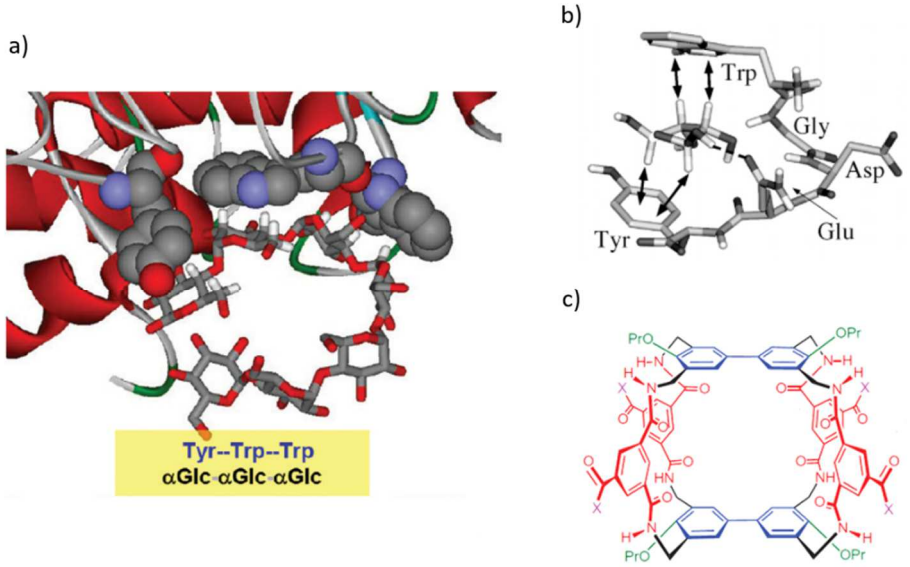

Figure 2: a) Example of carbohydrate binding-site topology and the structure of carbohydrate ligand. b) Minimized energy structure of Trp-Gly-Asp-Glu-Tyr-D-erythrose. Lines and dotted lines indicate CH-π and hydrogen-bonding interactions, respectively. c) Synthetic carbohydrate receptor composed of byphenyl surface and isopthalamides.

In 2016, Prins *et. al.* reported the formation of dynamic peptide surfaces via self-assembly of small peptides on the surface of AuNP **1** (Figure 3).[20] The resulting systems resembled nanosized synthetic proteins of which the structure could be easily varied. This approach inspired us to study whether such multivalent peptide surfaces would be able to form a binding pocket for carbohydrates.

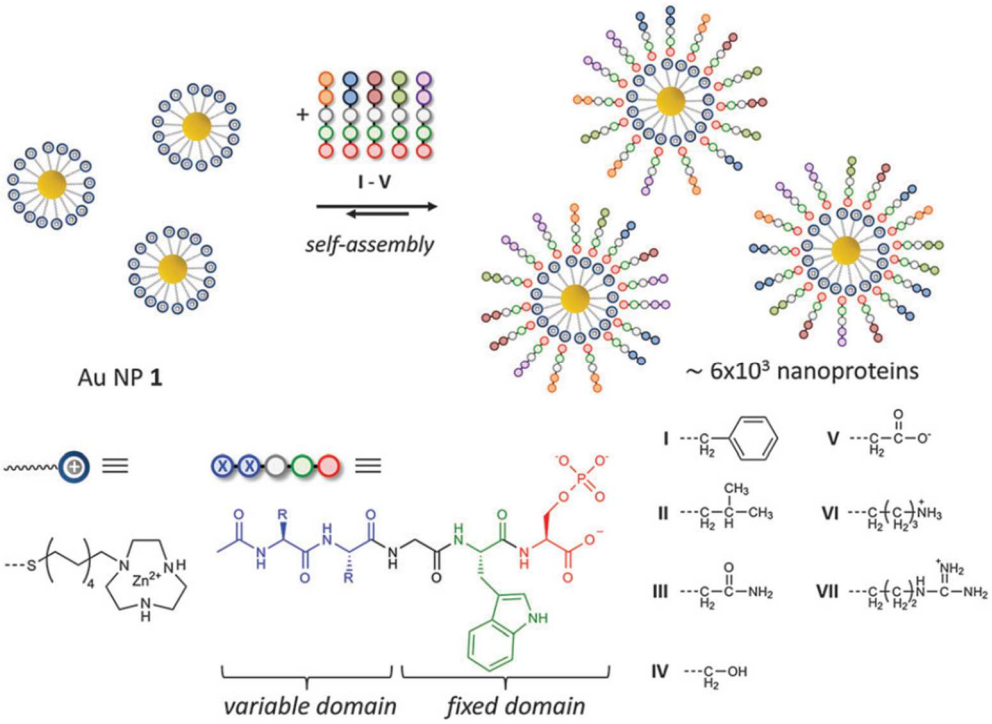

Figure 3: Schematic representation on the self-assembly of dynamic synthetic proteins.

Our strategy relied on the decoration of the surface of AuNP **1** with negatively charged peptides containing aromatic units as the carbohydrate recognition units. In addition, the co-localization on the surface of a (weaker binding) fluorescent probe introduces a way to detect complex formation by fluorescence measurements. The choice for amino acids containing aromatic units-residues was driven by the observation that the amino acids containing aromatic surfaces is a recurrent binding motif in both natural and synthetic receptors since can develop stabilizing interactions with carbohydrates through CH-π interactions (Figure 4).

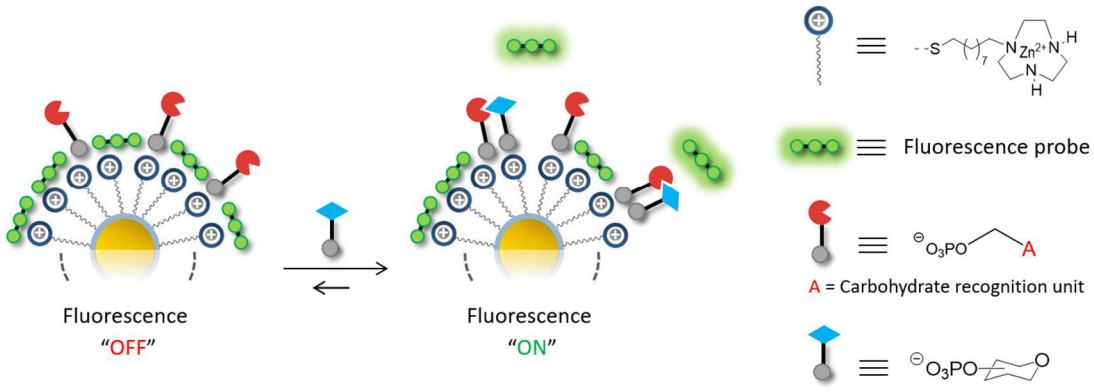

*Figure 4: Schematic representation of synthetic carbohydrate receptor based on AuNP **1** decorated with carbohydrate recognition units.*

4.3 Results and discussion

4.3.1 Synthesis and characterization of peptides

The peptides need to meet several requirements: a) the presence of aromatic-residues to interact with carbohydrates; b) the presence of a cluster of negative charges to ensure strong binding with AuNP **1**. Based on the carbohydrate receptors reported by Sugimoto along with the theoretical studies performed by Woolfson, tryptophan (W) was selected as the aromatic surface since the interaction with the carbohydrates through CH-π interactions is reportedly stronger than tyrosine or/and histidine.[18, 21] In addition, tryptophan possesses fluorescent properties. The small peptides used previously in the Prins' group for formation of the synthetic proteins, contained a C-terminal phosphoserine. The clustering of a phosphate and terminal carboxylate group was sufficient to ensure quantitative binding of the small peptides at low micromolar concentrations in water. Therefore, three peptides **I-III** (Ac-WS(OPO_3^{2-})-OH, Ac-WWS(OPO_3^{2-})-OH and Ac-WWWS(OPO_3^{2-})-OH) were designed in which the number of Trp-residues was increased in order to increase the number of recognition residues for carbohydrates (Figure 5).

The syntheses of these peptides were carried out by solid phase peptide synthesis (SPPS). All peptides were purified by High Performance Liquid Chromatography (HPLC) yielding peptides **I-III** with a purity over 96% in all the cases. Identification was carried out using Ultra Performance Liquid Chromatography – Mass Spectrometry (UPLC-MS).

The interaction of the peptides with AuNP **1** was studied through fluorescence titration experiments exploiting the fluorescence properties of tryptophan. The concentrations of the peptide stock solutions were determined using the molar extinction coefficients of tryptophan at 280 nm. (**I**: ε_{280} = 5579 M^{-1} cm^{-1}; **II**: 11158 M^{-1} cm^{-1}; **III**: 16737 M^{-1} cm^{-1}). The fluorescence intensity (F.I.) was plotted as a function of the concentration of the peptides. The resulting curves are characteristic of complex formation between peptides and AuNP **1** under saturation conditions. The surface saturation concentration (SSC) was calculated by extrapolation of the linear part of the curve to F.I. = 0. The SSCs obtained for peptide **I**, **II**, and **III** were 3.0 ± 0.1 μM, 3.3 ± 0.1 μM and 3.0 ± 0.2 μM, respectively, demonstrating that the number of peptides bound to AuNP **1** surface is practically the same (Figure 5). Considering that AuNP **1** is covered with approximately 70 thiols, these values indicate that at saturation around 20 peptides are bound to AuNP **1**.

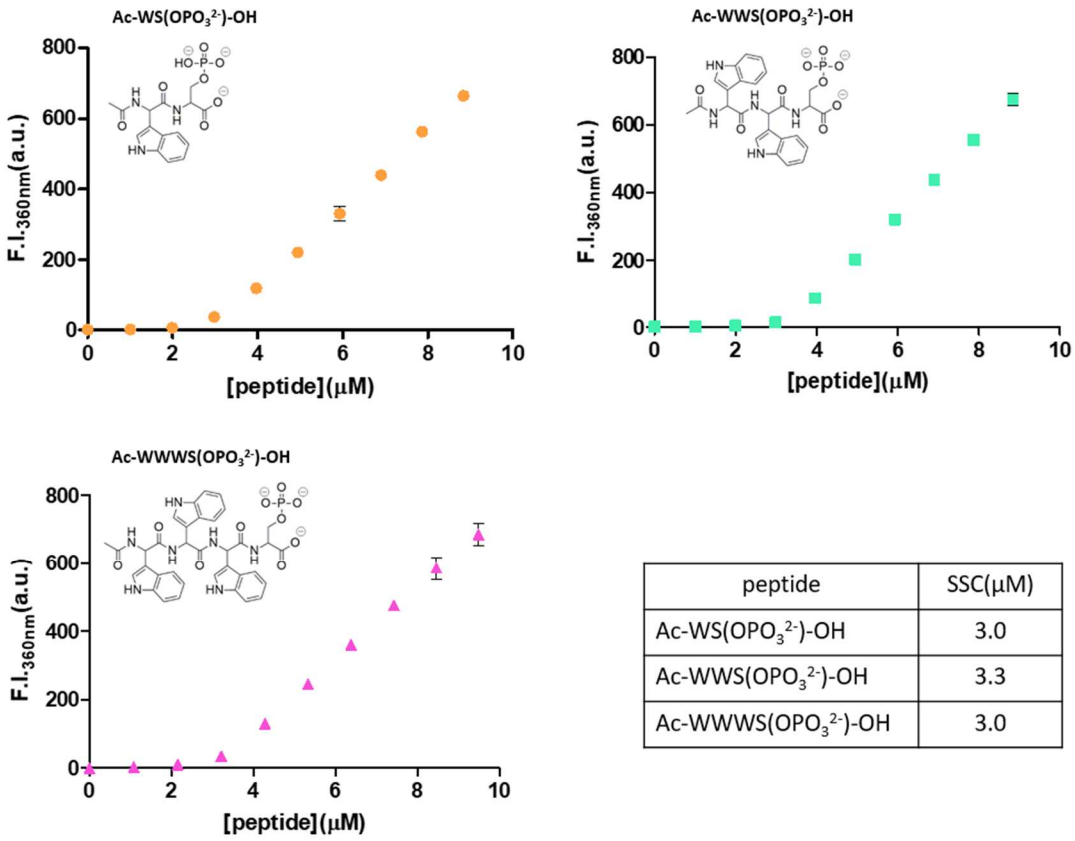

peptide	SSC(μM)
Ac-WS(OPO_3^{2-})-OH	3.0
Ac-WWS(OPO_3^{2-})-OH	3.3
Ac-WWWS(OPO_3^{2-})-OH	3.0

*Figure 5: Fluorescence intensity as a function of the amount of peptide added to a solution of AuNP **1** including SSC value per each peptide. Experimental conditions: [HEPES] = 10 mM, pH 7.0, [TACN·Zn^{2+}] = 10 μM, 37 ºC, $\lambda_{ex,\,Trp}$ = 280 nm, $\lambda_{em,\,Trp}$ = 360 nm, slits = 10.0/10.0 nm. Averaged values of from two independent measurements.*

4.3.2 Affinity study of peptides I-III for AuNP 1

The relative binding affinities of peptides **I-III** for AuNP **1** were determined through a series of displacement experiments. Peptides **I–III** were added at the surface saturation concentration to AuNP **1** and the increase of tryptophan fluorescence was measured upon the addition of the non-fluorescent competitor D-fructose-1,6-bisphosphate. The titrations were performed up to 1 mM concentration of competitor. Relative affinities were determined by comparing the amount of competitor needed to displace 40% of the peptide. To reach that level of displacement, 5, 100 and 1000 μM of competitor were needed for peptides **I**, **II** and **III** respectively. Interestingly, the obtained relative affinities of 1, 20, and 200, respectively, show that peptides **I–III** have a very different affinity for AuNP **1** despite the fact that all peptides contain the same phosphorylated Ser-residue. However, the observation is in line with prior studies of the Prins' group, which have shown that hydrophobic aromatic residues in peptides (such as Trp) can cause a significant increase in binding affinity. It is noted, though, that in all cases the absolute affinity of each peptide is sufficiently high to ensure binding under saturation conditions at the concentrations studied (Figure 6).

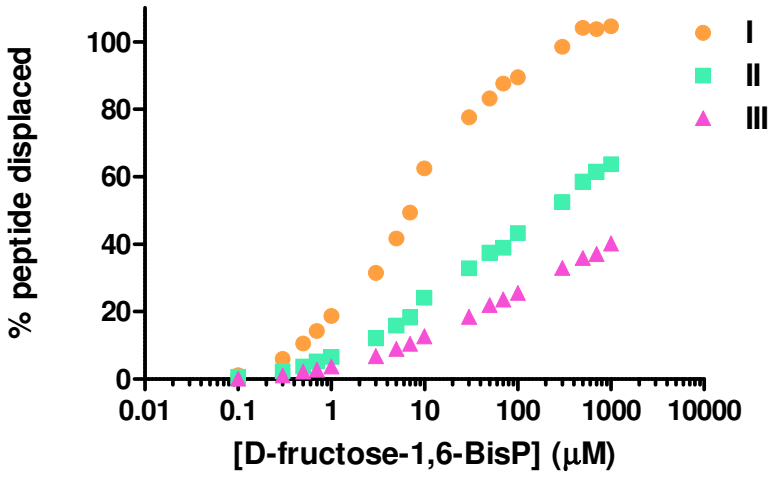

*Figure 6: Percentage of peptide displaced by D-fructose-1,6-bisphosphate as a competitor. Experimental conditions: [HEPES] = 10 mM, pH 7.0, [TACN·Zn^{2+}] = 10 μM, [peptide **I-III**] = 100 % SSC, 37 ºC, $\lambda_{ex, Trp}$ = 280 nm, $\lambda_{em, Trp}$ = 360 nm, slits = 10.0/10.0 nm.*

Overall, the results indicate that the binding of peptides **I-III** becomes stronger as the number of tryptophan residues increases.

Peptide	Relative binding affinity
I	1
II	20
III	200

*Table 1: Relative binding affinities of peptides for AuNP **1** taking as a reference peptide **I**. Experimental conditions: [HEPES] = 10 mM, pH 7.0, [TACN·Zn^{2+}] = 10 μM, [peptides **I-III**] = 100 % SSC, 37 ºC, $\lambda_{ex, Trp}$ = 280 nm, $\lambda_{em, Trp}$ = 360 nm, slits = 10.0/10.0 nm.*

4.3.3 Carbohydrate recognition by AuNP 1 decorated with peptides

Carbohydrate recognition by AuNP **1** covered with peptides **I-III** as carbohydrate recognition units was in first instance studied using fluorescence displacement experiments. The idea behind these experiments is to compare the ability of structurally similar phosphorylated carbohydrates to displace peptides **I-III** from the surface of AuNP **1**. It was hypothesized that any potential interaction between carbohydrates and peptides would be reflected by a difference in the displacement curves. Initial studies involved glucose phosphorylated in the C6- and C1–positions.

The displacement of peptides **I-III** from AuNP **1** by D-glucose-6P, α-D-glucose-1P and β-D-glucose-1P was monitored by measuring the fluorescence of tryptophan (λ_{ex} = 280 nm, λ_{em} = 360 nm). The titrations were carried out up to a 1 mM concentration of carbohydrate.

First, the C6-phosphorylated carbohydrates were assayed using peptide **I** in aqueous buffer at pH 7.0. Although the absolute difference amongst these carbohydrates is moderate, comparing the amount of peptide **I** displaced by the three carbohydrates at 1mM (34 ± 1.7%, 26 ± 1.2% and 30 ± 0.1% for D-glucose-6P, α-D-glucose-1P and β-D-glucose1P, respectively) showed modest selectivity for the C6-isomer. D-glucose-6P presented 1.38-fold and 1.15-fold higher binding affinity with regard to α-D-glucose-1P and β-D-glucose1P respectively (Figure 7a).

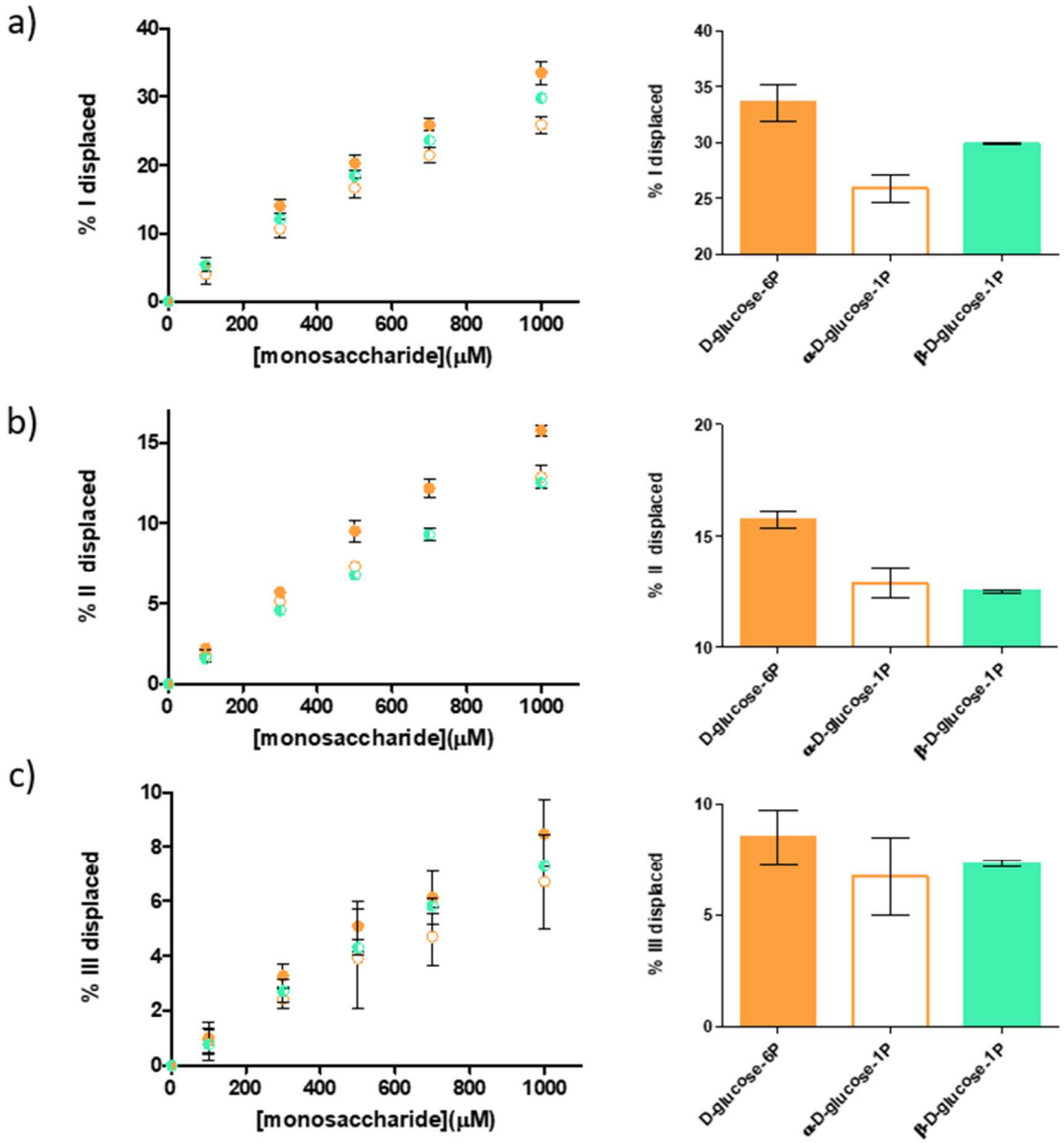

*Figure 7: Percentage of peptide **I-III** displaced as function of concentration of phosphorylated glucose along with histogram representing the percentage of peptide **I-III** displaced at 1 mM concentration of carbohydrate. Experimental conditions: [HEPES] = 10 mM, pH 7.0, [TACN·Zn^{2+}] = 10 μM, [peptides **I-III**] = 100 % SSC, 37 ºC, $\lambda_{ex,\,Trp}$ = 280 nm, $\lambda_{em,\,Trp}$ = 360 nm, slits = 10.0/10.0 nm. Averaged values of from two independent measurements.*

In the case of peptide **II** a minor displacement of peptide was observed by carbohydrates. It is line with the previous results since peptide **II** presented 20 times higher binding affinity regarding peptide **I**. Although the absolute difference observed amongst the

carbohydrates is moderate, also this system showed modest selectivity for D-glucose-6P observing a displacement of 16 ± 0.3% of peptide **II** at 1 mM concentration of carbohydrate against values for α-D-glucose-1P and β-D-glucose1P of 13 ± 0.7% and 12 ± 0.1%, respectively (Figure 7b). On the other hand, in presence of peptide **III** very low displacement of peptide was observed, in line with the 200 times higher binding affinity compared to peptide **I**. As a consequence the data had large errors and no reliable conclusions could be drawn (Figure 7c).

For both peptides **I** and **II** a higher affinity of the 6P-isomer was observed compared to both 1P-isomers. This is in line with that observed in Chapter 2 and is ascribed to the major distance in the 6P-isomer between the phosphate-group and the hydroxyl-groups, which are expected to negatively interfere with the cationic head groups. The fact that a similar ratio between 6P- and 1P-isomers was observed for peptides **I** and **II**, which is also similar to that observed for all fluorescent probes studied in Chapter 2 (except for probe **A**), indicate that these experiments provide no direct evidence for the involvement of either peptide **I** or **II** in the recognition process.

However, comparison between the α- and β-anomers of D-glucose-1P shows an interesting trend. For peptide **I** a higher affinity of the β-anomer is observed, which is in line with that observed for the pyrene-probes in Chapter 2.

Yet, the addition of another Trp-residue in peptide **II** results in a nearly equal affinity. This suggests that the presence of the second Trp-residue favours binding of the α-anomer. It is tempting to make the analogy with Chapter 2, in which it was shown that probe **A** was able to invert the selectivity for α- and β-anomers compared to the pyrene-probes, tentatively ascribed to the instalment of additional interactions between coumarin-unit and the carbohydrate.

Modest discrimination between the carbohydrates was observed. D-Glucose-6P presented a higher binding affinity with regard to α-D-glucose-1P and β-D-glucose-1P with ratios of 1.3 and 1.1 respectively (Figure 7a). The results suggested that the system has a discrete preference towards carbohydrates phosphorylated in C6 position than in C1. This was also observed in Chapter 2 for the pyrene probes.

4.3.4 Increasing the affinity of carbohydrate for AuNP 1 through the creation of binding pockets

The presence of peptides **I-III** in the system showed an effect, albeit weak, on the systems' response to the addition of phosphorylated carbohydrates. We reasoned that the weak effect may also have been a result of the full coverage of the surface with the peptides. Previous results in the Prins' group – and also the ITC-results discussed in Chapter 3 – strongly suggest that the same probe can bind with different affinities to the multivalent surface. A full coverage may lead to a displacement of the weaker binding probes, which would not reveal potentially stronger interactions. Therefore, we reasoned that the response might be enhanced in case lower amounts of peptides were used,

because, in an ideal case, this would lead to binding pockets on the monolayer surface. Thus, carbohydrates could interact with peptides without displacing them. Evidently, the question is how to generate a response from such a system. We reasoned that the combination of peptides **I-III** with a fluorescent probe – having weaker affinity for AuNP **1** compared to the peptides – would be a possibility. In this case, addition of the carbohydrate would displace the weaker binding fluorescent probe upon interacting with peptides **I-III**. Another advantage is that it would also allow us to explore the behaviour of peptide **III**, which by itself cannot be displaced by a monophosphorylated carbohydrate.

Criteria for the fluorescent probe were a lower binding affinity compared to the peptides, and the present of a fluorogenic moiety that could be monitored independently of tryptophan. Fluorescence probe **A** (λ_{ex} = 450 nm, λ_{em} = 493 nm) was selected as it fulfils the above requirements.

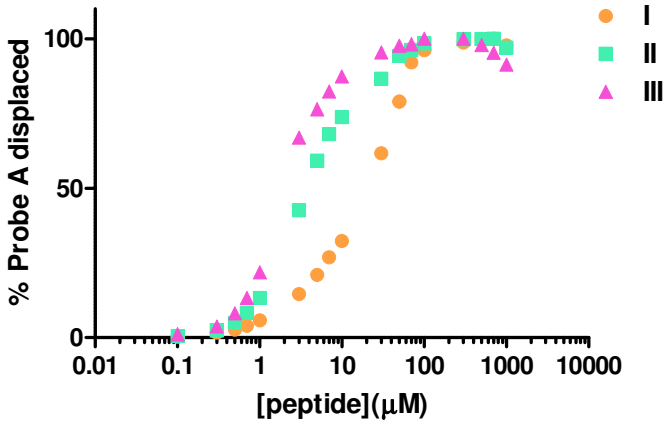

*Figure 9: a) Percentage of probe **A** displaced as function of [peptide **I-III**]. Experimental conditions: [HEPES] = 10 mM, pH 7.0, [TACN·Zn^{2+}] = 10 μM, [probe **A**] = 100 % SSC, 37 ºC, $\lambda_{ex,\ probe\ A}$ = 450 nm, $\lambda_{em,\ probe\ A}$ = 493 nm, slits = 2.5/5.0 nm.*

Our first studies were aimed at determining the relative binding affinities of peptides **I-III** and probe **A**. This was studied by adding increasing amounts of peptides **I-III** to a solution containing AuNP **1** and probe **A** at the surface saturation concentration. The titrations were performed until a concentration of 1 mM of peptide **I-III** was reached. In all cases, a full displacement of probe **A** was observed. In order to quantify the relative binding affinity of the peptides towards AuNP **1** coated with probe **A**, the peptide concentration required to displace 50% of the probe **A** was taken as a reference. The higher the concentration of the peptide needed to displace the probe **A** from the surface, the lower the affinity of the peptide for the AuNP **1**. Displacement of 50% of probe **A** required 17.5 μM, 4.0 μM and 2.2 μM of peptides **I-III**, respectively. This result is in line with the results described before (see section 4.3.2) (Figure 9). For the studied with phosphorylated carbohydrates, peptide concentrations were chosen such that they would cover around 25% of the AuNP **1** surface in the presence of a constant amount of probe **A**.

After optimization of the conditions, the response of the three systems towards D-glucose-6P was measured. Titrations up to 1 mM of carbohydrate were performed. Importantly, it was first verified whether peptides **I-III** would be displaced by glucose-6P under these conditions. Measurement of the fluorescence emission from tryptophan showed that up to a concentration of 600 µM none of the peptides **I-III** is displaced from AuNP **1** to a significant extent. At higher concentrations, just displacement of peptide **I** occurs reaching 20% at 1 mM of carbohydrate added. Peptides **II** and **III**, however, are not significantly displaced to any extent up till 1 mM. This implies that in this mixed system D-glucose-6P hardly displaces the peptides, which is an important prerequisite for our model (Figure 10).

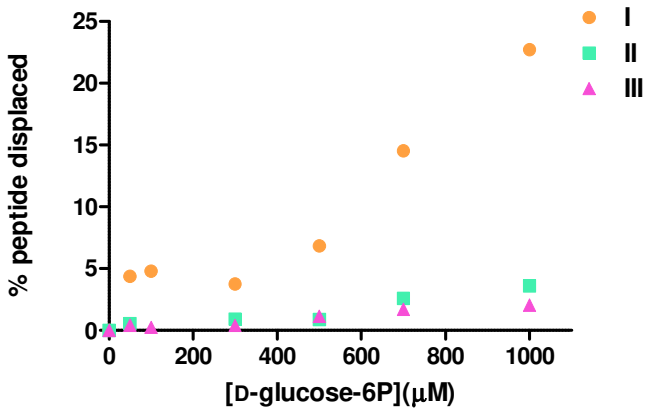

*Figure 10: a) Percentage of peptide displaced as function of [D-glucose-6P]. Experimental conditions: [HEPES] = 10 mM, pH 7.0, [TACN·Zn^{2+}] = 10 µM, [probe **A**] = 75% SSC, [peptide **I-III**] = 25% SSC, 37 ºC, $\lambda_{ex, Trp}$ = 280 nm, $\lambda_{em, Trp}$ = 360 nm, slits = 10.0/10.0 nm.*

Regarding probe **A**, it was noted that the addition of D-glucose-6P hardly provoked displacement in the absence of peptide (6 ± 0.5% probe displacement at 1 mM). However, excitingly, the same titration in the presence of peptides **I-III** revealed displacement of probe **A** already at much lower concentrations. When AuNP **1** was coated with peptide **I** along with the probe **A**, D-glucose-6P at 1 mM was able to displace 15 ± 1.0% of probe **A**. The system composed of AuNP **1** coated with probe **A** and peptide **II** showed even better results with 21 ± 3.5% of probe **A** displaced at 1 mM concentration of the carbohydrate. The same result was obtained for peptide **III** indicating that the increase from 2 to 3 units of tryptophan did not improve the interactions (Figure 11a).

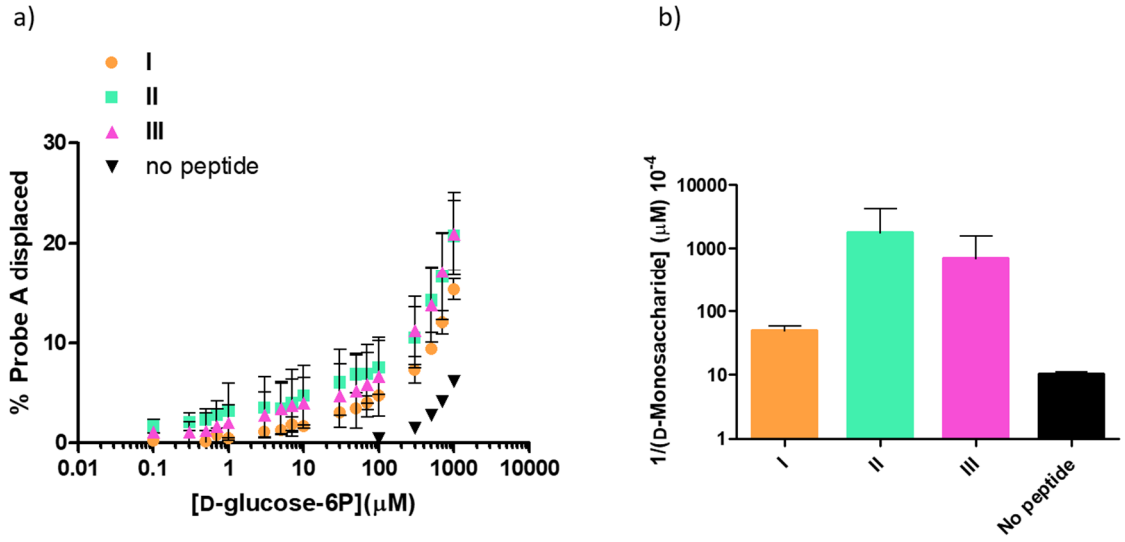

*Figure 11: a) Percentage of probe **A** displaced as function of [D-glucose-6P]. b) 1/[D-glucose-6P] required in order to displace 6% probe **A**. Experimental conditions: [HEPES] = 10 mM, pH 7.0, [TACN·Zn^{2+}] = 10 μM, [probe **A**] = 75% SSC, [peptide **I-III**] = 25% SSC, 37 ºC, $\lambda_{ex,\ probe\ A}$ = 450 nm, $\lambda_{em,\ probe\ A}$ = 493 nm, slits = 2.5/5.0 nm. Averaged values of from two independent measurements.*

The D-glucose-6P concentration required to displace 6% of probe **A** was taken as a value that quantifies the relative binding affinity of the carbohydrate. For graphical reasons 1/[carbohydrate](μM) was plotted to ensure that the highest value corresponds to a major affinity of the carbohydrate. It was observed that in the presence of peptide **I**, the sensitivity of the system increased 4.8-fold compared to the reference system in the absence of peptide. The sensitivity went up a further 36-fold (170-fold compared to the reference) when peptide **II** was used. The fact that the only difference is the presence of a Trp-residue strongly suggests that these play a role in the recognition process. Yet, the use of peptide **III** did not result in a further improvement and the results were similar as those of peptide **II** (Figure 11b). These results show that the presence of peptides **I-III** significantly increases the sensitivity of the system towards D-glucose-6P.

4.3.5 Study of the selectivity of binding pockets formed on AuNP 1

The response to the anomers α-D-glucose-1P and β-D-glucose-1P by a system composed of AuNP **1** covered with either one of the peptides **I-III** and probe **A** was studied by displacement experiments. The displacement experiments were performed as described in the previous section.

First of all, C1-phosposphorylated carbohydrates were assayed in presence of the mixture of probe **A** and peptide **I**. A comparison of the amount of probe **A** displaced by the carbohydrates at 1 mM concentration (11 ± 0.1% and 12 ± 1.6% for α-D-glucose-1P and β-D-glucose-1P, respectively) revealed no selectivity. Both carbohydrates showed a similar binding affinity for AuNP **1**. The same result was obtained for peptide **II**. At 1 mM concentration of α-D-glucose-1P and β-D-glucose-1P a displacement of 14 ± 1.6%

and 15 ± 0.8% of probe **A** were observed respectively. In the case of peptide **III**, similar results were obtained (Figure 12).

The results showed that the system composed of AuNP **1** covered with a mixture of peptide **I** and probe **A** did not present any selectivity for the anomers. Comparing this results with the results of Chapter 2 in which it was observed that the presence of probe **A** favours binding of the α-anomer with respect to the β-anomer, the presence of the peptides cause a loss of selectivity. The increase of number of Trp-residues in peptide **II** and **III** did not provide any improvement in term of selectivity.

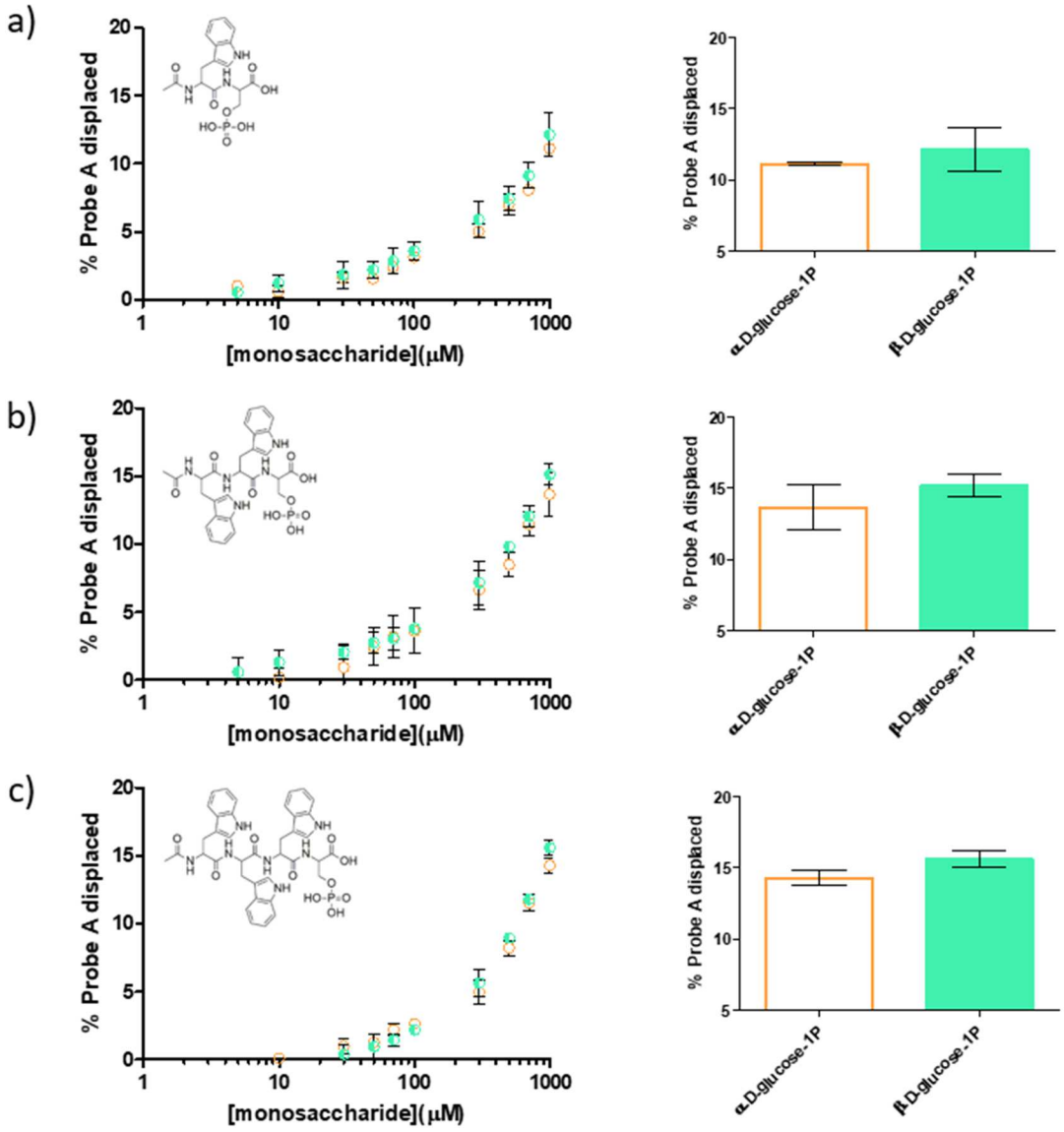

*Figure 12: Percentage of probe **A** displaced as function of concentration of C1 phosphorylated glucose anomers along with histogram representing the percentage of probe **A** displaced at 1 mM concentration of carbohydrates. Experimental conditions: [HEPES] = 10 mM, pH 7.0, [TACN·Zn^{2+}] = 10 μM, [probe **A**] = 75% SSC, [peptide **I-III**] = 25% SSC, 37 ºC, $\lambda_{ex,\ probe\ A}$ = 450 nm, $\lambda_{em,\ probe\ A}$ = 493 nm, slits = 2.5/5.0 nm. Averaged values of from two independent measurements.*

4.4 Conclusions

The peptides **I-III**, in which the number of Trp-residue was increased from 1 to 3, were synthesised and studied in presence of AuNP **1**, at 10 μM concentration in terms of head group, by means of fluorescence spectroscopy. Similar SSC values were determined for peptides **I-III** indicating that under saturation conditions the same number of molecules (around 30) are present on the AuNP **1** surface. However, peptide **II** and **III** have respectively a 20 and 200 higher affinity compared to peptide **I** indicating that Trp-residues interact with the monolayer, presumably via hydrophobic interactions.

D-Glucose-6P, α-D-glucose-1P and β-D-glucose-1P were studied in the presence of the AuNP **1** covered with peptides **I** and **II**. A modest selectivity was observed for the C6-isomer in both systems, indicating that an increase in distance between the phosphate group and the pyranose ring favors the interaction with AuNP **1**.

In the presence of peptide **I**, the β-anomer showed a higher binding affinity than the α-anomer, while in the presence of peptide **II** the α- and β-anomer have the same affinity. It can therefore be concluded that the additionial Trp-residue in peptide **II** favors binding of the α-anomer. Comparison of these results with those obtained in Chapter 2 using probe **A** – which had shown an inversion of the selectivity between anomer of C1-phosphorylated glucose – it can be concluded that the presence of the peptides affect the selectivity of the system in favour of the β-anomer.

D-Glucose-6P was assayed in the presence of AuNP **1** covered with either one of peptides **I-III** and probe **A**. It was observed that in the absence of peptide, the interaction of the carbohydrate with AuNP **1** was too weak to displace probe **A**. However, in the presence of peptide **I** a 4.8-fold increase in binding affinity of the carbohydrate was observed and a 170-fold increase in the presence of peptide **II** and **III**, compared to the system in absence of peptide. Therefore, the results suggest that Trp is involve in the recognition process improving binding of the carbohydrates. Tentatively, this increase may be ascribed to CH-π interactions between the C-H bond of carbohydrates and the aromatic moiety of Trp, but no direct evidence was obtained. No selectivity for α-D-glucose-1P and β-D-glucose-1P was detected.

4.5 Experimental section

4.5.1 Instrumentations

NMR Analysis

^{1}H-NMR spectra were recorded using a Bruker 400 Avance III spectrometer operating at 400 MHz for ^{1}H. Chemical shifts (δ) are reported in ppm using D_2O residual solvent value as internal reference.[22]

pH measurements

The pH of buffer solutions was determined at room temperature using a pH-meter Metrohm-632 equipped with a Ag/AgCl/KCl reference electrode.

UV-Vis and Fluorescence spectroscopy

UV-Vis measurements were recorded on a Varian Cary 50 spectrophotometer, while fluorescence measurements were recorded on a Varian Cary Eclipse Fluorescence spectrophotometer. Both the spectrophotometers were equipped with thermostatted cell holders.

LC/MS analysis

The UHPLC/MS measurements were performed on an Agilent 1290 Infinity LC/MS System equipped with an ESI sources, quadrupole system and diode array detector.

Flash chromatography system

Reveleris X2 flash chromatography system equipped with reveleris cartridge (FP ID C18 12 g) was used for the peptide purifications.

LIO5P freeze dryer

Lyophilisation was performed by the LIO-5P at minimum condensing temperature of -55 ºC under reduced pressure.

4.5.2 Materials

$Zn(NO_3)_2$ was of analytical grade. 4-(2-hydroxyethyl)-1-piperazineethanesulfonic acid (HEPES) was purchased from Sigma Aldrich and used without further purification. $Coumarin_{343}$-Gly-Asp-Asp (probe **A**) was synthesised previously in the group. D-Glucose-6-phosphate and D-fructose-1,6-bisphosphate were purchased from Sigma Aldrich. α-D-Glucose-1-phosphate, β-D-glucose-1-phosphate were purchased from CarboSynth. Fmoc-L-tryptophan(Boc)-OH, Fmoc-L-serine(PO(OBzl)OH)-OH and 2-CTC-chloride resin 100-200 BR-1060 were purchased from Sigma Aldrich, IrisBiotech and CBL respectively, and they were used without further purification. In all cases, the stock solutions were prepared using deionized water filtered with a milliQ-water-purifier (Millipore) and stored at 4 °C or -20 ºC.

4.5.3 Synthesis and purification of the peptides

The synthesis of peptides, which present the sequences Ac-WS(OPO_3^{2-})-OH (**I**), Ac-WWS(OPO_3^{2-})-OH (**II**) and Ac-WWWS(OPO_3^{2-})-OH (**III**), were performed by Fmoc-strategy Solid Phase Peptide Synthesis (SPPS) using 2-Chlorotrytil resins (2-CTC resin) (f = 1.0 mmol/g). The swelling was done using DMF and DCM for a duration of 20 minutes each. The active sites of the resin were capped using MeOH/DIPEA/DCM 2:1:17

(2 x 20 min). As always, 20% piperidine in DMF (2 x 10 min) was used to perform the Fmoc deprotection. The coupling step was performed using 4 equiv. Fmoc-aa-OH, 4 equiv. HBTU, 4 equiv. HOBT and 8 equiv. DIPEA. Finally, for the cleavage of the peptide from the resin an acidic mixture was used by mixing TFA/H_2O/TIS 95:2.5:2.5, which after filtering was removed by evaporation. Cold ether (x 2) was added for the precipitation and washing of the peptide.

Then, the purification of the peptides was performed using a flash chromatographic system equipped with Reveleris cartridge using A: H_2O + TFA 0.05% and B: ACN + TFA 0.05% as eluent and a FP ID C18 12 g column (Reveleris cartridge). After the purification the peptides were lyophilized. They were characterized by UPLC-MS using A: H_2O + HCOOH 0.1% and B: ACN + HCOOH 0.1% as eluent and Zorbax SB-C3 rapid resolution HT 3.0 x 100 mm 1.8-micron.

peptide	Gradient	RT (min)	Yield(%)
I	10%-10% B in 5 min 10%-100% B in 30 min	4	8.0
II	10%-10% B in 10 min 10%-100% in 15 min	15	8.2
III	10%-10% B in 10 min 10-100% B in 30 min	19	1.28

Table 2: Purification conditions for peptides using flash chromatographic system.

peptide	Gradient	RT (min)	Purity (%)	MASS $[M+H]^+$ (m/z)
I	5%-95% B in 12 min	2.664	99	414.0
II	5%-95% B in 12 min	4.151	98	600.1
III	5%-95% B in 12 min	5.141	96	786.1

Table 3: Peptide characterization by UPLC-MS.

4.5.4 Determination of the stock solution concentrations

The concentration of $Zn(NO_3)_2$ solution was determined by atomic absorption spectroscopy. The concentration of the fluorescence probe **A** and the peptides were determined by UV spectroscopy at pH 7.0. The concentration of phosphorylated carbohydrate solution were determined by ^{1}H-NMR using a coaxial tube along with pyrazine as internal standard as previously reported in the group.[23] The concentration of TACN head group was determined by kinetic titration using $Zn(NO_3)_2$.[24]

compound	Molar extinction coefficient (M^{-1} cm^{-1}) pH:7.0	Wavelength (nm)
Probe **A**	45000	450
I	5579	280
II	11158	280

III	16737	280

Table 4: Molar extinction coefficient and wavelength of the compounds used in this chapter.

4.5.5 Determination of surface saturation concentration of peptides

The fluorescence titration were performed by adding consecutive amounts of a stock solution of peptide in milliQ water to a 1 mL buffered aqueous solution ([HEPES] = 10 mM, pH 7.0) containing [TACN·Zn^{2+}] = 10 μM, in terms of head group, at 37 ºC monitoring the fluorescence of tryptophan (λ_{ex} = 280 nm, λ_{em} = 360 nm, slits = 10.0/10.0 nm). Then, the fluorescence intensity is plotted as a function of the concentration of peptide.

The Surface Saturation Concentration (SSC) was determined by the extrapolation of the linear part of the curve, in which the fluorescence intensity increased linearly as a function of the amount of probe ($y = mx + q$).

peptide	SSC (μM)
I	3.03 ± 0.12
II	3.29 ± 0.03
III	2.98 ± 0.17

Table 5: Values of SSC of the peptides. Averaged values of from two independent measurements

In order to avoid any kinetic problems, the first fluorescence titrations were always performed by following the evolution of the F.I. after each addition of the peptide (8 to 10 minutes between each addition).

4.5.6 Affinity studies of peptides for AuNP 1

In order to study the relative binding affinity of the peptides towards the AuNP **1**, displacement experiments were performed by adding consecutive amount of a stock solution of D-fructose-1,6-bisphosphate in milliQ water to a 1 mL aqueous solution ([HEPES] = 10 mM, pH 7.0) containing [TACN·Zn^{2+}] = 10 μM, in terms of head group, coated with the peptide at 100% of the surface saturation concentration at 37 ºC and monitoring the fluorescence of tryptophan (λ_{ex} = 280 nm, λ_{em} = 360 nm, slits = 10.0/10.0 nm).

To ensure that a stable signal was obtained, the displacement studies were performed by measuring the fluorescence intensity in time after each addition until a constant value was observed (8 to 10 minutes between each addition).

At the end of the displacement it was verified that the maximum value was close to the value obtained by the extrapolation of the linear part of the titration curve of SSC experiments (see above). Then, this value was used to normalize the F.I. and to plot the percentage of peptide displaced as a function of the concentration of the D-fructose-1,6-bisphosphate. However, in some cases the full displacement of the peptide was not

achieved and it was assumed that the F.I. maximum for the peptide was the interception value of the equation obtained from SSC experiments of that peptide ($y = mx + \boldsymbol{q}$).

peptide	F.I. max (theoretical)	F.I. max observed
I	335.93	346.3
II	400.66	304.24
III	347.25	186.41

*Table 6: F.I. max, theoretical and observed, for the peptides **I-III** displaced by competitor at 1 mM concentration. . Experimental conditions: [HEPES] = 10 mM, pH 7.0, [TACN·Zn^{2+}] = 10 μM, [**I-III**] = 100 % SSC, 37 ºC, $\lambda_{ex, Trp}$ = 280 nm, $\lambda_{em, Trp}$ = 360 nm, slits = 10.0/10.0 nm.*

4.5.7 Carbohydrate recognition by AuNP 1 decorated with peptides

In order to study the carbohydrate recognition by AuNP **1** covered with the peptide, displacement experiments were performed by adding consecutive amount of a stock solution of phosphorylated carbohydrate in milliQ water to a 1 mL aqueous solution ([HEPES] = 10 mM, pH 7.0) containing [TACN·Zn^{2+}] = 10 μM, in terms of head group, covered with the peptide **I-III** at 100% of the surface saturation concentration at 37 ºC and monitoring the fluorescence of tryptophan (λ_{ex} = 280 nm, λ_{em} = 360 nm, slits = 10.0/10.0 nm).

To ensure that a stable signal was obtained, the displacement studies were performed by measuring the fluorescence intensity in time after each addition until a constant value was observed (8 to 10 minutes between each addition).

A full displacement of the peptides from the AuNP **1** surface was not observed by phosphorylated carbohydrates. In order to quantify the amount of peptide displaced, it was assumed that the F.I. max for the peptide when it is fully displaced was the interception value of the equation obtained from SSC experiments of that peptide ($y = mx + \boldsymbol{q}$). Then, this value was used to normalize the F.I. and to plot the percentage of peptide **I-III** displaced as a function of the concentration of the phosphorylated glucose isomers.

4.5.8 Increasing the affinity of carbohydrate for AuNP 1 through the creation of binding pockets

4.5.8.1 Study of binding affinity of peptides towards AuNP 1 covered with probe A

The binding affinity of peptide **I-III** towards AuNP **1** covered with fluorescence probe **A** was studied through displacement experiments monitoring the fluorescence of probe **A** (λ_{ex} = 450 nm, λ_{em} = 493 nm, slits = 2.5/5.0 nm). The experiments were performed by adding consecutive amount of a stock solution of peptide in milliQ water to a 1 mL aqueous solution ([HEPES] = 10 mM, pH 7.0) containing [TACN·Zn^{2+}] = 10 μM, in

terms of head group, coated with [probe **A**] = 3.6 μM, which correspond to 100% of the surface saturation concentration and it was determined in Chapter 2, at 37 ºC.

To ensure that a stable signal was obtained, the displacement studies were performed by measuring the fluorescence intensity in time after each addition until a constant value was observed (8 to 10 minutes between each addition).

The experiments were performed up to 1 mM concentration of carbohydrate. A plateau was observed in all the cases corresponding to F.I. max. Then that value was taken to normalize the F.I. and to plot the percentage of probe **A** displaced as a function of the concentration of peptide.

peptide	F.I. max observed
I	372
II	365
III	303

*Table 7: F.I. max observed owing to the displacement of probe **A** by the peptides **I-III**. Experimental conditions: [HEPES] = 10 mM, pH 7.0, [TACN·Zn^{2+}] = 10 μM, [probe **A**] = 100 % SSC, 37 ºC, $\lambda_{ex,\ probe\ A}$ = 450 nm, $\lambda_{em,\ probe\ A}$ = 493 nm, slits = 2.5/5.0 nm.*

4.5.8.2 Study of C6 and C1 isomers of carbohydrates for AuNP 1 covered with mixture of peptide and probe A

D-glucose-6P, α-D-glucose-1P, β-D-glucose-1P recognition by AuNP **1** covered with a mixture of probe **A** and the peptides **I-III** were studied through fluorescence displacement experiments monitoring the fluorescence of probe **A** (λ_{ex} = 450 nm, λ_{em} = 493 nm, slits = 2.5/5.0 nm). The experiments were done preparing 1 mL aqueous solution ([HEPES] = 10 mM, pH 7.0) containing [TACN·Zn^{2+}] = 10 μM, in terms of head group, coated with [probe **A**] = 3.6 μM, which correspond to 100% of the SSC, at 37 ºC. Upon the stabilization of the F.I., the peptide was added ([peptide **I**] = 5 μM, [peptide **II**] = 2 μM, [peptide **III**] = 1 μM) to the solution and then consecutive amount of a stock solution of carbohydrate in milliQ water were added to the mixture.

To ensure that a stable signal was obtained, the displacement studies were performed by measuring the fluorescence intensity in time after each addition until a constant value was observed (8 to 10 minutes between each addition).

In order to quantify the displacement of the probe **A** from the AuNP **1** surface, it was necessary to determined F.I. max for probe **A** under these experimental conditions. Therefore, displacement experiments were performed adding consecutive amount of D-fructose-1,6-bisphosphate in milliQ water to 1 mL aqueous solution ([HEPES] = 10 mM, pH 7.0) containing [TACN·Zn^{2+}] = 10 μM, in terms of head group, coated with [probe **A**] = 3.6 μM and the peptide ([peptide **I**] = 5 μM, [peptide **II**] = 2 μM, [peptide **III**] = 1 μM). The probe **A** was fully displaced and the F.I. max were determined for each system.

AuNP 1 + peptide	F.I. max observed
Ac-WS(OPO_3^{2-})-OH	360.98
Ac-WWS(OPO_3^{2-})-OH	385.92
Ac-WWWS(OPO_3^{2-})-OH	375.08

*Table 8: F.I. max observed owing to the displacement of probe **A** by D-fructose-1,6-bisphosphate. Experimental conditions: [HEPES] = 10 mM, pH 7.0, [TACN·Zn^{2+}] = 10 μM, [probe **A**] = 75% SSC, [peptide **I-III**] = 25% SSC, 37 ºC, $\lambda_{ex,\ probe\ A}$ = 450 nm, $\lambda_{em,\ probe\ A}$ = 493 nm, slits = 2.5/5.0 nm.*

Once F.I. max for probe **A** was determined for each system, those values were taken to normalize the F.I. and to plot the percentage of probe **A** displaced as a function of the concentration of carbohydrates.

4.5.8.3 Study of the stability of the peptides on AuNP 1 surface in presence of carbohydrates

The stability of the peptides **I-III** when they are covering the AuNP **1** along with the probe **A** in presence of carbohydrate were studied through displacement experiments monitoring the fluorescence of tryptophan (λ_{ex} = 280 nm, λ_{em} = 360 nm, slits = 10.0/10.0 nm). The experiments were performed preparing 1 mL aqueous solution ([HEPES] = 10 mM, pH 7.0) containing [TACN·Zn^{2+}] = 10 μM, in term of head group, saturated with [probe **A**] = 3.6 μM, which correspond to 100% of the SSC, at 37 ºC. Upon the stabilization of the F.I., the peptide was added ([peptide **I**] = 5 μM, [peptide **II**] = 2 μM, [peptide **III**] = 1 μM) to the solution and then consecutive amount of a stock solution of D-glucose-6P in milliQ water were added to the mixture.

To ensure that a stable signal was obtained, the displacement studies were performed by measuring the fluorescence intensity in time after each addition until a constant value was observed (8 to 10 minutes between each addition).

In order to quantify the displacement of the peptides from the AuNP **1** surface, it was necessary to determined F.I. max for each peptide under these experimental conditions. Hence, peptide solution ([peptide **I**] = 5 μM, [peptide **II**] = 2 μM, [peptide **III**] = 1 μM) was prepared in 1 mL aqueous solution ([HEPES] = 10 mM ,pH 7.0) with [probe **A**] = 3.6 μM. Then, F.I. was recorded for each peptide under these experimental conditions.

peptide	F.I. (a.u.)
I	577
II	265
III	145

*Table 9: F.I. determined for peptides free in solution. Experimental conditions: [HEPES] = 10 mM, pH 7.0, [probe **A**] = 3.6 μM, 37 ºC, $\lambda_{ex,\ Trp}$ = 280 nm, $\lambda_{em,\ Trp}$ = 360 nm, slits = 10.0/10.0 nm.*

Once F.I. max for each peptide were determined, those values were taken to normalize the F.I. and to plot the percentage of peptide displaced as a function of the concentration of carbohydrate.

4.6 Bibliography

1. Zeng, X.; Andrade, C. S.; Oliveira, M. L.; Sun, X.-L., Carbohydrate–protein interactions and their biosensing applications. *Anal. Bioanal. Chem.* **2012,** *402* (10), 3161-3176.

2. (a) Davidson, B.; Berner, A.; Nesland, J. M.; Risberg, B.; Kristensen, G. B.; Tropé, C. G.; Bryne, M., Carbohydrate antigen expression in primary tumors, metastatic lesions, and serous effusions from patients diagnosed with epithelial ovarian carcinoma: Evidence of up-regulated Tn and Sialyl Tn antigen expression in effusions. *Hum. Pathol.* **2000,** *31* (9), 1081-1087; (b) Kyselova, Z.; Mechref, Y.; Al Bataineh, M. M.; Dobrolecki, L. E.; Hickey, R. J.; Vinson, J.; Sweeney, C. J.; Novotny, M. V., Alterations in the Serum Glycome Due to Metastatic Prostate Cancer. *J. Proteome Res.* **2007,** *6* (5), 1822-1832; (c) Adamczyk, B.; Tharmalingam, T.; Rudd, P. M., Glycans as cancer biomarkers. *Biochim. Biophys. Acta Gen. Subj.* **2012,** *1820* (9), 1347-1353.

3. Vaillant, O.; Cheikh, K. E.; Warther, D.; Brevet, D.; Maynadier, M.; Bouffard, E.; Salgues, F.; Jeanjean, A.; Puche, P.; Mazerolles, C.; Maillard, P.; Mongin, O.; Blanchard-Desce, M.; Raehm, L.; Rébillard, X.; Durand, J.-O.; Gary-Bobo, M.; Morère, A.; Garcia, M., Mannose-6-Phosphate Receptor: A Target for Theranostics of Prostate Cancer. *Angew. Chem. Int. Ed.* **2015,** *54* (20), 5952-5956.

4. Miron, C. E.; Petitjean, A., Sugar Recognition: Designing Artificial Receptors for Applications in Biological Diagnostics and Imaging. *ChemBioChem* **2015,** *16* (3), 365-379.

5. Zhang, X.-t.; Liu, G.-j.; Ning, Z.-w.; Xing, G.-w., Boronic acid-based chemical sensors for saccharides. *Carbohydr. Res.* **2017,** *452*, 129-148.

6. (a) Solís, D.; Bovin, N. V.; Davis, A. P.; Jiménez-Barbero, J.; Romero, A.; Roy, R.; Smetana Jr, K.; Gabius, H.-J., A guide into glycosciences: How chemistry, biochemistry and biology cooperate to crack the sugar code. *Biochim. Biophys. Acta Gen. Subj.* **2015,** *1850* (1), 186-235; (b) Davis, A. P., Synthetic lectins. *Org. Biomol. Chem.* **2009,** *7* (18), 3629-3638.

7. Nikitina, V.; Loshchinina, E.; Vetchinkina, E., Lectins from Mycelia of Basidiomycetes. *Int. J. Mol. Sci.* **2017,** *18* (7), 1334.

8. Lemieux, R. U., How Water Provides the Impetus for Molecular Recognition in Aqueous Solution. *Acc. Chem. Res.* **1996,** *29* (8), 373-380.

9. (a) Spiwok, V., CH/π Interactions in Carbohydrate Recognition. *Molecules* **2017,** *22* (7), 1038; (b) Asensio, J. L.; Ardá, A.; Cañada, F. J.; Jiménez-Barbero, J., Carbohydrate–Aromatic Interactions. *Acc. Chem. Res.* **2013,** *46* (4), 946-954; (c) Nishio, M.; Umezawa, Y.; Hirota, M.; Takeuchi, Y., The CH/π interaction: Significance in molecular recognition. *Tetrahedron* **1995,** *51* (32), 8665-8701; (d) F. A. Quiocho, Protein-carbohydrate interactions: basic molecular features. *Pure Appl. Chem.* **1989,** *61*, 1293.

10. Davis, A. P.; Wareham, R. S., Carbohydrate Recognition through Noncovalent Interactions: A Challenge for Biomimetic and Supramolecular Chemistry. *Angew. Chem. Int. Ed.* **1999,** *38* (20), 2978-2996.

11. Kim, Y.-H.; Hong, J.-I., Molecular Recognition of Carbohydrates through Directional Hydrogen Bonds by Urea-Appended Porphyrins in Organic Media. *Angew. Chem. Int. Ed.* **2002,** *41* (16), 2947-2950.

12. Mazik, M.; Radunz, W.; Sicking, W., High α/β-Anomer Selectivity in Molecular Recognition of Carbohydrates by Artificial Receptors. *Org. Lett.* **2002,** *4* (26), 4579-4582.

13. (a) Hall, D. G., Structure, Properties, and Preparation of Boronic Acid Derivatives. Overview of Their Reactions and Applications. In *Boronic Acids*, Wiley-VCH Verlag GmbH & Co. KGaA: 2006; pp 1-99; (b) Peters, J. A., Interactions between boric acid derivatives and saccharides in aqueous media: Structures and stabilities of resulting esters. *Coord. Chem. Rev.* **2014,** *268*, 1-22.

14. (a) Jin, S.; Cheng, Y.; Reid, S.; Li, M.; Wang, B., Carbohydrate recognition by boronolectins, small molecules, and lectins. *Med. Res. Rev.* **2010,** *30* (2), 171-257; (b) Pal, A.; Bérubé, M.; Hall, D. G., Design, Synthesis, and Screening of a Library of Peptidyl Bis(Boroxoles) as Oligosaccharide Receptors in Water: Identification of a Receptor for the Tumor Marker TF-Antigen Disaccharide. *Angew. Chem. Int. Ed.* **2010,** *49* (8), 1492-1495.
15. Lis, N. S. H., *Lectins*. 2 ed.; Springer Netherlands: 2007.
16. (a) Siebert, H.-C.; Lü, S.-Y.; Frank, M.; Kramer, J.; Wechselberger, R.; Joosten, J.; André, S.; Rittenhouse-Olson, K.; Roy, R.; von der Lieth, C.-W.; Kaptein, R.; Vliegenthart, J. F. G.; Heck, A. J. R.; Gabius, H.-J., Analysis of Protein–Carbohydrate Interaction at the Lower Size Limit of the Protein Part (15-Mer Peptide) by NMR Spectroscopy, Electrospray Ionization Mass Spectrometry, and Molecular Modeling. *Biochemistry* **2002,** *41* (30), 9707-9717; (b) Sharon, N.; Lis, H., The structural basis for carbohydrate recognition by lectins. *Adv Exp Med Biol* **2001,** *491*, 1-16; (c) Sauerborn, M. K.; Wright, L. M.; Reynolds, C. D.; Grossmann, J. G.; Rizkallah, P. J., Insights into carbohydrate recognition by Narcissus pseudonarcissus lectin: the crystal structure at 2 Å resolution in complex with α1-3 mannobiose1. *J. Mol. Biol* **1999,** *290* (1), 185-199; (d) Seetharaman, J.; Kanigsberg, A.; Slaaby, R.; Leffler, H.; Barondes, S. H.; Rini, J. M., X-ray Crystal Structure of the Human Galectin-3 Carbohydrate Recognition Domain at 2.1-Å Resolution. *J. Biol. Chem.* **1998,** *273* (21), 13047-13052.
17. Nishio, M.; Umezawa, Y.; Fantini, J.; Weiss, M. S.; Chakrabarti, P., CH-[small pi] hydrogen bonds in biological macromolecules. *Phys. Chem. Chem. Phys.* **2014,** *16* (25), 12648-12683.
18. Sugimoto, N.; Miyoshi, D.; Zou, J., Development of small peptides recognizing a monosaccharide by combinatorial chemistry. *Chem. Commun.* **2000,** (23), 2295-2296.
19. Barwell, N. P.; Crump, M. P.; Davis, A. P., A Synthetic Lectin for β-Glucosyl. *Angew. Chem. Int. Ed.* **2009,** *48* (41), 7673-7676.
20. Garcia Martin, S.; Prins, L. J., Dynamic nanoproteins: self-assembled peptide surfaces on monolayer protected gold nanoparticles. *Chem. Commun.* **2016,** *52* (60), 9387-9390.
21. Hudson, K. L.; Bartlett, G. J.; Diehl, R. C.; Agirre, J.; Gallagher, T.; Kiessling, L. L.; Woolfson, D. N., Carbohydrate-aromatic interactions in proteins. *J. Am. Chem. Soc.* **2015**.
22. Gottlieb, H. E.; Kotlyar, V.; Nudelman, A., NMR Chemical Shifts of Common Laboratory Solvents as Trace Impurities. *J. Org. Chem.* **1997,** *62* (21), 7512-7515.
23. Neri, S.; Pinalli, R.; Dalcanale, E.; Prins, L. J., Orthogonal Sensing of Small Molecules Using a Modular Nanoparticle-Based Assay. *ChemNanoMat* **2016,** *2* (6), 489-493.
24. Bonomi, R.; Cazzolaro, A.; Sansone, A.; Scrimin, P.; Prins, L. J., Detection of Enzyme Activity through Catalytic Signal Amplification with Functionalized Gold Nanoparticles. *Angew. Chem. Int. Ed.* **2011,** *50* (10), 2307-2312.

Chapter 5: Carbohydrate recognition through enzyme-mediated signal generation

5.1 Summary

In Chapter 2 it was observed that the weak interactions between phosphorylated carbohydrates and AuNP **1** covered with fluorescence probe led to low levels of probe displacement and, concomitantly, signals of low fluorescence intensity. In this Chapter, a novel strategy is reported to increase the signal strength relying on enzyme mediated dephosphorylation. It will be shown that enzyme substrate selectivity can cause a differentiated response of the sensing system towards carbohydrates.

5.2 Introduction

The studies described in the previous chapters showed that systems composed of AuNP **1**, fluorescent probes and additional recognition modules – *i.e.* peptides – were able to generate a response to phosphorylated carbohydrates with some degree of selectivity. Although interesting from a conceptual point of view, the observed signal intensities and selectivities never reached the magnitude to make the system practical from an applicative point of view. In addition, non-phosphorylated carbohydrates – which are the most attractive targets – never induced any effect. For that reason, we decided to explore an entire different approach towards carbohydrate sensing relying on one feature that emerged as critical for carbohydrate binding to AuNP **1**: the presence of negative charges in the analyte. Comparative studies had shown a strong difference in affinity between non-phosphorylated carbohydrates (no binding), monophosphorylated binding (mM regime) and diphosphorylated binding (μM regime). These results were fully in line with previous results obtained in the Prins' group for nucleotides and peptides.[1] Also for those compounds it was observed that the addition of each negative charged caused an increase in the affinity for AuNP **1** of one order of magnitude. Prins *et. al.* reported the use of catalytic AuNPs, coated with thiol chain containing TACN·Zn^{2+} as head group, for the detection of enzyme activity.[1b] It was found that in the presence of this AuNPs the transphosphorylation process of 2-hydroxypropyl-4-nitrophenyl phosphate (HPNPP) presented a rate acceleration over $3x10^4$ (k_{cat}/k_{uncat}) under saturation conditions at neutral pH owing to the cooperative effects of two head groups. The presence of oligoanions, such as ATP and Ac-Asp-Asp-Asp-OH, provoked the inhibition of the catalytic process due to the strong interaction with the polycationic surface of AuNP avoiding the formation of p-nitrophenol as reporter molecule. Yet, the presence of an enzyme able to hydrolyse ATP or the peptides in smaller fragments with low affinity for Au NP **1** resulted in the activation of catalysis. This could be easily detected by the formation of a yellow color.

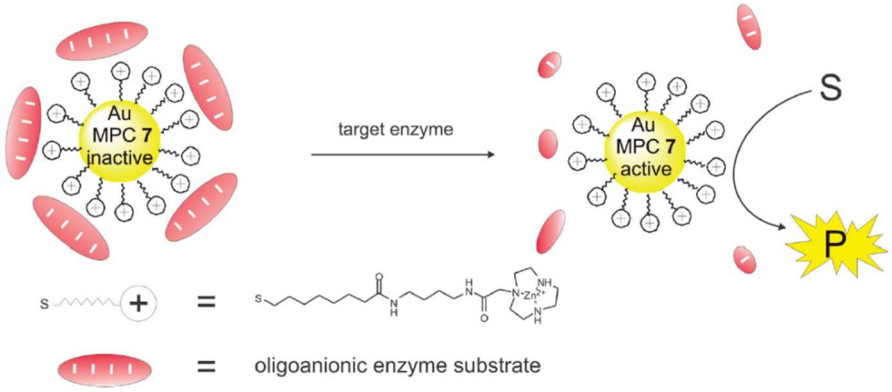

Figure 1: The catalytic activity of Au MPC 7 is inhibited in the presence of oligoanions. The addition of an enzyme able to hydrolyse the substrate in small fragments restores the catalytic activity of Au MPC 7.

We posed ourselves the question whether it would be possible to exploit a related strategy for the detection of non-phosphorylated carbohydrates. Thus, through enzyme-mediated phosphate transfer to a non-phosphorylated carbohydrates we would increase the affinity of the carbohydrate for AuNP **1** leading to a displacement of a fluorogenic probe. In principle, the use of enzymes could also introduce an element of selectivity in case phosphate-transfer would take place selectively to certain carbohydrates (Figure 2).

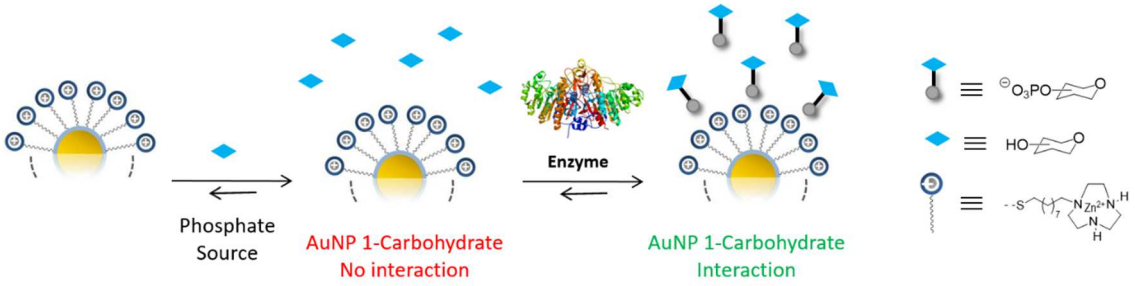

*Figure 2: Schematic representation of carbohydrate recognition by AuNP **1** through the transformation of non-phosphorylated carbohydrate to phosphorylated carbohydrate via transphosphorylation performed by enzyme.*

In natural processes transphosphorylation is carried out by different classes of enzymes.[2] It is well known that hexokinase (HK), which belongs to the transferase family, plays an important role in the first step in glycolysis. HK is able to transfer an inorganic phosphate group from adenosine triphosphate (ATP), as phosphate source, to glucose, as phosphate acceptor, yielding glucose-6-phosphate as product and adenosine diphosphate (ADP) as by-product (Figure 3).[3]

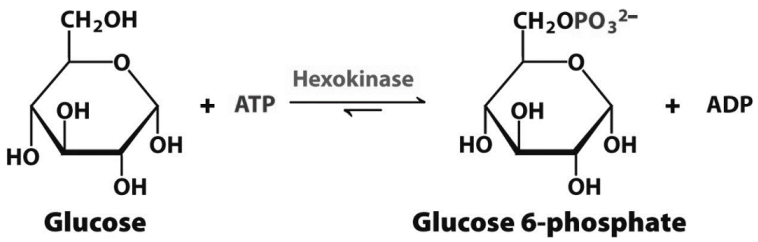

Figure 3: Transphosphorylation process performed by Hexokinase using ATP as phosphate source and glucose as acceptor yielding D-glucose-6-phosphate and ADP.

Yet, this example immediately marks the main challenge, which is that typically enzymes use ATP as phosphate source in transphosphorylation reactions. The use of ATP, however, is incompatible with the proposed sensing system. Prins *et. al.* reported that oligophosphate compounds, such as ATP and ADP, present a stronger binding affinity for AuNP **1** than polycarboxylate compounds or monophosphate compounds, such as probe **A** or glucose-6-phosphate respectively.[1a, 4] This implies that ATP cannot be used as phosphate donor since it would strip all other compounds from the surface of AuNP **1**. For this reason, it was necessary to carry out the transphosphorylation process using an enzyme which uses a phosphate source with low binding affinity for AuNP **1**.

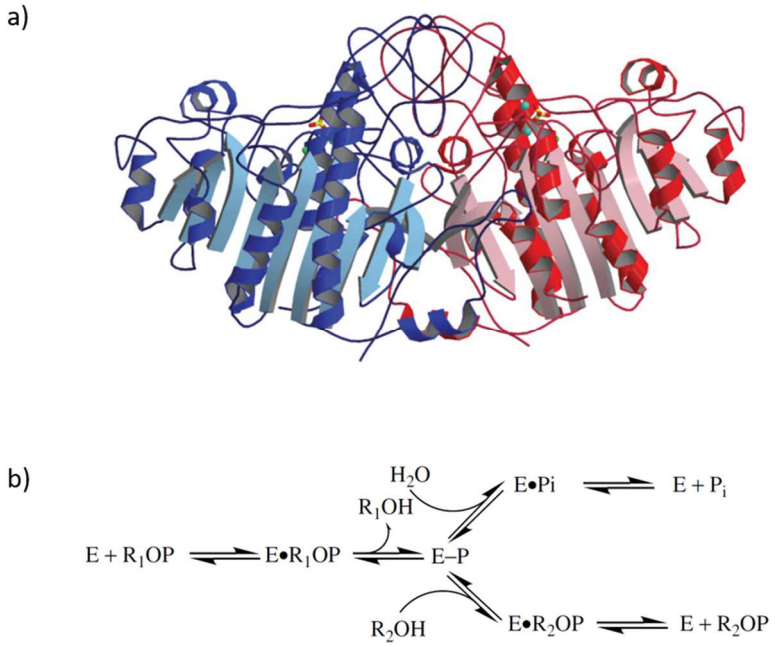

Figure 4: a) Schematic representation of the 3D structure of dimeric E. coli AP the monomers are shown in blue and red. b) Kinetic scheme for the enzymatic hydrolysis/transphosphorylation of phosphate monoester by AP.

Alternative enzymes capable of catalysing transphosphorylation reactions were investigated and alkaline phosphatase (AP) was selected for further studies. AP is a ubiquitous membrane-bound glycoprotein that catalyses the hydrolysis of phosphate monoesters from a wide variety of substrates at basic pH values.[5] However, it has been reported that under specific conditions AP is able to transfer the phosphate group from a monophosphate source to an acceptor with a hydroxyl group (Figure 4).[6] Pradines *et. al.* reported the use of AP for the synthesis of glycerol-1-phosphate, reaching yield of 41%, using phosphate salts as phosphate source under the reverse hydrolysis conditions.[7]

5.3 Results and discussion

5.3.1 Transphosphorylation studies

Several factors are relevant in order to shift the enzymatic process from hydrolysis, which is favoured, to transphosphorylation. To investigate this possibility we modified several parameters, such as the type of phosphate donor, the type of acceptor, the donor: acceptor ratio and the type of buffer.

The transphosphorylation process was investigated through fluorescence kinetic experiments. Experiments were performed by preparing 1 mL solutions of AuNP **1** and probe **A** in aqueous buffer to which different phosphate donors and non-phosphorylated carbohydrates, were added as acceptor. Kinetics were started by adding AP to the mixture and monitored by measuring the fluorescence emission from probe **A**. All attempts are listed in Table 1.

Entrance	Buffer (pH)	Phosphate donor (µM)	Phosphate acceptor (µM)	AP (U/mL)
1	HEPES (7)	Phenyl Phosphate (150)	Fructose (300)	3
2	TRIS (8)	Phenyl Phosphate (150)	Fructose (300)	3
3	HEPES (7)	TMP (100)	Glucose (100)	3
4	HEPES (7)	dGMP (100)	Glucose (200)	3
5	HEPES (7)	Phenyl Phosphate (100)	Glucose (1000)	3
6	MOPS (7.9)	Phenyl Phosphate (200)	Glucose (2000)	3
7	MES (6.7)	Phenyl Phosphate (200)	Glucose (2000)	3
8	MOPS (7.9)	PNPP(100)	Glucose (1000)	3
9	MES (6.7)	PNPP(100)	Glucose (1000)	3
10	MOPS (7.9)	Phenyl Phosphate (200)	Glucose (1000)	4
11	MOPS (7.9)	Phenyl Phosphate (200)	Mannose (1000)	4
12	HEPES (7)	Fructose-1,6-BisPhosphate (200)	Glucose (500)	4
13	HEPES (7)	Phenyl Phosphate (200)	Glucose-6P (1000)	4

*Table 1: Experimental conditions assayed for transphosphorylation process. Experimental conditions: [buffer] = 100 mM, [TACN·Zn^{2+}] = 10 µM, [probe **A**] = 100 % SSC, 37 ºC, $\lambda_{ex\ probe\ A}$ = 450 nm, $\lambda_{em\ probe\ A}$ = 493 nm, slits 2.5/5 nm.*

Different phosphate donors were tested such as phenyl phosphate, thymidine monophosphate (TMP), deoxy-guanidine monophosphate (dGMP), para-nitro-phenyl phosphate (PNPP) and also the diphosphorylated carbohydrate D-fructose-1,6-bisphosphate. In addition, a series of non-phosphorylated carbohydrates such glucose, mannose and fructose were used. Finally, different donor:acceptor ratios and buffer systems were tested.

However, in nearly all cases addition of the enzyme resulted in a decrease of fluorescence intensity indicating that enzyme activity resulted in the formation of products with a lower affinity compared to the starting materials (Figure 5a).

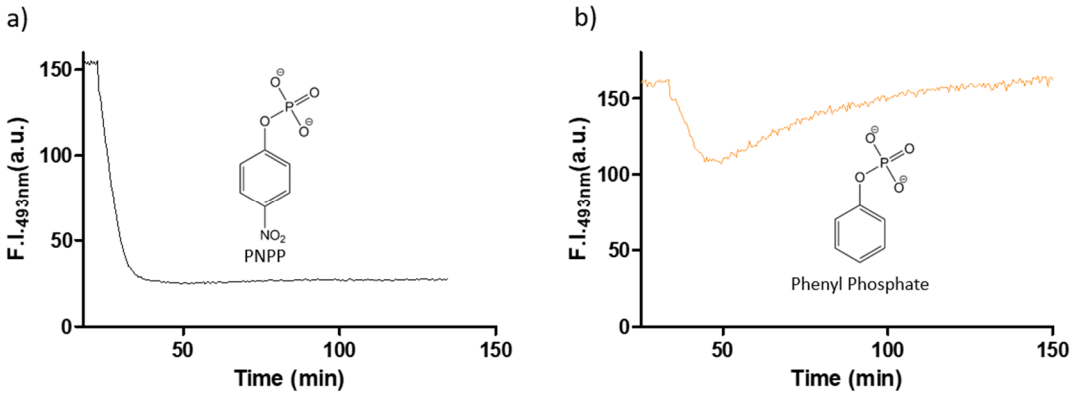

*Figure 5: Fluorescence intensity of 493 nm as a function of time upon the addition of alkaline phosphatase as chemical triggers in presence of D-glucose (left) and D-glucose-6P (right) as acceptors. Experimental conditions a) [MES] = 10 mM, pH 6.7, [TACN·Zn^{2+}] = 10 µM, [glucose] = 1000 µM, [probe **A**] = 100% SSC, [PNPP] = 100 µM, [Alkaline Phosphatase] = 3 U/mL, 37 ºC, $\lambda_{ex,\ probe\ A}$= 450 nm $\lambda_{em,\ probe\ A}$= 493 nm, slits = 2.5/5.0 nm. Experimental conditions b) [HEPES] = 10 mM, pH 7.0, [TACN·Zn^{2+}] = 10 µM, [D-glucose-6P] = 1 mM, [probe **A**] = 100% SSC, [Phenyl Phosphate] = 200 µM, [Alkaline Phosphatase] = 4 U/mL, 37 ºC, $\lambda_{ex,\ probe\ A}$= 450 nm $\lambda_{em,\ probe\ A}$= 493 nm, slits = 2.5/5.0 nm.*

Excitingly, in just one case we observed an increase of F.I. upon the addition of AP to the solution. This occurred when D-glucose-6-phosphate was used as an acceptor and phenyl phosphate as the donor (Figure 5b). Our reason for inserting D-glucose-6-phosphate was that transfer of the phosphate group to one of the hydroxyl-moieties would lead to a diphosphorylated carbohydrate which would be easier to distinguish from the donor and acceptor, which are both monophosphorylated.

We studied this system in further detail to obtain confirmation that transphosphorylation was the source for the observation. This turned out not to be the case, because the addition of AP to a solution containing just D-glucose-6-phosphate – in the absence of a phosphate donor - provoked the same effect. Indeed, this result demonstrates clearly that phenyl phosphate does not play any role in increase of F.I. (Figure 6).

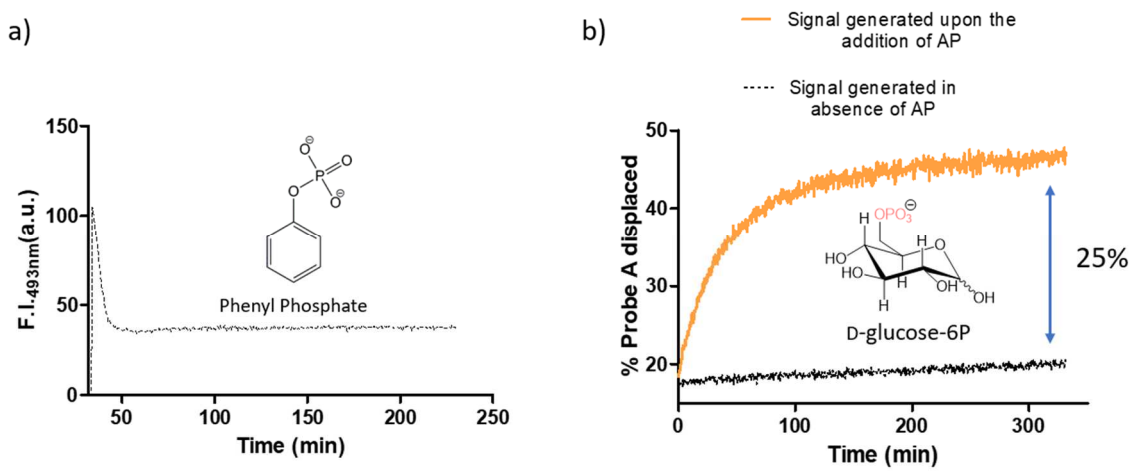

*Figure 6: a) Fluorescence intensity of 493 nm as a function of time upon the addition of alkaline phosphatase as chemical triggers in presence of phenyl phosphate. Experimental conditions:[HEPES] = 10 mM, pH 7.0, [TACN·Zn^{2+}] = 10 μM, [probe **A**] = 100% SSC, [phenyl phosphate] = 200 μM, [Alkaline Phosphatase] = 4 U/mL, 37 ºC, $\lambda_{ex,\ probe\ A}$= 450 nm $\lambda_{em,\ probe\ A}$= 493nm, slits = 2.5/5.0 nm. b) Percentage of probe **A** displaced as function of the time in presence and absence of AP. Experimental conditions: [HEPES] = 10 mM, pH 7.0, [TACN·Zn^{2+}] = 10 μM, [probe **A**] = 100% SSC, [D-glucose-6P] = 1 mM, [Alkaline Phosphatase] = 4 U/mL, 37ºC, $\lambda_{ex,\ probe\ A}$= 450 nm $\lambda_{em,\ probe\ A}$= 493 nm, slits = 2.5/5.0 nm.*

On the other hand the process was clearly caused by enzymatic action, because in the absence of enzyme the signal was basically stable as a function of time.

A more detailed investigation was carried out by measuring the rate of fluorescence increase at different concentrations of alkaline phosphate. Fluorescence kinetic experiments were performed by adding fixed amounts of AP to 1 mL solution of AuNP **1** covered with probe **A** in the presence of D-glucose-6P in aqueous buffer (Figure 7). It was observed that an increase in AP concentration resulted in a higher rate (Figure 8).

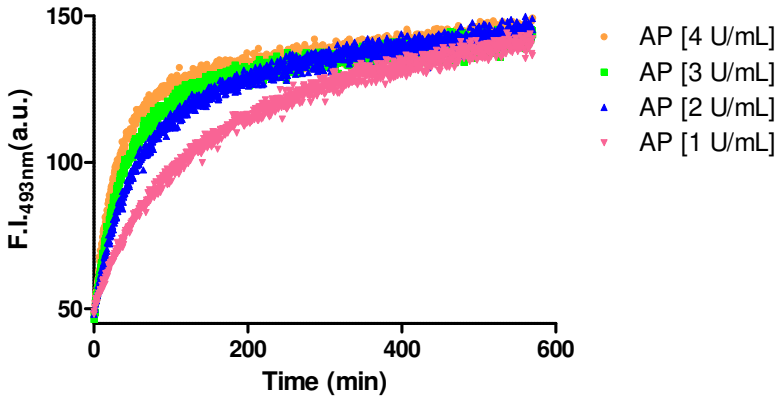

*Figure 7: Fluorescence intensity of 493 nm as a function of time upon the addition of different concentration of alkaline phosphatase as chemical triggers in presence of D-glucose-6P. Experimental conditions: [HEPES] = 10 mM, pH 7.0, [TACN·Zn^{2+}] = 10 μM, [probe **A**] = 100% SSC, [D-glucose-6P] = 1 mM, 37 ºC, $\lambda_{ex,\ probe\ A}$= 450 nm $\lambda_{em,\ probe\ A}$= 493 nm, slits = 2.5/5.0 nm.*

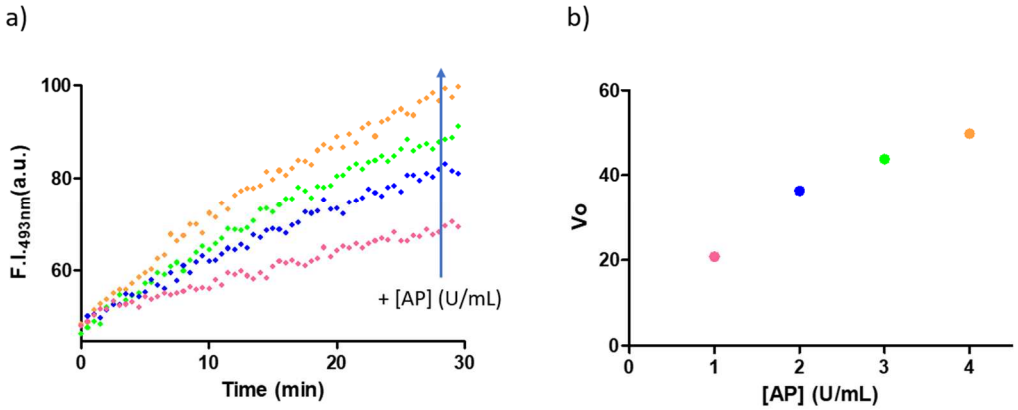

*Figure 8: Fluorescence intensity of 493 nm as a function of time upon the addition of different concentration of alkaline phosphatase as chemical triggers in presence of D-glucose-6P. b) Initial rate (V_o) as function of AP concentration. Experimental conditions: [HEPES] = 10 mM, pH 7.0, [TACN·Zn^{2+}] = 10 µM, [probe **A**] = 100% SSC, [D-glucose-6P] = 1 mM, 37 ºC, $\lambda_{ex,\ probe\ A}$= 450 nm $\lambda_{em,\ probe\ A}$= 493 nm, slits = 2.5/5.0 nm.*

^{31}P-NMR spectroscopy was then used to obtain a direct insight in the chemical conversion. Several experimental conditions were studied and under optimized conditions kinetic experiments were performed to monitor changes in the mixture. Prior to the addition of AP, the signals of the α- and β-anomers of D-glucose-6P and H_3PO_4, as reference, were observed at 3.85 ppm, 3.76 ppm and 0.0 ppm respectively. Upon AP addition, a gradual disappearance of the anomer signals was observed accompanied with the formation of a new signal at 1.49 ppm (Figure 9 left).

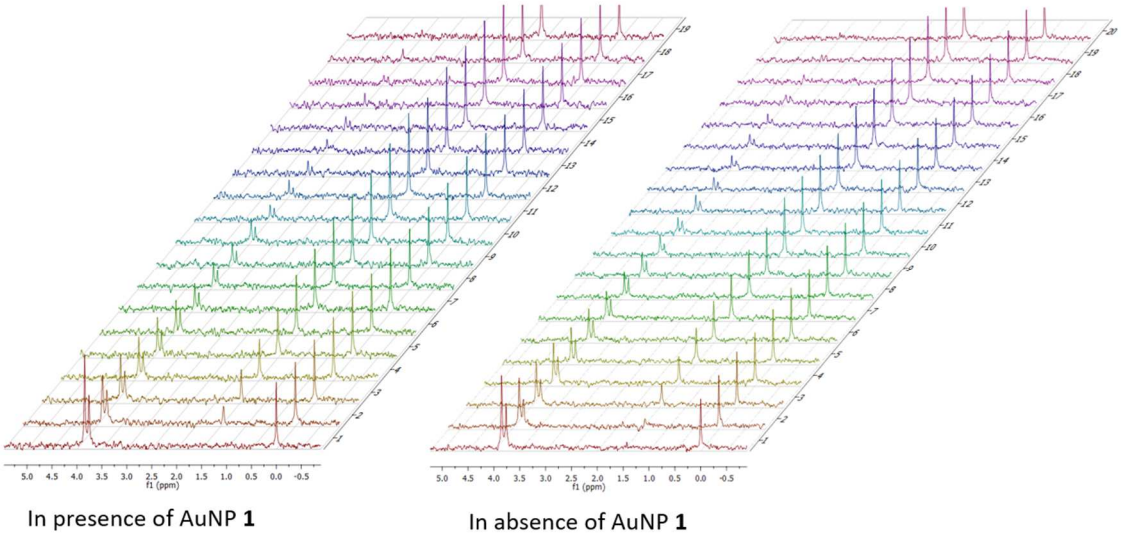

*Figure 9: Partial ^{31}P-NMR spectra from the kinetic experiments in presence and absence of AuNP **1**. Experimental conditions: [HEPES] = 10 mM, pH 7.0, [TACN·Zn^{2+}] = 10 µM, [D-glucose-6P] = 2 mM, [Alkaline Phosphatase] = 6 U/mL, 301 K.*

In an additional experiment, it was investigated whether the presence of AuNP **1** affected the reaction rate (Figure 9b). Preliminary results in the Prins' group have provided evidence that the TACN-Zn^{2+} complexes in the monolayer can activate phosphate compounds for enzymatic cleavage. In order to quantify the consumption of D-glucose-

6P and the formation of the phosphorylated compound, the peak of H_3PO_4 was taken as a reference and the signals of both compounds were integrated with regard to the reference. No distinction was made between α- and β-anomers. An additional control showed no difference in rate between the anomers. The graphs confirmed that AuNP **1** did not affect the rates (Figure 10).

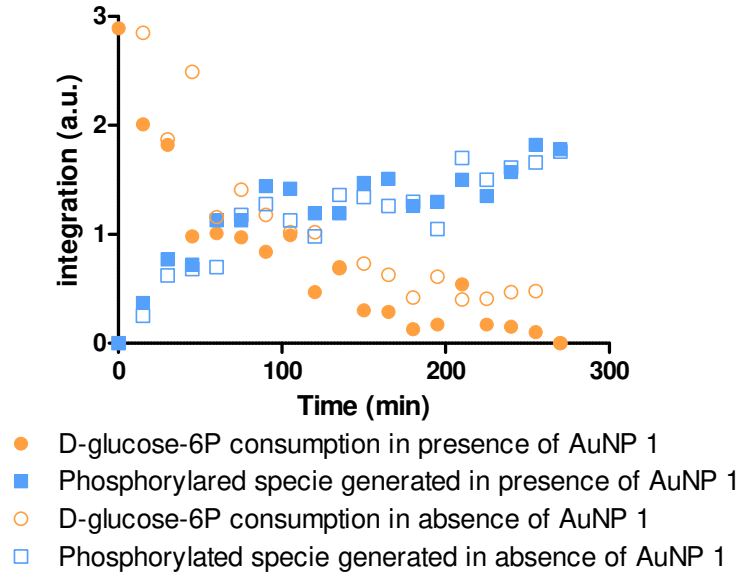

Figure 10: Integration of D-glucose-6P and phosphorylated compound signals as function of time. Experimental conditions: [HEPES] = 10 mM, pH 7.0, [TACN·Zn^{2+}] = 10 μM, [D-glucose-6P] = 2 mM, [Alkaline Phosphatase] = 6 U/mL, 301 K.

After reaction, the mixture was purified by size-exclusion chromatography, using milliQ water as the eluent, collecting several fractions. Surprisingly, the analysis showed unequivocally that the new phosphorylated compound corresponded to inorganic phosphate. Therefore, the process leading to an increase in fluorescence intensity originated simply from the hydrolysis of D-glucose-6P.[8] This came as a surprise, because even though many dephosphorylation reactions on different compounds and using different enzymes have been carried out previously in the Prins' group, this is the first example in which dephosphorylation results in an increase in fluorescent intensity.

This implies that the waste products (inorganic phosphate and glucose) have a higher affinity compared to the starting material D-glucose-6P. This was verified using displacement experiments. The displacement experiments consisted of titration of glucose or inorganic phosphate stock solutions to a solution containing AuNP **1** and probe **A**.

As expected, D-glucose was unable to displace probe **A** from the surface even at 1 mM concentration (3%). However, inorganic sodium phosphate displaced 18% of the probe at the same concentration (Figure 11). The combined displacement of 21% closely matches the 25% probe displacement observed during the initial kinetics.

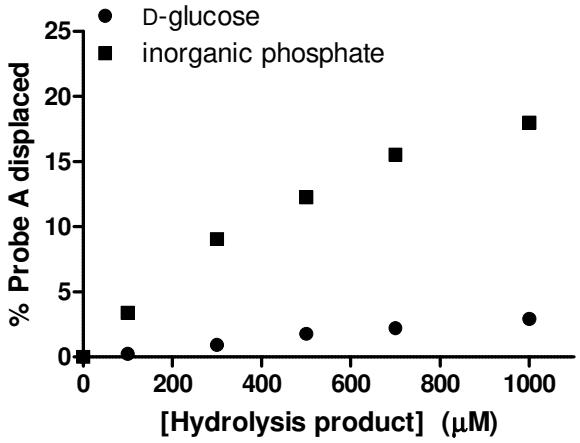

*Figure 11: Percentage of probe **A** displaced as function of [hydrolysis product]. Experimental conditions: [HEPES] = 10 mM, pH 7.0, [TACN·Zn^{2+}] = 10 μM, [probe **A**] = 100% SSC, 37 ºC, $\lambda_{ex,\ probe\ A}$ = 450 nm $\lambda_{em,\ probe\ A}$ = 493 nm, slits = 2.5/5.0 nm.*

5.3.2 Study of C1- and C6-phosphorylated carbohydrates

Although different than designed, the observation that enzymatic activity leads to increased signal strength enables a different approach to the sensing of monophosphorylated carbohydrates. Indeed, compared to the direct titrations performed in previous chapters, the increase in signal intensity is significantly higher. Yet, a possible discrimination between carbohydrates cannot rely on the final fluorescence values, because these derive from the liberated phosphate which is independent of the substrate. This emerged clearly from a comparative study of D-glucose-1P, D-mannose-1P and D-galactose-1P. Nearly superimposable kinetic traces were obtained reaching identical end values (Figure 12).

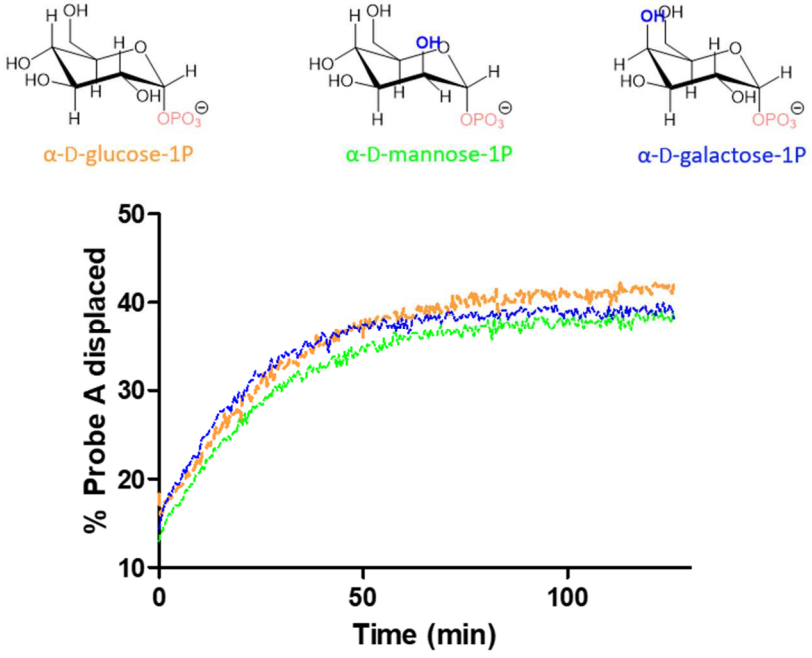

*Figure 12: Percentage of probe **A** displaced as a function of time upon the addition of alkaline phosphatase as chemical trigger in presence of phosphorylated carbohydrates in C1 position. Experimental conditions: [HEPES] = 10 mM, pH 7.0, [TACN·Zn^{2+}] = 10 μM, [probe **A**] = 100% SSC, [D-carbohydrate-1P] = 1 mM, 37 ºC, $\lambda_{ex,\ probe\ A}$= 450 nm $\lambda_{em,\ probe\ A}$= 493 nm, slits = 2.5/5.0 nm.*

However, this screening method could exploit enzyme selectivity to generate a differentiated response between different analytes. Although AP is not the best enzyme of choice because of its broad substrate scope, the following experiments indicate nonetheless the feasibility. Whereas the carbohydrates phosphorylated in position 1 were structurally too similar to be differentiated by the enzyme, this was not the case for the analogous carbohydrate series phosphorylated in position 6. Thus, the hydrolysis of D-glucose-6P, D-mannose-6P and D-galactose-6P proceeded with very different rates. Whereas hydrolysis of D-galactose-6P proceeded very slowly and was not complete after 100 minutes, D-glucose-6P was hydrolysed very rapidly. The difference emerges from a comparison of the initial rates. An overall 2.7-fold difference was observed between the best (D-glucose-6P) and worst (D-galactose-6P) substrate (Figure 13).

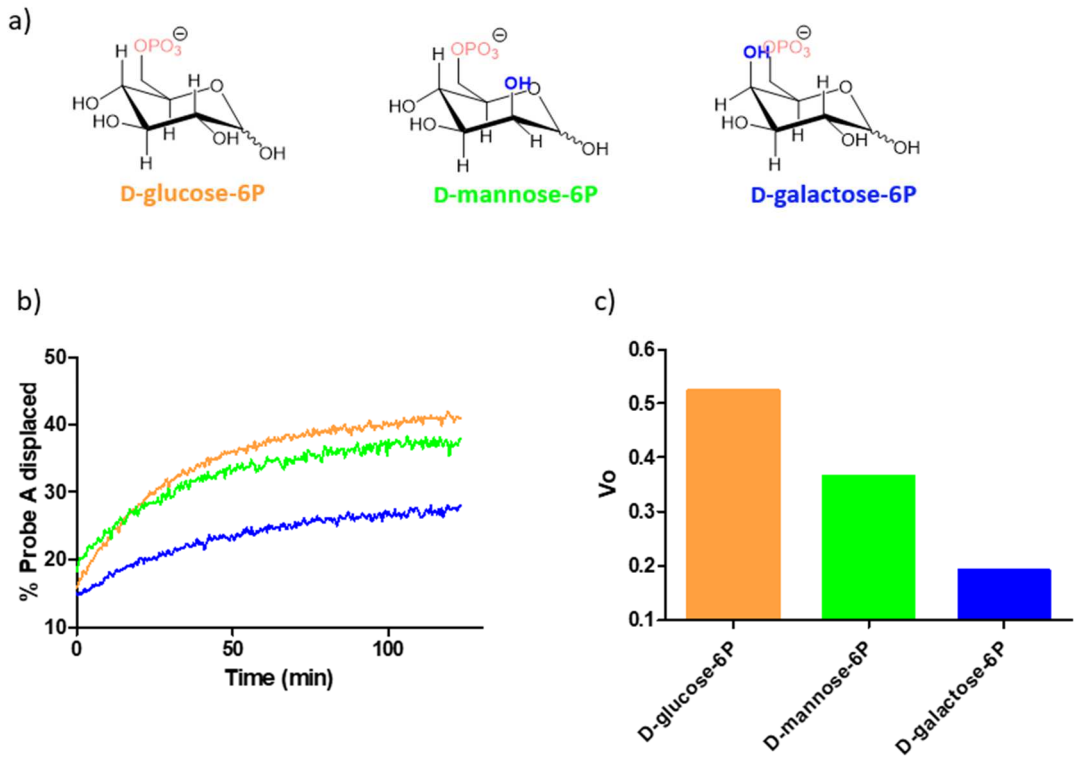

*Figure 13: a) Phosphorylated carbohydrates in C6 position selected. b) Percentage of probe **A** displaced as a function of time upon the addition of alkaline phosphatase as chemical trigger in presence of phosphorylated carbohydrates in C6 position. c) Initial rates for hydrolysis process of D-carbohydrates-6P in presence of AP. Experimental conditions: [HEPES] = 10 mM, pH 7.0, [TACN·Zn^{2+}] = 10 μM, [probe **A**] = 100% SSC, [D-carbohydrate-6P] = 1 mM, 37 ºC, $\lambda_{ex,\ probe\ A}$= 450 nm $\lambda_{em,\ probe\ A}$= 493nm, slits = 2.5/5.0 nm.*

5.4 Conclusions

A new approach has been developed for the sensing of non-phosphorylated carbohydrates by AuNP **1** relying on the introduction of a phosphate group by means of an enzyme-mediated transphosphorylation process. However, no experimental conditions within the boundary conditions of our system could be found in which AP-catalysed transphosphorylations was detected.

On the other hand, signal generation was observed for C6- and C1-phosphorylated carbohydrates because of AP-catalysed dephosphorylation. The reason for signal intensity increase was the fact that the waste products had a higher affinity for AuNP **1** compared to the phosphorylated carbohydrates. So far, this had not been observed in the Prins' group. The different rates of hydrolysis for C6-phosphorylated carbohydrates permitted their discrimination by AuNP **1**. On the other hand, no selectivity was observed for C1.

5.5 Experimental section

5.5.1 Instrumentations

NMR Analysis

^{1}H-NMR spectra were recorded using a Bruker 400 Avance III spectrometer operating at 400 MHz for ^{1}H. Chemical shifts (δ) are reported in ppm using D_2O residual solvent value as internal reference.[9] ^{31}P-NMR experiments were performed using a Bruker 400 Avance III spectrometer operating at 162 MHz for ^{31}P using a solution of H_3PO_4 (15 mM) as external standard for calibration.

pH measurements

The pH of buffer solutions was determined at room temperature using a pH-meter Metrohm-632 equipped with a Ag/AgCl/KCl reference electrode.

Uv-Vis and Fluorescence spectroscopy

Uv-Vis measurements were recorded on a Varian Cary 50 spectrophotometer, while fluorescence measurements were recorded on a Varian Cary Eclipse Fluorescence spectrophotometer. Both the spectrophotometers were equipped with a thermostatted cell holders.

LC/MS analysis

The UHPLC/MS measurements were performed on an Agilent 1290 Infinity LC/MS System equipped with an ESI sources, quadrupole system and diode array detector.

LIO5P freeze dryer

Lyophilisation was performed by the LIO-5P at minimum condensing temperature of -55 ºC under reduced pressure.

5.5.2 Materials

$Zn(NO_3)_2$ was analytical grade products. 4-(2-hydroxyethyl)-1-piperazineethanesulfonic acid (HEPES), 2-amino-2-(hydroxymethyl)propane-1,3-diol (TRIS), 3-(N-morpholino)propanesulfonic (MOPS), 2-morpholinoethanesulfonic acid sodium salt (MES), Sephadex® G-25 and alkaline phosphatase (from calf intestine, EC number 3.1.3.1) were purchased from Sigma Aldrich and used without further purification. $Coumarin_{343}$-Gly-Asp-Asp (probe **A**) was synthesised previously in the group. D-Glucose-6-phosphate, D-mannose-6-phosphate, D-galactose-6-phosphate, α-D-mannose-1-phosphate and α-D-galactose-1-phosphate were purchased from Sigma Aldrich. α-D-Glucose-1-phosphate, β-D-glucose-1-phosphate were purchased from CarboSynth. In all cases, stock solutions were prepared using deionized water filtered with a milliQ-water-purifier (Millipore) and stored at 4 °C or -20 ºC.

5.5.3 Determination of the stock solution concentrations

The concentration of $Zn(NO_3)_2$ solution was determined by atomic absorption spectroscopy. The concentration of the fluorescence probe **A** stock solution ($\varepsilon_{(450\ nm)}$ = 45000 M^{-1} cm^{-1}) was determined by UV spectroscopy at pH 7.0. The concentration of phosphorylated carbohydrate solution were determined by ^{1}H-NMR using pyrazine as internal standard.[10] The concentration of TACN head group was determined by kinetic titration using $Zn(NO_3)_2$.[1b]

5.5.4 Determination of surface saturation concentration

The SSC of fluorescence probe **A** on AuNP **1** was determined from a fluorescence titration of probe **A** to AuNP **1** (10 μM) in HEPES buffer (10 mM) at 25 ºC.[11] The F.I. at 493 nm was measured as a function of amount of probe **A** added. Fitting of the experimental values yielded a SSC of 3.6 μM (equivalent to 100% SCC).

5.5.5 Fluorescence kinetic experiments

Study of the transphosphorylation process

To carry out the study of experimental conditions of transphosphorylation process performed by alkaline phosphatase, AP stock solution (U/mL) was added to a mixture of AuNP **1** (10 μM), probe **A** (3.6 μM), phosphate donor (μM) and carbohydrate (μM)

prepared in 1 mL aqueous buffer (10 mM) at 37 ºC. Upon the addition of AP at t = 15 minutes, the fluorescence intensity of probe **A** (λ_{ex} = 450 nm, λ_{em} = 493 nm) was monitored with time. The concentrations of each reagents are described in Table 1.

Study of C-1 and C6-phosphorylated carbohydrates

Phosphorylated carbohydrates in C1 and C6 positions were studied through kinetic displacement experiments. The experiments were performed preparing 1 mL solution containing AuNP **1** (10 μM), probe **A** (3.6 μM) and phosphorylated carbohydrate (1 mM) in HEPES (10 mM, pH 7.0) at 37 ºC. Upon the addition of AP stock solution in milliQ water to the mixture reaching a concentration of 4 U/mL, the fluorescence of probe **A** was monitored with time.

In order to normalize the F.I. values, it was assumed as F.I. max the value of the interception of the equation obtained from SSC experiments ($y = mx + \boldsymbol{q}$). Then, this value was used to normalize the F.I. and to plot the percentage of probe displaced as function of time.

Initial rate for the process (V_o) were determined by following the changes in fluorescence (Fluorescence Intensity (a.u.)/ minutes).

Study of the effect of AP concentration on the signal generation process

The influence of AP concentration to signal generation was investigated through kinetic displacement experiments. The experiments were performed preparing 1 mL solution containing AuNP **1** (10 μM), probe **A** (3.6 μM) and D-glucose-6P (1 mM) in HEPES (10 mM, pH 7.0) at 37 ºC. Upon the addition of AP stock solution in milliQ water to the mixture reaching a concentrations of 1, 2, 3, and 4 U/mL, the fluorescence of probe **A** was monitored in time. Then, F.I at 493 nm was plotted as function of time.

Initial rate for the process (V_o) were determined by following the changes in fluorescence (Fluorescence Intesity (a.u.)/ minutes), plotted as a function of alkaline phosphatase concentration (U/mL).

5.5.6 Investigation of the new compound formed by several techniques

^{31}P-NMR spectroscopy

The ^{31}P-NMR spectra (256 scan, delay time: 3 s) were recorded using a coaxial tube: an aqueous solution of 15 mM H_3PO_4 was placed inside and employed as a chemical shift reference (H_3PO_4 give δ= 0.0 ppm as a singlet), whereas the mixture of 0.5 mL of D-glucose-6P (2 mM), AuNP **1** (10 μM) in HEPES (10 mM, pH 7.0) was placed in the external tube. The first spectrum was acquired for the mixture with 10% of D_2O (v/v)

(employed as a locking signal). Afterwards, alkaline phosphatase stock solution in milliQ water was added to the mixture reaching final concentration of 6 U/mL. The process was monitored for 360 minutes at 301K, in which every 15 minutes a spectra was recorded. The same experiments were performed in absence of AuNP **1** under the similar experimental conditions.

In order to quantify the process of the consumption of D-glucose-6P and the formation of the new phosphorylated compounds, the intensity of the peak corresponding to H_3PO_4, in ^{31}P-NMR spectra, was normalized to 1 and this was taken as a reference. The peaks corresponding to D-glucose-6P and the phosphorylated compound were integrated. Afterwards, these values were plotted as function of time.

Purification and UPLC/MS analysis

The sample preparation consisted of preparation of a mixture of 0.5 mL containing AuNP **1** (10 µM), D-glucose-6P (2 mM) in HEPES (10 mM, pH 7.0). Upon the addition of alkaline phosphatase stock solution in milliQ water to the mixture, the sample was stirred for 360 minutes at room temperature. Then, the sample was purified by size-exclusion chromatography (Sephadex G25, eluent milliQ water) and collected in fractions. They were characterized by UPLC/MS using A: H_2O + HCOOH 0.1% and B: ACN + HCOOH 0.1% as eluent and Zorbax SB-C3 rapid resolution HT 3.0 x 100 mm 1.8-micron passing from 5% B to 95% B in 15 minutes.

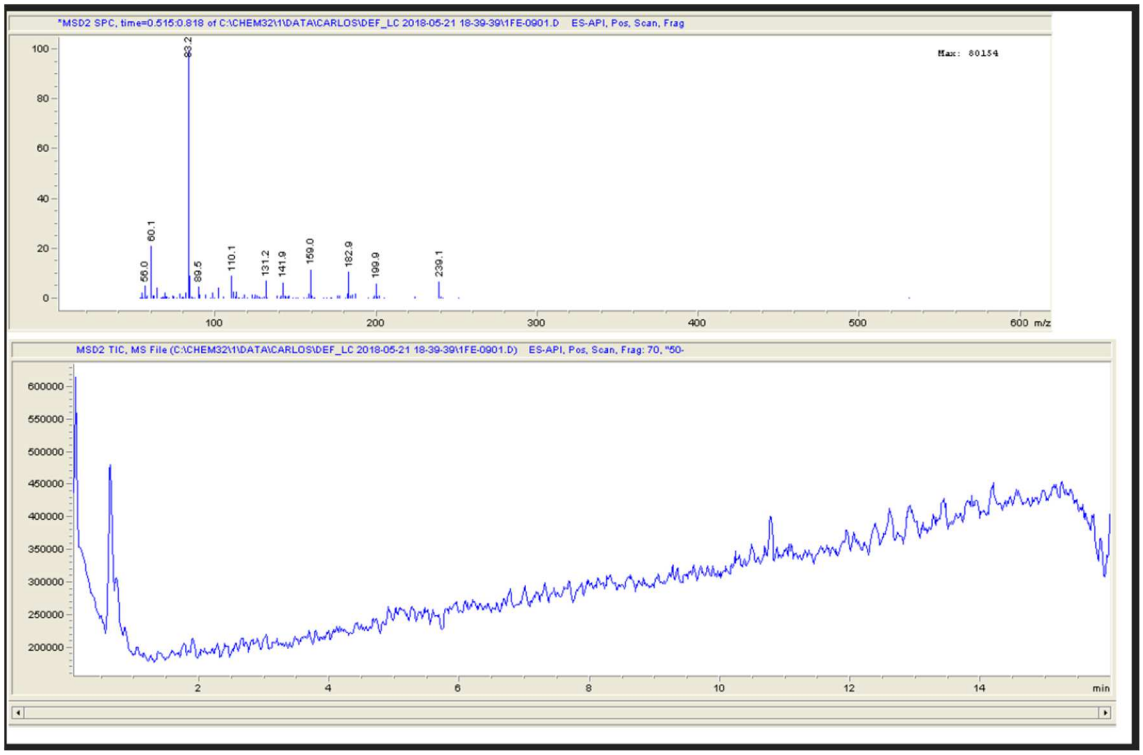

Fluorescence experiments

The fluorescence experiments consisted of displacement experiments using the hydrolysis product. D-Glucose and sodium phosphate (inorganic phosphate) stock solutions in milliQ water were used.

The displacement experiments were performed by adding consecutive amounts of stock solutions of hydrolysis products in milliQ water to a 1 mL aqueous solution of HEPES (10 mM, pH 7.0) containing the AuNP **1** (10 μM) in presence of fluorescence probe **A** (3.6 μM) at 37 ºC.

In order to quantify the F.I. at 493 nm, similar procedure as above was followed. Then, the F.I. values were normalized, as percentage of probe displaced, and plotted as function of concentration of the hydrolysis product.

5.6 Bibliography

1. (a) Pieters, G.; Pezzato, C.; Prins, L. J., Controlling Supramolecular Complex Formation on the Surface of a Monolayer-Protected Gold Nanoparticle in Water. *Langmuir* **2013,** *29* (24), 7180-7185; (b) Bonomi, R.; Cazzolaro, A.; Sansone, A.; Scrimin, P.; Prins, L. J., Detection of Enzyme Activity through Catalytic Signal Amplification with Functionalized Gold Nanoparticles. *Angew. Chem. Int. Ed.* **2011,** *50* (10), 2307-2312.

2. Nelson, D. L.; Cox, M. M.; Lehninger, A. L., *Lehninger principles of biochemistry*. W.H. Freeman: New York, 2013.

3. Tornheim, K., Glucose Metabolism and Hormonal Regulation. In *Reference Module in Biomedical Sciences*, Elsevier: 2018.

4. Pezzato, C.; Lee, B.; Severin, K.; Prins, L. J., Pattern-based sensing of nucleotides with functionalized gold nanoparticles. *Chem. Commun.* **2013,** *49* (5), 469-471.

5. Sharma, U.; Pal, D.; Prasad, R., Alkaline Phosphatase: An Overview. *Indian J. Clin. Biochem.* **2014,** *29* (3), 269-278.

6. Kantrowitz, E. R., E. coli Alkaline Phosphatase. In *Handbook of Metalloproteins*, John Wiley & Sons, Ltd: 2006.

7. Pradines, A.; Klaebe, A.; Perie, J.; Paul, F.; Monsan, P., Large-scale enzymatic synthesis of glycerol 1-phosphate. *Enzyme Microb. Technol.* **1991,** *13* (1), 19-23.

8. (a) Weiss, P. M.; Cleland, W. W., Alkaline phosphatase catalyzes the hydrolysis of glucose-6-phosphate via a dissociative mechanism. *J. Am. Chem. Soc.* **1989,** *111* (5), 1928-1929; (b) Tewari, Y. B.; Steckler, D. K.; Goldberg, R. N.; Gitomer, W. L., Thermodynamics of hydrolysis of sugar phosphates. *J. Biol. Chem.* **1988,** *263* (8), 3670-3675.

9. Gottlieb, H. E.; Kotlyar, V.; Nudelman, A., NMR Chemical Shifts of Common Laboratory Solvents as Trace Impurities. *J. Org. Chem.* **1997,** *62* (21), 7512-7515.

10. Neri, S.; Pinalli, R.; Dalcanale, E.; Prins, L. J., Orthogonal Sensing of Small Molecules Using a Modular Nanoparticle-Based Assay. *ChemNanoMat* **2016,** *2* (6), 489-493.

11. Pieters, G.; Cazzolaro, A.; Bonomi, R.; Prins, L. J., Self-assembly and selective exchange of oligoanions on the surface of monolayer protected Au nanoparticles in water. *Chem. Commun.* **2012,** *48* (13), 1916-1918.

Summary

Carbohydrates participate in many biological processes which are involved in the recognition process of selective protein-carbohydrate interactions. Therefore, it is important to develop new strategies for carbohydrate recognition since it can be useful to understand the process better and also for its application in medical and diagnostic fields. However, carbohydrate recognition in water is not trivial. Carbohydrates are hydrophilic molecules which resemble cluster of water molecules and therefore the differentiation of it from the solvent is difficult. Despite their large varieties, they usually have very subtle structural differences which in turn makes it more difficult to differentiate them. Lectins, which are natural carbohydrate receptors, are able to differentiate carbohydrates in a biological context as a consequence of the presence of binding pockets with multiple recognition units for carbohydrates relying on multiple non-covalent interactions. Inspired by these natural systems, supramolecular chemists designed synthetic counterparts. Initially, most synthetic strategies developed were operative only in organic solvents however their applicability was limited in medical and diagnostic fields. Recently, the attention has shifted towards designing synthetic receptors for recognition of carbohydrates that are able to operate in water. AuNPs present very interesting features which can be exploited for the design of novel chemical and biological sensors. This characteristic gives it an advantage with regard to conventionally used synthetic receptors.

In this PhD thesis AuNP **1**, which are gold nanoparticles (d = 1.8 ± 0.4 nm) covered with hydrophobic C9-thiols terminating with a 1,4,7-triazacyclonone (TACN)·Zn^{2+}, have been used to study carbohydrate recognition. The main purpose was provide the initial bases for the development of innovative synthetic receptor for recognition of carbohydrates able to operate in water using non-covalent interactions.

Initially, study of different carbohydrates, such as glucose, mannose and galactose, phosphorylated in C6 and C1 positions in presence of AuNP **1** covered with different fluorescent probes, such probe **A**, MSP and BSP, were performed. The results showed the AuNP **1** was able to bind to phosphorylated carbohydrates. Besides, certain selectivity was observed for C6-isomers in presence of MSP and BSP while an inversion of the selectivity was observed in presence of probe **A**. In addition, only in the case of probe **A** selectivity was observed between the carbohydrates. Therefore, these system were able to differentiate between isomers and epimers in presence of probe **A**. The study of α- and β-anomers showed that the systems are able to differentiate them, also the selectivity is affected by the type of probe on the surface. Therefore, this also suggests along with the inversion of the selectivity between isomers that the probe could play a role in the recognition process.

After this, the carbohydrate recognition by AuNP **1** was used as an ideal system in order to study the interactions between AuNP **1** and small molecules. In addition, it was used to study the role of the probe in the process. Several techniques were investigated such as fluorescence correlation spectroscopy (FCS), isothermal titration calorimetry (ITC), Diffusion-ordered spectroscopy (DOSY) and ^{31}P-NMR. The results showed that all the

techniques allowed the detection of the interaction between AuNP **1** and phosphorylated carbohydrates despite the fact that all of them provide different grades of selectivity. Owing to the weak interactions of the system, it was not possible to obtain reliable data in all the cases. Related with the recognition process, it was observed that in the absence of the fluorescent probe, phosphorylated glucose in the C1 and C6 positions present similar binding affinity for the AuNP **1** giving an idea about the role of the probe in the recognition process. Besides, it was observed that the binding process presents a different behaviour compared to the 1:1 binding model indicating a higher level of complexity.

Based on the previous results obtained, a new strategy was designed by combining AuNP **1** and small peptides, containing **I-II-III** Trp residues as carbohydrate recognition units, along with fluorescence probe **A** yielding a synthetic receptor capable of recognizing carbohydrates in water via non-covalent interactions. The systems were assayed in presence of D-glucose-6P and an increase of 4.8-folds was observed in the case of **I**, when compared to the same system in absence of peptides. Even higher binding affinity was observed in presence of **II** and similar results were obtained in the presence of **III** with no drastic increase. Therefore, these results suggested that the presence of Trp on the AuNP **1** surface is involved in the recognition process by improving the binding probably through CH-π interactions with the carbohydrates. However, these system did not show any selectivity in presence of α-D-glucose-1P and β-D-glucose-1P. Hence, these systems are not able to differentiate between anomers of carbohydrates.

To overcome the above drawback a novel strategy was developed to produce an increase of the signal strength by performing hydrolysis of phosphorylated carbohydrates using alkaline phosphatase. Several phosphorylated carbohydrates in C1 and C6 positions were studied. The results showed that AP presented different rates of efficiency and therefore different selectivity for C6-isomers. However, no differentiation was observed in the case of C1-isomers.

Acknowledgements

On completing this project successfully, many people have best owned upon me their heart pledged help and support for which I would like to express my sincere gratitude. Foremost, I would like to thank my supervisor, Prof. Leonard J. Prins for giving me this opportunity and also for his constant guidance, encouragement and constructive feedback throughout this journey. I would like to extend my gratitude to the Marie Curie ITN-MULTI-APP programme for the financial support (Nº 642793) and all the training received.

I wish to thank Prof. Bart Jan Ravoo from the University of Münster and Prof. Jurriaan Huskens from the University of Twente for giving me the opportunity to visit their labs and collaborate with them. Also, the group of "MULTI-APP" including the PI´s, Post Doctoral fellows and PhD students for organizing such wonderful conferences and meetings.

A special gratitude to all the people with whom I shared some wonderful and memorable moment; Sushmitha, for the great moments spent inside the lab either discussing chemistry, or watching the computer screen for prolonged periods waiting for the expected results or in general just working late nights in Bunker. Also for all the activities outside the lab like dinners, parties, birthdays, beers and the discussions about life. Rui, my dear colleague and now friend, for all the moments shared having coffees in Aurora and the many discussions about the synthesis of gold nanoparticles. Andrea, for all the great moments spent in the lab and in the bar. Elisa, for her great kindness and delicious sweets and chocolates that she brought to bunker office to brighten people's days. Antonio, for all funny moments that we shared together in Padova and Pula. Last but not least, Lucía for always supporting me and cheering me up whenever I needed, for the countless moments we shared together (birthdays, dinners, trips…and many more), and most importantly for giving me a different perspective about life with her kindness and positive attitude.

Finally, I would like to thank to my mother, Pilar, sister, Claudia, and father, Carlos, for supporting me throughout this time despite the distance. Also, all my friends in Barcelona (Victor, Javier, Adrià, Santiago, Carlos, David y Daniel) for their support and company whenever I returned home. Marta, despite not being able to work things out as expected, I thank her for all the moments we shared and also for her motivation and inspiration to progress and never give up.